ANL-7438

Argonne National Laboratory

REACTOR DEVELOPMENT PROGRAM PROGRESS REPORT

March 1968

Printed in the United States of America
Available from
Clearinghouse for Federal Scientific and Technical Information
National Bureau of Standards, U. S. Department of Commerce
Springfield, Virginia 22151
Price: Printed Copy $3.00; Microfiche $0.65

ANL-7438
Reactor Technology
(TID-4500)
AEC Research and
Development Report

ARGONNE NATIONAL LABORATORY
9700 South Cass Avenue
Argonne, Illinois 60439

REACTOR DEVELOPMENT PROGRAM PROGRESS REPORT

March 1968

Robert B. Duffield, Laboratory Director
Stephen Lawroski, Associate Laboratory Director

Division	Director
Chemical Engineering	R. C. Vogel
Idaho	M. Novick
Metallurgy	M. V. Nevitt
Reactor Engineering	L. J. Koch
Reactor Physics	R. Avery
Remote Control	D. P. Mingesz (Acting)

Report Coordinated by
C. L. Chernick and A. Glassner

Issued April 26, 1968

FOREWORD

The Reactor Development Program Progress Report, issued monthly, is intended to be a means of reporting those items of significant technical progress which have occurred in both the specific reactor projects and the general engineering research and development programs. The report is organized in accordance with budget activities in a way which, it is hoped, gives the clearest, most logical overall view of progress. Since the intent is to report only items of significant progress, not all activities are reported each month. In order to issue this report as soon as possible after the end of the month editorial work must necessarily be limited. Also, since this is an informal progress report, the results and data presented should be understood to be preliminary and subject to change unless otherwise stated.

The issuance of these reports is not intended to constitute publication in any sense of the word. Final results either will be submitted for publication in regular professional journals or will be published in the form of ANL topical reports.

The last six reports issued in this series are:

September 1967	ANL-7382
October 1967	ANL-7391
November 1967	ANL-7399
December 1967	ANL-7403
January 1968	ANL-7419
February 1968	ANL-7427

REACTOR DEVELOPMENT PROGRAM

Highlights of Project Activities for March 1968

EBR-II

The reactor was operated for 293 MWdt in Runs 27B and 27C during March. Each run was terminated after the detection of an increase in fission gas activity in the primary cover gas. Two previously suspected experimental subassemblies had been reinserted in the reactor for these runs: XG05 was present during Run 27B, and XA08 during Run 27C. A positive identification of the source(s) of the fission gas has not yet been made. The cumulated total of EBR-II operation is 16,117 MWdt.

Normal production was resumed in the FCF hot line and the cold line following the adoption of a larger acceptance limit for the diameter of the lower ends of the fuel-element jackets. The new, conservatively chosen limit allows most of the elements to pass inspection despite a small amount of deformation from impact bonding. Studies are being made to evaluate methods for reducing the deformation and to define precisely the limit at which the deformation becomes harmful.

ZPR-3

In a continuation of experiments on Assembly 51, measurements were made of the worths of depleted uranium, U_3O_8, Pu, Na, Ta, and B_4C in various positions. A fuel-compaction experiment was performed by moving a section of fissile and fertile material axially from the core-reflector boundary toward the center of the core, displacing sodium.

ZPPR

Full-load deflection testing of the bed and tables was completed satisfactorily. After the reactor knees were installed, a full complement of matrix tubes was loaded and reloaded in an effort to develop a clamping procedure that would minimize tube deflection.

The backup containment structure was leak tested satisfactorily following replacement of uncertified filters.

AARR

Thermal analyses of the reflector shroud and pedestal continued. New steady-state temperature calculations indicate that the highest temperature, 259°F, occurs in the upper support ring.

Confirmation testing of the beam-tube reflector liner indicates no appreciable leakage past the liner.

Underwater life-cycle tests of the hydraulic-rabbit loading station have been terminated after successfully completing 13,000 cycles, equivalent to an estimated 5-yr operating period.

Load and deflection tests were made on the blind beam tubes.

Vibration problems in the preliminary flow tests of the ITC prototype were traced to a temporary flat-plate orifice that was not a part of the prototype. When the plate was removed, the vibration ceased.

TABLE OF CONTENTS

TABLE OF CONTENTS

TABLE OF CONTENTS

I. PLUTONIUM UTILIZATION--CIVILIAN--EBWR

A. Research and Development

1. Operational Consultation and Support

a. Materials Surveillance (N. Balai)

Last Reported: ANL-7371, p. 1 (Aug 1967).

(i) Postirradiation Vessel Surveillance. After the remotely controlled 240 ft-lb Riehle impact-test machine was refurbished, measurements of irradiation effects on the impact strength of the EBWR pressure-vessel SA212B steel, rounded-corner, Charpy vee-notch specimens were started. Before a reasonable calibration with Watertown Arsenal standardization specimens could be achieved, the testing machine's hammer bearing was replaced, the anvil faces were machined, and the machine was removed from its dolly and bolted to the floor (it had been mounted on a wheeled carriage so it could be moved into and from the caves). The machine is still slightly out of calibration at the higher energies, as is shown in Table I.A.1, but is satisfactory for use at the lower energies required for the fracture of SA212B steel.

TABLE I.A.1. Calibration of Impact-test Machine at Room Temperature

Watertown Arsenal Charpy Impact Standard Identity			Test-machine Results (ft-lb)	
Series	Impact Strength (ft-lb)	Specimen No.	Wheeled-dolly Mounting	Fixed Mounting (Bolted and Grouted)
I-3	14.5 ± 1	868	17.0[a]	
		004	16.5[a]	
		244	16.0[b]	
		776	15.0[b]	
		872	15.5[b]	
		184		14.0[b]
		343		15.2[b]
		307		14.3[b]
		410		16.2[b]
		377		14.3[b]
H-5	50.1 ± 2.5	056	50.8[a]	
		667	49.9[a]	
		465	52.6[a]	
		656	45.2[a]	
		431	49.8[a]	
		796		50.6[b]
		615		50.4[b]
		825		52.0[b]
		163		45.0[b]
		103		49.1[b]
G-4	84.4 ± 4.2	966	93.5[a]	
		449	96.6[a]	
		222	89.2[b]	
		898	100.0[b]	
		173	102.0[b]	
		145		93.0[b]
		215		86.2[b]
		392		97.0[b]
		769		91.0[b]

[a]120 ft-lb max hammer.
[b]240 ft-lb max hammer.

Capsule 4 was examined first; it contained 15 rounded-corner, Charpy vee-notch control specimens for determining the temperature effects during the residence period for the five capsules. During the residence time, approximately 4800 hr at an average power of 44 MW, this capsule lost its helium-gas charge (500-psi fill pressure). Although several drops of water were found when the stainless steel container was opened and the impact specimens were coated with a dark oxide, no thermal effects were found when the impact transition curve for the specimens was compared with curves obtained previously. However, preliminary results from bars in Capsule 5 (a "bare" tube irradiation) indicate substantial irradiation embrittlement during the 4800 hr of exposure. The source strength of each of these bars is about 4 R/hr at a distance of 3 in.

(a) Cracks in the Cladding. It was reported previously* that the cladding cracked more severely in the 2-in.-thick "practice" plate and that the mechanism differed from that for the EBWR vessel cladding. A review of the mill test reports for the cladding materials reveals that the cladding used for the 1959 practice plate was significantly hardened by cold work at the mill before delivery to the fabricator. This stainless cladding was then resistance-welded to the SA212B backing plate to produce the practice plate that was used at the Laboratory to pretest the welding procedures used in uprating the EBWR to the 100 MW capability of 1960. The multiple effects of cold rolling of cladding, forming of the clad plate to the 84-in.-dia circular segment, and of subsequent stress relief resulted in the severe sensitization of the stainless steel as shown by Fig. 10 of ANL-7117. The earlier deductions concerning the cladding failure mechanisms, namely, thermal-stress ruptures, are supported by the data abstracted from the mill test reports. Table I.A.2 summarizes the finish, hardness, and related data for the two heats of cladding.

TABLE I.A.2. Summary of Mill Test Report Data for EBWR Vessel and for Practice-plate Cladding Material

Heat No.	Mill Invoice Date	Hardness (R_B)	Specification, Grade, Finish
EBWR-vessel cladding from Allegheny-Ludlum			
334053	5/19/55	75-77	Allegheny Metal 18-8-S, Type 304, No. 1 finish (ferrite/austenite = 1.50[a])
Practice-plate cladding from Republic			
H-26800	10/23/57	82	SA240, Gr. S, Enduro 18-8-S, Type 304 CR Sheets, No. 4 finish, one side polished (ferrite/austenite = 1.625[a])

[a]Calculated from the compositions and the relations given by the Schaeffer diagram.

*Balai, N., Sutton, C. R., Wimunc, E. A., and Jones, R. F., Inspection, Evaluation, and Operation of the EBWR Reactor Vessel, ANL-7117 (Nov 1965).

II. LIQUID-METAL FAST BREEDER REACTORS--CIVILIAN

A. Fuel Development--LMFBR

1. Metallic

a. Fuel Element Performance (W. F. Murphy)

Last Reported: ANL-7427, pp. 1-2 (Feb 1968).

Two metallic fuel elements are being irradiated in EBR-II Subassembly XG05. This subassembly has been moved to the storage rack while attempting to locate a leaking fuel element or capsule. It is scheduled for reinsertion if it is determined that the leak is not in this subassembly.

Revised data indicate that the two metallic fuel elements (U-15 w/o Pu-10 w/o Zr and U-15 w/o Pu-10 w/o Ti, both clad in V-20 w/o Ti) in Subassembly XG05 had accumulated 92% of the scheduled exposure. The estimated burnup for these two fuel elements is 6.9 a/o.

Fifteen U-15 w/o Pu-10 w/o Zr fuel elements (Group M-3) have accumulated ~0.6 a/o burnup in EBR-II. The primary objectives and design and operating parameters of these elements have been given previously (see Progress Report for December 1967, ANL-7403, pp. 3-5).

The fuel elements for the M-4 irradiation experiment have been reassembled, and are being bonded and inspected. The M-4 experiment will investigate the irradiation of U-15 w/o Pu-12 w/o Zr fuel alloy at 14 kW/ft in stainless steel and vanadium alloy claddings.

(i) Studies of Cladding-Fuel Interaction (D. W. Walker)

Additional work with fuel elements irradiated in Subassembly XA07 has been done to determine the degree of interaction between the U-15 w/o Pu-9 w/o Zr alloy fuel and the cladding materials (see Progress Report for November 1967, ANL-7399, pp. 1-4). The samples studied were sections of Type 316 stainless steel and Hastelloy-X claddings that had been irradiated to 4.9 a/o burnup at a maximum cladding temperature of 615°C. Evaluation of the cladding-core reaction was performed by metallographic examination and by microprobe analysis. The samples were small transverse sections that had been cleaned carefully to remove any trace of fuel alloy. Control samples of unirradiated tubing that had been heat-treated at 600°C for 96 hr were also prepared for comparison.

Metallographic examination indicated that the stainless steel cladding had reacted with the U-Pu-Zr fuel; a reaction zone of approximately 32-μ thickness had formed. In addition, carbide precipitate was found

in the grain boundaries, and a fine particulate phase had formed within the grains. The control sample also showed that carbide precipitate formed, and the grain size was essentially identical with that of the irradiated material. However, no fine particulate phase was distributed within the grains.

A microprobe analysis was made on the irradiated stainless steel sample; a reaction zone 25 μ wide was investigated. The analysis consisted of (1) X-ray spectral profiles to detect the presence of carbon, oxygen, and nitrogen, as well as all elements above atomic number 11; and (2) mechanical scans that show the linear distribution of all elements detected.

The results of the mechanical scans, summarized in Fig. II.A.1, were similar to those obtained with Type 304L stainless steel irradiated in contact with U-Pu-Zr fuel (see ANL-7399, p. 3). A major difference, however, was the presence of significant amounts of plutonium and uranium in the reaction layer of the sample examined in the present study; maximum buildup occurred approximately 5 μ from the interface. In order to determine if the plutonium and uranium present at the fuel-cladding interface were in the form of a ceramic compound, the characteristic X-ray line of oxygen was sought in the plutonium-rich layer. A high concentration of oxygen was associated with this layer, which suggested that plutonium and uranium were present as $(U,Pu)O_2$ in a concentration of approximately 70 w/o Pu and 20 w/o U.

An extensive reaction zone extended approximately 152 μ into the cladding of the irradiated Hastelloy-X sample. This zone appeared brittle, as indicated by a number of cracks observed. The grain structure of the unreacted portion of the sample was not revealed. The structure of the Hastelloy-X control sample appeared normal, but had a large grain size. A microprobe analysis will be performed on the irradiated sample.

2. Oxide

a. Fuel Element Performance (F. L. Brown)

Last Reported: ANL-7427, p. 2 (Feb 1968).

Four fuel elements irradiated in experimental Subassembly XO11 to burnups of approximately 3.5 a/o are being destructively examined. A fifth element (SOV-3) still in its irradiation capsule will be returned to Idaho and reinserted in EBR-II to complete the target burnup of 5 a/o (element SOV-1 will be reinserted also). Element SOV-7, also irradiated in Subassembly XO11, is to be returned from EBR-II for examination in place of SOV-3. Design parameters and irradiation conditions for the seven elements originally in Subassembly XO11 were reported previously (see Progress Report for September 1967, ANL-7382, Table II.D.1, p. 73).

Two of the elements being examined (HOV-4 and HOV-10) had failed during irradiation. The bond sodium had leaked out of HOV-4, which

caused severe overheating of this element. Transverse sections were made through the capsule (containing HOV-4) at quarter-points along the length of the fuel column. Examination of the as-sectioned surfaces confirmed that the cladding was in intimate contact with the capsule. Also, the melting

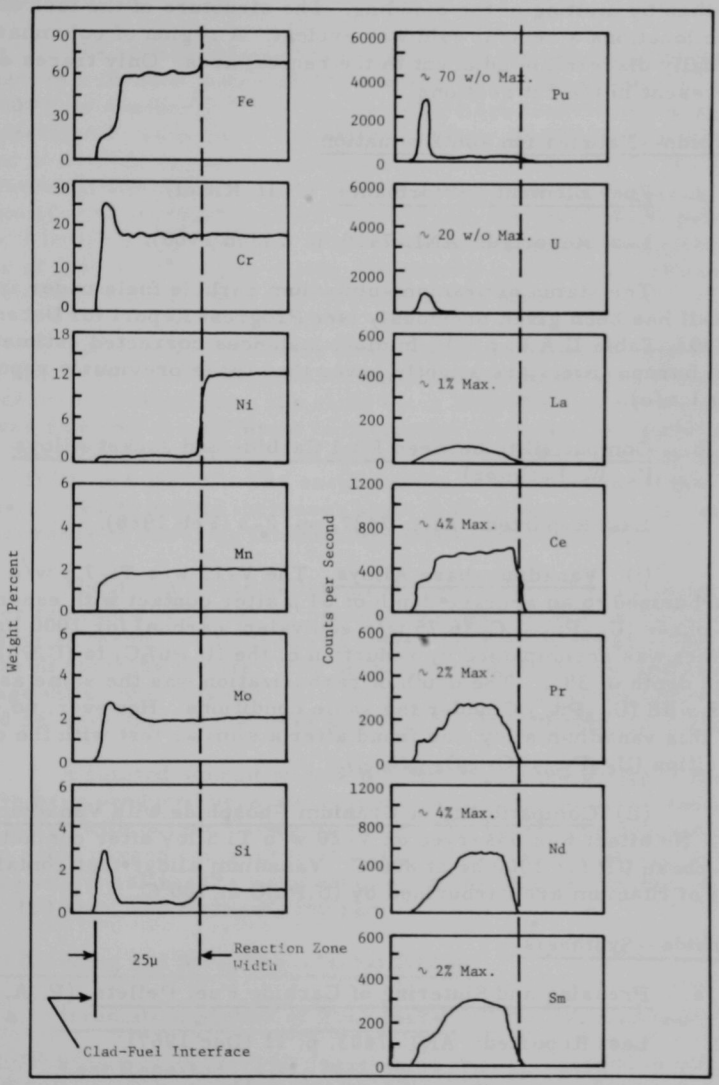

Fig. II.A.1. Typical Distribution of Elements in Surface Layer in Irradiated Type 316 Stainless Steel Cladding (U-Pu-Zr fuel)

point (1290°C) of the cladding had been exceeded, at least along the lower half of the fuel column. The cladding along the upper half of the fuel column was in slightly better condition; temperatures had been lower, and failure evidently was propagated by longitudinal and transverse cracking rather than by melting of the cladding. The structure of the fuel varied; in some locations a central void was evident. A region of columnar grains was usually discernible adjacent to the central area. Only traces of sodium were present in the cut sections.

3. Carbide--Fabrication and Evaluation

a. Fuel Element Performance (J. H. Kittel)

Last Reported: ANL-7419, p. 2 (Jan 1968).

The status of uranium-plutonium carbide fuels under irradiation in EBR-II has been given previously (see Progress Report for December 1967, ANL-7403, Table II.A.4, p. 9). In most instances corrected estimates of the current burnup levels are slightly lower than those previously reported (by about 0.1 a/o).

b. Compatibility between Fuel Carbide and Jacket Alloys (T. W. Latimer)

Last Reported: ANL-7427, pp. 2-3 (Feb 1968).

(i) Vanadium-base Alloys. The V-15 w/o Ti-7.5 w/o Cr alloy was carburized to an average depth of 64 μ after contact with essentially single-phase $(U_{0.8}Pu_{0.2})_2C_3$ (6.75 w/o equivalent carbon) for 1000 hr at 800°C. The effect was accompanied by reduction of the $(U,Pu)_2C_3$ to (U,Pu)C to an average depth of 38 μ. The depth of carburization was the same as that found in tests with $(U_{0.8}Pu_{0.2})C$ under the same conditions. However, no carburization of this vanadium alloy was found after a similar test with the oxycarbide composition $(U_{0.8}Pu_{0.2})(C_{0.62}O_{0.38}N_{0.01})$.

(ii) Compatibility of Uranium Phosphide with Vanadium-base Alloys. No effect was observed on V-20 w/o Ti alloy after contact with single-phase UP for 1000 hr at 800°C. Vanadium alloys that contain this amount of titanium are carburized by (U,Pu)C at 700°C.

4. Carbide--Synthesis

a. Pressing and Sintering of Carbide Fuel Pellets (P. A. Nelson)

Last Reported: ANL-7403, p. 11 (Dec 1967).

High-purity UC and (U-15 w/o Pu)C powders prepared by the metal-methane reaction (see Progress Report for February 1968, ANL-7427, pp. 4-5) are being pressed and sintered into pellets suitable for irradiation

testing. The pellets are pressed at 75,000 psi in a double-acting hydraulic press. Green (unsintered) densities of the UC and (U,Pu)C pellets are 7.4 ± 0.1 and 8.0 ± 0.1 g/cc, respectively. The required density of sintered carbide pellets is 85 ± 3% of theoretical, and the specification for diameter is 0.255 ± 0.001 in.

The current procedure for sintering the pellets involves degassing them in a furnace heated with a graphite resistance heater at 10^{-5} Torr until 1000°C is reached (~1/2 hr). The pellets are then heated to the sintering temperature. To achieve the desired density, the (U,Pu)C pellets are sintered at 2115°C, and the UC pellets are sintered at 1725°C. The sintering temperature is reached about one hour from the time the degassing operation commences, and is maintained for 30 to 40 min for the (U,Pu)C pellets and for 2 to 3 hr for the UC pellets. The furnace atmosphere is maintained at 15 Torr of high-purity argon during the sintering operation. The furnace is subsequently cooled to room temperature in one hour.

The effect of sintering temperature on pellet density was investigated in a series of sintering experiments. Several batches of about ten pellets each were pressed from the same batch of (U,Pu)C powder, and each batch was sintered at a different temperature. Five batches sintered at 2115°C had a density of 85 ± 1% of theoretical. Pellets were also sintered at 1800, 1900, and 2215°C. The results of these tests indicated that the density of (U,Pu)C pellets increases about 2.5% of theoretical for each 100°C increase in sintering temperature from 1800 to 2215°C.

About half of the pellets produced at 2115°C do not meet the diameter tolerance of ±0.001 in. because of slight distortion due to shrinkage during sintering. A centerless grinder is being installed to reduce the diameter of oversize pellets. The percentages of diametral and axial shrinkage differ only slightly. At 2115°C the (U,Pu)C pellets undergo 12.0 ± 0.5% shrinkage in diameter and 10.7 ± 0.5% shrinkage in length.

A limited amount of data is available on the purity of the pellets that have been produced because, in many cases, the powders used have been contaminated with oxygen during handling. In a recent run precautions were taken to avoid oxygen contamination of the (U,Pu)C feed material and the following analytical results were obtained on the pellets: carbon, 4.99 w/o; oxygen, 150 ppm; and nitrogen, 300 ppm.

5. Fuel Cladding and Structure--Jacket Alloys

a. Irradiation Studies of Fuel Jacket Alloys (R. Carlander)

Last Reported: ANL-7427, pp. 6-7 (Feb 1968).

In previous experiments (see Progress Reports for May 1967, ANL-7342, pp. 75-77, and August 1967, ANL-7371, pp. 80-83), V-20 w/o Ti alloy (heat treated for 1 hr at 900°C) was irradiated to a nominal fluence of

5×10^{21} at 600 ± 100°C. The postirradiation tensile tests showed a maximum increase in yield strength of approximately 43% at a test temperature of 550°C. Moreover, the uniform elongation of the irradiated specimens decreased from approximately 18 to 12% at the same test temperature. Additional tensile tests at 400 and 650°C (see Progress Report for December 1967, ANL-7403, pp. 11-13) revealed that the yield strength of the irradiated alloy was about the same as that at 550°C. The uniform elongations at 400 and 650°C, however, were higher than that at 550°C.

Two series of tensile tests were made with V-20 w/o Ti alloy: (1) Specimens irradiated to a nominal fluence of 5×10^{21} at 600 ± 100°C were tested at 750°C to determine if the observed changes in strength (due to irradiation) persisted over the postirradiation-test-temperature range of 400 to 750°C. (2) Specimens irradiated to a nominal fluence of 3×10^{22} at a calculated irradiation temperature of 580°C were tested at 550 and 650°C to determine the effect of higher fluence levels on postirradiation tensile strength. The tensile tests were conducted at a constant crosshead speed of 0.05 cm/min with a gauge length of 2.5 cm.

The results from tests on the irradiated specimens were compared with results from tests conducted on unirradiated specimens at approximately the same test temperature, 400, 600, and 800°C (see Progress Report for October 1967, ANL-7391, pp. 9-12). The comparison is presented in Fig. II.A.2.

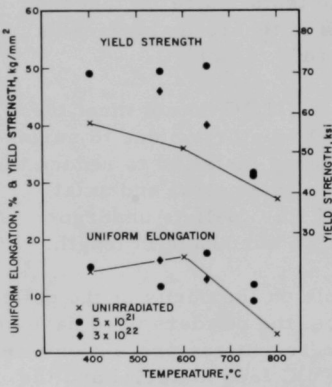

Fig. II.A.2

Effect of Irradiation of the Yield Strength and Uniform Elongation of V-20 w/o Ti as a Function of Test Temperature

The postirradiation yield strength of the specimens irradiated at both fluence levels decreased as the temperature was increased from 400 to 750°C. The difference between the irradiated and unirradiated yield strengths at ~750°C was small because recovery probably occurred at this test temperature. The uniform elongation of specimens irradiated to 5×10^{21} and 3×10^{22} over the test temperature range of 400 to 750°C was similar to that of the unirradiated alloy (except for the 550°C test of the specimen irradiated to 5×10^{21}).

The results of the tensile tests indicate that (1) irradiation up to a nominal fluence of 3×10^{22} does not appear to affect the ductility of V-20 w/o Ti alloy over the postirradiation-temperature range of 400 to 750°C, and (2) although strengthening occurs as a result of irradiation, the original strength of the alloy may be recovered by postirradiation annealing at a temperature around 750°C.

B. Physics Development--LMFBR

1. Theoretical Reactor Physics--Fast Critical Experiments--Theoretical Support (F. W. Thalgott, R. B. Nicholson, and R. G. Palmer)

Last Reported: ANL-7427, pp. 9-10 (Feb 1968).

a. Updated Safety Analysis of ZPR-3. The safety analysis of ZPR-3 has been updated to include plutonium loadings in the Fast Test Reactor (FTR) format up to 800 kg of plutonium. A parametric survey of a startup accident has shown that, even assuming pessimistic values for the feedback coefficients, the circuit delay times, and the reactivity ramp rates, the excursions were terminated by scram action before core-damaging temperatures were reached in the most concentrated fuel, i.e., the ZPR-3 plutonium metal plates. The temperature rises in the Pu-U alloy plates were lower by a factor of about three. The assumptions in the accident were a gross core overloading, a complete failure of the period trips, and scram action being initiated by the power-level trips.

b. Modifications to RABID. An improved method of evaluating sums of exponential integrals of the form

$$S = \sum_{k=0}^{\infty} E_n(z+kh)$$

$$= \int_1^{\infty} \frac{e^{-zt}}{(1-e^{-ht})} \frac{dt}{t^n}$$

$$\cong \sum_{i=1}^{M} w_i e^{-zt_i}$$

by Gaussian quadrature (rather than by adding the first few terms and extrapolating geometrically to infinitely many terms) has led to speed increases of up to 50% for RABID. Numerical accuracy is also improved. The quadrature weights w_i and nodes t_i were computed for n = 0 (1) 10 and for M = 2 (1) 10. Accuracy sufficient for use in RABID was obtained by using M = 4.

An N-region problem requires a running time proportional to N for RABBLE, and to N^2 for RABID, with RABID being quicker for small N. Also, accurate results are obtained from RABID with a smaller N than required in RABBLE. Consequently RABID may be best used for a few "benchmark" calculations when dealing with very complicated cells.

2. Experimental Reactor Physics--Fast Critical Experiments--Experimental Support (Idaho) (W. G. Davey)

Last Reported: ANL-7427, pp. 10-12 (Feb 1968).

a. Neutron Spectrometry

(i) High-count-rate Electronics. Work has been initiated toward integration of a pole-zero compensated preamp and linear amplifier into the present pulse-shape discrimination system. Preamplifier power cables were run from the Argonne Fast Source Reactor (AFSR) and ZPR-3 to the spectrometer laboratory. Preamplifiers were mounted in two ZPR-3 drawers. This equipment will be installed in AFSR, and count-rate tests will be performed. Several different neutron spectra will be studied to check the overlap of the proton-recoil spectra. These data will give the information needed to complete the optimum preamplifier design.

(ii) Computer Software. Work has started on streamlining the present proton-recoil software package. The present computer program is very detailed and lengthy. The final product of this effort will be a more compact program in assembly language. This will facilitate future measurements of neutron spectra in a more standardized manner.

b. Heterogeneity Studies. The analysis of the exposure of ^{238}U foils in AFSR is almost complete. Several gamma-ray peaks appear to be suitable for foil-activation measurements.

The intensity ratios of the gamma-ray peaks in two fission product mass chains were found to be quite constant, which indicates that the activations are being interpreted correctly. Gamma-ray peaks from ^{97m}Nb-^{97}Nb, with a half-life of 17 hr, had nearly the same intensity ratio over a period of 50 hr. Several gamma-ray peaks from ^{132}I, with an effective half-life of 78 hr, were found to have essentially constant intensity ratios for a period of several days. Other possibilities are ^{134}I, ^{135}I, ^{105}Ru, ^{138}Cs, and ^{91}Sr-^{91m}Y. There is considerable scatter in the gamma-ray peak-intensity ratios for these isotopes from the ^{238}U exposure, but the better resolution of our new electronics may improve this condition in subsequent runs.

A ^{239}Pu exposure in AFSR has been completed, but the data have not yet been analyzed. Preliminary evaluation does indicate, however, that another exposure will be needed, preferably with a thin foil instead of the 30-mil sample used. Procurement of suitable thin foils has been initiated.

An exposure of a ^{235}U foil in ZPR-3 is now in progress. This will permit the evaluation of the count rates and the necessary exposures

for foils in ZPPR. In addition, it will provide some indication of the counting times that will be needed to obtain the required statistical accuracy.

c. Computer Applications. The Request for Proposals for the ZPPR Computer System has been modified to incorporate final comments from the Reactor Physics Division and is ready to be issued to computer vendors.

The Justification Document has been revised to incorporate the most recent data from other areas of reactor equipment development on ZPPR.

The ZPPR fuel inventory procedures and the application of automation to these have been investigated. A standard logging form from which IBM cards can easily be punched has been designed. A CDC-1604 program for building and updating a fuel-inventory master tape is in preliminary stages, and should be operational before fuel arrives for storage in the ZPPR vault.

A computer program for recording ZPPR core-loading information is in its formative stage. This program will produce a magnetic tape for each loading, containing all information including descriptions of drawer masters, fuel-plate identification, and drawer position. This information will be in such form that atomic densities, plutonium mass, and other pertinent parameters can be obtained from the computer. These programs will be designed so that the logic will be compatible with the ZPPR Computer System.

Bids have been received on the interim data-recording system. Low bidders have been contacted for clarification of technical details prior to issuance of a purchase order.

3. Experimental Reactor Physics--Fast Critical Experiments--Experimental Support (Argonne)

a. Basic Reactor Data (R. Gold)

Last Reported: ANL-7391, p. 120 (Oct 1967).

(i) Absolute Measurements of Fission Neutron Yield. The process of neutron generation in a reactor is related to either of two combined parameters, $\nu\sigma_f$ or $\eta\sigma_a$, specifying the neutron yield per absorption in fissionable material. Neither of these pairs yields sufficient information because of structural effects, but each is a basis of calculational procedures. At present there are greater inconsistencies in reported data for both ν and σ_f than for both η and σ_a.

Although relationships between the neutron yield per fission, ν, and other nuclear data have long been recognized, desire for high precision has become more significant due to the strong influence of ν in various methods of in-core determination of breeding ratios for advanced reactors. Furthermore, the foundation underlying all ν values are the absolute measurements, mainly those of ^{235}U and ^{252}Cf.

From a recent study* of current values of the fundamental fission parameters, underlying characteristics of the various measurements of neutron yield have been isolated and examined for susceptibility to systematic error. One may classify these experiments into two categories, gated and nongated, with variations in each group. Certain weaknesses of each method can be distinguished, and efforts made to evaluate or remedy the possible sources of error are examined. New published and unpublished data on $\nu(^{235}U)$ and $\nu(^{252}Cf)$ can be brought into the picture. An evaluation has been made of the prospects for improvements based on new techniques in neutron detection, particularly with the manganese bath. There have also been a number of additional improvements in neutron detection which are applicable to evaluation of neutron yields. Both British** and American† groups are pursuing better data and better agreement. Because the yields may be determined by two widely different experimental methods, and because ^{252}Cf can be established as a convenient reference standard, it is likely that 0.33% accuracy is eventually attainable in ν.

4. ZPR-3 Operations and Analysis (W. G. Davey and R. L. McVean)

Last Reported: ANL-7427, p. 12 (Feb 1968).

a. Mockup Studies. Experiments with Assembly 51, the first core of the FTR Phase-B critical experiments, continued. The following measurements were made:

(1) the worths of depleted uranium metal, U_3O_8, and sodium by material replacement in half of the core drawers; these drawers were distributed over the entire core;

(2) the worth of substituting sodium for the core materials and axial-reflector materials in the P-16 matrix position of both halves;

*De Volpi, A., Current Values of Fundamental Fission Parameters, Reactor and Fuel Processing Technology 10(4), 271-288 (Fall 1966).

**Colvin, D. W., Sowerby, M. G., and McDonald, R. I., Confirmatory Experimental Data on the Harwell Boron Pile $\bar{\nu}$ Values, Proc. Conf. Nuclear Data, Paris, October 1966 (IAEA, Vienna, 1967), Vol. I, p. 307.

†De Volpi, A., and Porges, K. G., Direct and Absolute Measurements of Average Fission Neutron Yield from ^{235}U and ^{252}Cf, ibid., p. 297.

(3) the worth of sodium by removing sodium from the normal core composition in a central zone in both halves of the reactor; both axial and radial reactivity worths of the sodium were determined;

(4) the worth of a 7-in.-long region of normal core composition, as a function of axial position, as it is moved within a column of sodium occupying the P-16 matrix position in both halves;

(5) the worth of compacting the fuel by moving the fissile and fertile material at one core-axial reflector boundary in the P-16 matrix position toward the center of the core, displacing sodium;

(6) the central worths of tantalum and enriched B_4C in the P-16 matrix position;

(7) the worths of depleted uranium metal, U_3O_8, and plutonium in the P-16 matrix position.

(i) Distributed Sodium Worth. In this experiment, the reactivity effect of removing one 17-in. column of sodium from A-type drawers was measured. The column removed was the interior column of the two in the A-type drawers. Reactivity measurements were taken with 24, 42, and 112 drawers perturbed. The reactor loading was the reference geometry containing 112 A-type drawers of which two are control drawers. Stainless steel frames were placed in the vacated sodium positions.

Tables II.B.1 and II.B.2 summarize the material changes in each A-type drawer and the experimental results for each step:

TABLE II.B.1. Composition Change for Distributed Sodium Worth Experiment

Drawer	Material Removed per Drawer		Stainless Steel Added per Drawer (g)	Stainless Steel Change (g)
	Sodium (g)	Stainless Steel (g)		
A	103.09	157.79	161.22	+3.43
Control	100.71	157.94	151.37	-6.57

TABLE II.B.2. Experimental Results for Distributed Sodium Worths

Total No. of Drawers	Perturbed Drawers in Each Half	Sodium Removed (g)	Stainless Increase (g)	Reactivity (Ih)	Reactivity Change (Ih)
0	None	0	0	+41.588	0
24	K-18, L-18, M-18, N-18, O-18, P-18, L-20, M-20, N-20, O-20, P-20, P-22	2474.42	82.32	-10.346	-51.934
42	Above, plus Q-18, R-18, S-18, T-18, U-18, Q-20, R-20, S-20, T-20	4329.78	144.06	-47.193	-88.781
112	Above, plus the remaining A-type drawers including two control drawers	11541.32	364.16	-160.03	-201.618

(ii) Worth of Sodium in Position P-16. The reactivity loss which occurred when all the drawer contents in the P-16 matrix location, in both core and axial reflector, were removed and replaced with sodium contained in stainless steel cans was measured. Excluding drawer ends and spring gaps, the sodium occupied 58 in. in the P-16 matrix location. The reactor loading was the reference geometry except for P-16, which initially contained the normal loading of fuel with the stainless steel split into two half-high columns (i.e., the same reference as in the uranium and plutonium removal experiment).

As mentioned previously, the loss of material is the total contents of the core and reflector drawers excluding changes in material associated with the drawers or spring gaps. The sodium and associated stainless steel added are summarized in Table II.B.3 and are distinguished by region to facilitate calculations.

TABLE II.B.3. Composition of P-16 Matrix Position with Sodium Substituted

	Half One		Half Two		
	Reflector (g)	Core (g)	Core (g)	Reflector (g)	Total (g)
Na	580.2	830.0	829.9	579.9	2820.0
SS	863.2	1255.2	1255.7	856.4	4230.5

The reactivity decreased from +41.19 to -721.89 Ih, making the reactivity worth of the interchange -763.08 Ih.

(iii) Radial and Axial Worth of Sodium. In this series of measurements, sodium cans were removed from selected positions within drawers to determine the axial dependence of sodium reactivity worth. A measure of the radial dependence was obtained by removing sodium from the same drawer positions in an increasing number of drawers. Each time sodium was removed, the vacated positions were filled with stainless steel frames which simulate empty sodium cans. The material change is primarily the loss of sodium from the perturbed drawers with a small correction for the stainless steel change. Except for the perturbed drawers, the reactor loading was the reference geometry.

(a) Axial Sodium Worth. The perturbed region was a central 9-drawer array in both halves (i.e., 18 drawers) in which the sodium was removed from the drawers in three different (axial) lengths, 0 to 7 in., 7 to 17 in., and 0 to 17 in., the zero position being the reactor midplane. The material changes and reactivity worths associated with each step are summarized in Table II.B.4.

TABLE II.B.4. Sodium Worths

Axial Location of the Perturbation	Number of Drawers Perturbed[a]		Material Removed (g)		Stainless Steel Added (g)	Reactivity (Ih)	Reactivity Change (Ih)
	Type A	Type A*	Sodium	Stainless Steel			
None	0	0	0	0	0	39.937	0
0 to 7 in.	6		519.0	795.72	795.3	49.049	+9.112
		12	519.0	795.72	795.3		
0 to 17 in.	6		1237.08	1893.48	1934.6	21.309	-18.628
		12	1237.08	1893.48	1934.6		
7 to 17 in.	6		718.08	1097.76	1139.39	15.051	-24.886
		12	718.08	1097.76	1139.39		
0 to 7 in.	22		1903.0	2917.64	2916.10	50.303	+10.366
		20	865.0	1326.20	1325.50		

[a]A--Drawers in even-numbered matrix columns; A*--Drawers in odd-numbered matrix columns.

(b) Radial Sodium Worth. The perturbed region from which the sodium was removed was 0 to 7 in. in the axial direction as measured from the midplane. Measurements were made for a central 9-drawer array in both halves and for a central 21-drawer array in both halves. The material changes and the reactivity associated with each step are summarized in Table II.B.4.

(iv) Fuel Compaction. The effect of fuel compaction was measured by moving a 5-in. section of plutonium metal, depleted uranium, and ZPPR fuel from the 12- to 17-in. axial position in Drawer 1-P-16 to the 0- to 5-in. axial position, displacing sodium which was moved to fill the vacated position.

The experiment involved a spatial rearrangement of material with no net change in quantity, and was done in one drawer, 1-P-16, in Half I. Table II.B.5 summarizes the material that was moved in the drawer.

TABLE II.B.5. Fuel Compaction Experiment

Material (Piece Length, in.)	^{239}Pu (g)	^{240}Pu (g)	^{241}Pu (g)	^{242}Pu (g)	^{238}U (g)	^{235}U (g)	Na (g)	Stainless Steel (g)	Al (g)
ZPPR Fuel (5)	136.79	18.23	2.36	0.21	380.54	0.84		52.318	
Pu Metal (3)	99.085	4.746	0.459	0.0063				24.659	1.16
(2)	65.620	3.141	0.2692	0.00055				16.789	0.77
Depleted U (3)					223.29	0.46			
(2)					147.86	0.31			
Total Compacted	301.495	26.117	3.0882	0.21685	751.69	1.61		93.766	1.93
Sodium Transferred, Two 5-in. Cans							59.84	91.48	

The worth of the compaction was measured twice, and the average increase in reactivity was +125.39 Ih.

The reactor loading was one drawer less than the reference geometry. The worth of this one drawer, 2-0-10, has been measured to be 95.68 Ih.

(v) Worths of B_4C and Tantalum. The relative worths of B_4C and tantalum were measured in the P-16 matrix location. The test region in the P-16 matrix location was 1/2 by 2 by 36 in., excluding drawer ends. During the reference measurement, the test region was approximately half filled with stainless steel. When the test region was occupied alternately by tantalum and B_4C, the stainless steel was rearranged in the drawers so there was no net change in material other than B_4C and tantalum.

Table II.B.6 gives the material changes and the experimental results. The reference geometry was the reactor loading.

TABLE II.B.6. B_4C and Tantalum Worths

	Test Region	Excess Reactivity of Core (Ih)	Reactivity Change Relative to Void (Ih)
Reference:	Contained half-height stainless steel which was rearranged for measurements	-740	0
Ta:	9432 g of Ta consisting of 72 pieces, 1/8 x 2 x 2 in.	-1313	-573
B_4C:	1262.2 g of natural B_4C consisting of 96 pieces, 1/4 x 1/2 x 3 in. ^{10}B = 13.67 w/o; ^{11}B = 63.31 w/o; C = 23.02 w/o.	-1646	-905

(vi) Worth of Uranium and Plutonium in Position P-16. The worth of uranium and plutonium was measured in the P-16 matrix position. In the reference geometry, the loading of this position included two half-height stainless steel columns in the 1/8-in.-wide stainless steel location. In the worth measurement, one of the half-height columns was placed in the U_3O_8 position and empty sodium cans (8, 2, and 7 in. in length) were placed in the ZPPR-fuel and Pu + ^{238}U positions. The net material change consisted of (a) a loss of all the depleted uranium metal, U_3O_8, plutonium metal, ZPPR fuel, and the stainless steel associated with the plutonium metal and ZPPR fuel cans, and (b) a gain in the stainless steel contained in the empty sodium cans. This change was made in the core drawers in both halves of the P-16 matrix location. The reactor loading was the reference geometry.

Table II.B.7 summarizes the material changes and the measured reactivities. The net worth of this change was -752.47 Ih.

TABLE II.B.7. Uranium and Plutonium Worth Experiment

	^{239}Pu + ^{241}Pu (g)	^{240}Pu + ^{242}Pu (g)	^{235}U (g)	^{238}U (g)	Mo (g)	O (g)	Stainless Steel[a] (g)	Excess Reactivity (Ih)
Reference Case (Material to be removed)	2076.34	179.56	12.83	5978.0	94.48	150.86	627.75	+41.586
Perturbed Case (Material added)	0	0	0	0	0	0	650.24	-710.88

[a]Stainless Steel Analysis: 73.4% Fe, 17% Cr, 8.4% Ni, 0.75% Mn, and 0.45% Si by weight.

b. Doppler Experiments. Measurements of the Doppler effect in uranium were initiated during this reporting period and are continuing.

5. ZPR-6 and -9 Operations and Analysis

a. Integral Studies of Large Systems (W. Y. Kato)

Last Reported: ANL-7427, pp. 12-16 (Feb 1968).

(i) ZPR-6. The central reactivity worths of various 2 x 2 x 1-in. samples were measured in the 4000-liter oxide core, Assembly 6 of ZPR-6. These samples were measured by the period method relative to void. A reference run (void) was made before and after each measurement of the sample worth. Table II.B.8 shows the results. The uncertainties in the measured values are based on the differences in the "before and after" reference runs and on the propagation of errors.

TABLE II.B.8. Central Reactivity Worths in Assembly 6 of ZPR-6

Sample	Wt of Sample (g)	Can[a] Type	Can Wt (g)	Gross Sample Worth (Ih)	Net Sample Worth (Ih)	Specific Sample Worth (Ih/kg)
Inconel X	507.0	Bare	-	-0.785 ± 0.018	-0.785 ± 0.013	-1.548 ± 0.026
Ti	90.42	SS	56.88	-0.040 ± 0.012	+0.026 ± 0.013	+0.288 ± 0.181
SS Can	72.607	Bare	-	-0.084 ± 0.005	-0.084 ± 0.005	-1.157 ± 0.069
UO_2	106.5	Al	20.1	-0.337 ± 0.013	-0.317 ± 0.014	-2.977 ± 0.131
C	103.0	Bare	-	+0.366 ± 0.001	+0.366 ± 0.001	+3.553 ± 0.010
Be	114.308	Bare	-	+1.304 ± 0.003	+1.304 ± 0.003	+11.408 ± 0.026
Cr	220.73	SS	56.30	-0.287 ± 0.006	-0.222 ± 0.008	-1.006 ± 0.036
B_4C	59.62	SS	64.70	-6.443 ± 0.010	-6.368 ± 0.011	-106.810 ± 0.185
Nb	481.2	SS	30.10	-3.560 ± 0.008	-3.525 ± 0.009	-7.325 ± 0.019
$(CH_2)_n$	58.986	Bare	-	+12.324 ± 0.003	+12.324 ± 0.003	+208.927 ± 0.051
Mo	599.0	Bare	-	-3.115 ± 0.021	-3.115 ± 0.021	-5.200 ± 0.035
Depleted U	1153.58	Bare	-	-3.764 ± 0.003	-3.764 ± 0.003	-3.263 ± 0.003
Zn	414.2	SS	26.3	-1.040 ± 0.006	-1.010 ± 0.008	-2.438 ± 0.019
Zr	406.0	Bare	-	-0.443 ± 0.007	-0.443 ± 0.007	-1.091 ± 0.017
Ni	546.0	Bare	-	-0.832 ± 0.008	-0.832 ± 0.008	-1.524 ± 0.015
Na	51.38	SS	56.42	-0.052 ± 0.006	+0.013 ± 0.008	+0.253 ± 0.156
W	1052.0	Bare	-	-5.095 ± 0.001	-5.095 ± 0.001	-4.843 ± 0.001
V	183.67	SS	55.30	-0.161 ± 0.003	-0.097 ± 0.006	-0.528 ± 0.033
Mn	209.58	SS	55.92	-0.545 ± 0.003	-0.481 ± 0.006	-2.295 ± 0.029
Fe	488.0	Bare	-	-0.450 ± 0.004	-0.450 ± 0.004	-0.922 ± 0.008
TaO	101.144	SS	71.645	-1.689 ± 0.013	-1.607 ± 0.014	-15.889 ± 0.139
Al Block	165.33	Bare	-	-0.122 ± 0.010	-0.122 ± 0.010	-0.738 ± 0.061
Fe_2O_3	296.4	Bare	-	-0.106 ± 0.003	-0.106 ± 0.003	-0.358 ± 0.010
SS Block	480.9	Bare	-	-0.530 ± 0.003	-0.530 ± 0.003	-1.102 ± 0.006
ZrH	107.01	Al	26.874	+2.638 ± 0.004	+2.664 ± 0.006	+24.874 ± 0.056
Li	28.60	SS	56.72	-0.582 ± 0.007	-0.517 ± 0.009	-18.077 ± 0.315
Al Can	26.2098	Bare	-	-0.026 ± 0.004	-0.026 ± 0.006	-0.992 ± 0.229
^{10}B	29.29	SS	55.73	-23.272 ± 0.011	-23.208 ± 0.012	-792.352 ± 0.410
Eu Oxide	34.0	Al	20.4	-2.673 ± 0.013	-2.653 ± 0.014	-78.029 ± 0.412
Hf	806.0	Bare	-	-8.931 ± 0.017	-8.931 ± 0.017	-11.081 ± 0.021

[a]Some samples were canned in either stainless steel or aluminum cans.

The reactivity effect of having ^{238}U plates next to ^{235}U plates was tested in the following manner:

1. The reactivity worth of 16 (2 x 2 x 0.004-in.) ^{235}U foils was measured at the center of the core in a cavity with a volume of 2 x 2 x 2 in. These foils were equivalent to the 1/16-in. plate of ^{235}U used in the core.

2. The reactivity worth of 25 (2 x 2 x 0.005-in.) ^{238}U foils was measured in a similar manner. These foils were equivalent to the 1/8-in. ^{238}U plate used in the core.

3. The reactivity worth of the 25 ^{238}U foils stacked on top of the 16 ^{235}U foils was measured together.

4. The 16 ^{235}U foils were sandwiched among the 25 ^{238}U foils, and the worth of the whole packet was measured.

Table II.B.9 shows these results. Also included in Table II.B.9 are the worths of plutonium samples as a function of sample thickness.

TABLE II.B.9. Central Reactivity Worths of Uranium and Plutonium in Assembly 6 of ZPR-6

Sample Description	Sample Wt (g)	Can Type	Can Wt (g)	Gross Sample Worth (Ih)	Net Sample Worth (Ih)	Specific Sample Worth (Ih)
Depleted Uranium[a]						
25 (2 x 2 x 0.005-in.) foils	147.1234	Bare	-	-0.5136 ± 0.002	-0.5136 ± 0.002	-3.491 ± 0.017
Enriched Uranium[b]						
16 (2 x 2 x 0.0045-in.) foils	76.634	Bare	-	+2.960 ± 0.001	+2.960 ± 0.001	+38.625 ± 0.004
Enriched and Depleted Uranium						
25 ^{238}U foils on top of 16 ^{235}U foils	223 757	Bare	-	+2.486 ± 0.006	+2.486 ± 0.006	-
16 ^{235}U foils sandwiched among 25 ^{238}U foils	223.757	Bare	-	+2.478 ± 0.003	+2.478 ± 0.003	-
Plutonium[c]						
2 x 2 x 0.015 in.	11.25	SS	18.39	+0.458 ± 0.003	+0.480 ± 0.003	+42.667 ± 0.267
2 x 2 x 0.020 in.	22.60	SS	18.48	+0.998 ± 0.002	+1.020 ± 0.003	+45.133 ± 0.133
2 x 2 x 0.050 in.	35.00	SS	18.56	+1.597 ± 0.001	+1.619 ± 0.003	+46.257 ± 0.086
2 x 2 x 0.080 in.	57.57	SS	18.56	+2.722 ± 0.001	+2.744 ± 0.002	+47.664 ± 0.052
2 x 2 x 0.200 in.	151.16	SS	25.17	+7.569 ± 0.008	+7.599 ± 0.008	+50.271 ± 0.053

[a] 0.21 w/o ^{235}U.
[b] 93.13 w/o ^{235}U.
[c] 72.24 w/o ^{239}Pu, 22.28 w/o ^{240}Pu, 4.63 w/o ^{241}Pu.

The reactivity worths of ^{235}U, ^{238}U, iron, and nickel were measured as a function of sample size by the oscillation technique. The accuracy of this technique is quite dependent on the knowledge of the differential worth of the autorod. The data on the calibration of the autorod as well as the worths of the materials are being analyzed.

b. Doppler Effect (C. E. Till)

Last Reported: ANL-7419, p. 15 (Jan 1968).

In order to extend the temperature range over which Doppler-effect measurements can be made, effort has been directed toward the development of a Doppler element that can achieve very high temperatures. The design that has given the best results uses graphite for the heater,

sample container, and supporting pieces. Beryllia insulators are used to support the graphite heater. The high-temperature element can use samples up to 12 in. long and 0.860 in. in diameter.

Measurements were made in ZPR-9 with this element and results were obtained from room temperature to approximately 2000°K, thus effectively doubling the temperature range of the Doppler measurements at ANL.

The measurements were made in Assembly 23, which is almost identical to Assembly 19, a uranium oxide-zoned core described in Progress Report for November 1967, ANL-7399, pp. 30-31. Assemblies 19 and 23 were designed to have central real and adjoint spectra typical of a large, dilute, ^{235}U-fueled oxide core. Based on the results of the sample environment studies reported in ANL-7419, a 1/4-in. stainless steel filter was loaded into the eight core drawers surrounding the central drawer occupied by the Doppler oscillator. This gave a total stainless steel radial thickness of approximately 1/2 in. between the sample and the core. The radial thickness of carbon surrounding the sample was 0.16 in.

The Doppler oscillator in ZPR-9 was modified to provide the additional cooling required by the high-temperature element. The counterflow type of air cooling system has been found to give adequate cooling for up to 4 kW of heater power.

The modified Doppler oscillator has no dummy-sample position, and balancing between "sample in" and "sample out" is obtained by means of a newly installed shim rod with position reproducibility of ±0.001 in. This small uncertainty in the position of the shim rod results in an uncertainty in reactivity of ±0.0015 Ih. The observed standard deviations for a set of at least five measurements at a given temperature varied from a minimum of 0.0015 Ih to a maximum of 0.025 Ih. The source of the poorer precision was isolated and will be eliminated.

The Doppler effect was measured for the following materials during this series of runs: UO_2 (natural uranium), tungsten, molybdenum, rhenium, and tantalum.

The chemical reaction that occurs between carbon and UO_2 at high temperatures has been observed in the form of a deterioration of the vacuum in the Doppler capsule beginning at about 1400°C and becoming progressively worse at higher temperatures. Analysis of residual gas showed the presence of CO. To eliminate this problem, a 0.002-in.-thick tantalum liner was used between the graphite sample container and the samples. An additional measurement was made to determine the Doppler effect of the empty capsule (with liner).

The analysis of the measurements is not yet complete; however, preliminary results indicate good agreement between the data obtained for UO_2 with the new high-temperature element and those obtained earlier in Assembly 19 with the standard ANL freely expanding Doppler element.

Of the refractory metals, tantalum showed the largest temperature coefficient, with a change in worth of over 3 Ih/kg from 300 to 2100°K. Listed in order of decreasing Doppler effect per kilogram, the materials fall in this order: tantalum, rhenium, ^{238}U, molybdenum, and tungsten. Before final results are available a number of corrections must be considered, including expansion corrections and accurate determination of average sample temperature.

6. ZPPR Operations and Analysis (W. G. Davey and P. I. Amundson)

Last Reported: ANL-7427, pp. 17-20 (Feb 1968).

a. Basic Studies of Large Plutonium Systems

(i) Program. Detail design work for the ZPPR Core I continues. The scope has been increased to evaluate the relationships between possible alternative detail designs and material utilization for Cores 1, 2, and 3.

(ii) Experimental Equipment. The development of major reactor-associated experimental devices continues. The status of the development effort is as follows:

The design of the perturbation sample changer is complete. Detailed drawings have been completed and checked. The bid package is being reviewed and will be submitted to Purchasing shortly.

The perturbation-sample specifications have been established. Potential material suppliers have been identified. The perturbation-sample containers and traverse holders have been designed and approved.

The design of the axial traverse drive system has been completed and detailed drawings are 80% complete.

Of the two design options established for the axial-traverse sample changer, the most feasible design has been selected. Design work is underway.

Fabrication work continues on the autorod system.

A remote communications system for the ZPPR cell has been tested. The necessary components for the system have been ordered.

b. Doppler Coefficients. The detail and assembly drawings have been compiled for the entire system, except for minor detailing which will depend on the actual dimensions of commercially supplied components. Additional orders have been placed for components which could be specified before approval of the final design.

A bid on the motor-drive system has been received from one of the manufacturers. Additional information has been supplied to a second bidder, and the bid will be received shortly. Choice of the drive will be made as soon as a second bid is received.

Several components have already been received and construction of the Doppler system will begin as soon as the final design is checked and approved.

The RABBLE Program has been studied relative to ZPPR Doppler measurements. Initial work with the code will be coordinated with the Theoretical Support Group and will entail a study of the Doppler measurements on ZPR-3 Assembly 51.

c. Sodium Coefficients. Developmental work on the axial sample-drive mechanism continues. A sample-changer concept has been established and design work has been started. These equipment items are multipurpose and have been covered in Sect. II.B.6.a(ii).

Gross sodium-void techniques used with ZPR-3, -6, and -9 are being studied relative to their applicability to study of the large systems to be constructed in ZPPR.

d. Reactor Technique Development

(i) Precision Reactivity Measurements. An experiment has been run with ZPR-3 Assembly 51 to determine the effect of detector efficiency and power level on the accuracy of autorod-position determinations. The power level was varied from 80 to 0.2 W, and five detectors were used with efficiencies varying from about 10^{-4} to about 5×10^{-8}. Preliminary analysis of the results indicates that the error varies in the expected manner, remaining constant at high efficiencies and increasing rapidly for very low efficiencies. The data obtained will be used to optimize the detectors on ZPPR.

(ii) Doppler Balance Code. Corrections to the test-case input data indicate that the computer program which will predict the preferred Doppler-rod loading for minimum reactivity swing is working correctly. The Doppler-rod loadings for ZPR-3 Assembly 51 and the measured reactor responses have been obtained. These data will be analyzed to establish further the validity of the balance code.

(iii) Foil Techniques. Specification of equipment for the ZPPR counting room is complete. The purchase of equipment is proceeding. Major items will be sent out shortly for bid.

Activation analysis work on ^{235}U and ^{238}U has been essentially completed. Acquisition of thin ^{239}Pu and ^{233}U foils has been initiated.

The experimental technique development for this effort is discussed in Sect. II.B.2.

(iv) Automation of Data Acquisition. This program covers work on control and readout equipment for the experiments on ZPPR that necessitate automation.

(a) Digital Position Indicators. Development and testing of the logic circuits has been completed. Completion of the prototype will follow delivery of specified printed circuit boards.

(b) Digital Multiplexer. The Digital Multiplexer will sample position information from all devices using shaft encoders, such as control rod and autorod. Development and testing of the logic circuits is in progress.

(c) Autorod Control. Construction of the autorod-control system has been initiated. Procurement is complete except for the constant-temperature component oven. It is planned to utilize the Donner-3500 analog computer as a reactor simulator to verify the calculated stability of the finished equipment.

(d) Data Acquisition and Recording System. Bids have been received from five vendors. The two low bidders have been contacted for clarification of certain details.

(v) Training. The technician-training course has commenced. Initial sessions indicate that the desired course structure and teaching level have been achieved. The course is intensive and covers 92 sessions of scheduled instruction including lectures, problem sessions, supplementary films, demonstrations, reviews, and examinations.

The initial portion of the reactor technology training course will be completed this month. System training sessions are now being formulated. They will follow the reactor technology course.

7. ZPPR Construction (H. Lawroski)

Last Reported: ANL-7427, pp. 16-17 (Feb 1968).

Beneficial occupancy of the mound area was obtained by ANL on February 21, and installation of the ZPPR reactor components was started on February 22.

Full-load (180-ton) testing of the bed and tables was completed on March 7. Deflection measurements were made at loads of 0, 60, 120, and 180 tons, and again at no load following the tests. A Brunson optical system, capable of accuracies of 1 second of angle, was used to check against the bed-and-tables manufacturer's instruments which were electronic levels with accuracies of 1 part in 250,000. The results of the two systems agreed within 0.001 in. Analysis of the measurements revealed that the areas of the table surfaces where the matrix and the rod drives will be mounted are within ±0.002 in. of levelness. One area on the movable table near the rear corner was a maximum of 0.004 in. high. This is not a critical area, and no corrective action is required.

The transmission, lubrication system, ball-screw-and-nut assembly, electrical system, emergency scram system, and position-indication system checked satisfactorily.

Both sets of reactor knees were placed on the tables and aligned. A full complement of matrix tubes was stacked between the knees of both halves, and the tie-down beams were installed. The purpose of this preliminary stacking of the tubes was to check the tie-down system and the alignment of the tubes between the two halves.

During the clamping of the matrix, movement of the front edges of the tubes with respect to a vertical plane was measured. The tubes were not anchored, and no attempt was made to restrict their movement. By varying the clamping procedure, i.e., moving the knees in first and then clamping down with the tie-down beams, or clamping down the tie-down beams and moving the knees concurrently, the front edges of the tubes could be manipulated with respect to a vertical plane. Development of a technique for loading the tubes and clamping the matrix to minimize deflection during the final assembly with the alignment plates was then undertaken.

The two platform-support T-beams were set and aligned in the loading platform pit.

Approximately 40% of the electrical work on the reactor control and instrumentation system has been completed.

Wiring for the loading-tube drive mechanism was installed through the access-corridor bulkheads. Modifications on the air compressors in the support wing were completed and checked out. Replacements for the relays in the suspect-exhaust and supply-air fans were installed. Ninety-eight percent of the wiring in the cable trays in the cable routing room has been run.

The construction contractor replaced 13 uncertified filters in the backup containment structure. The replaced filters were inspected, and a

satisfactory leak test of the backup containment structure was performed. Four uncertified filters in the suspect-exhaust systems of the mound and the support wing were also replaced.

A satisfactory leak test was performed on the bulkhead of seal door D74. The contractor continued attempting to obtain the required leak tightness in the escape-tunnel-transition connection.

All 55 of the concrete storage bins for fuel were received and placed in the fuel storage vault.

An ANL representative visited the manufacturer of fuel storage canisters. Aluminum die casting of the canisters, which are made in two parts, has been completed; they are now being assembled and leak tested. Delivery of the canisters was scheduled to start during the last week of March.

The additional information requested by the AEC on the Final Safety Analysis Report was supplied.

8. FFTF Critical Experiment Program (D. Meneghetti)

Last Reported: ANL-7427, pp. 23-25 (Feb 1968).

a. Additional Studies of a Simple Method for Approximating Solutions of Axially-Split Cylindrical Cores. In ANL-7427 a method is described by which a finite cylindrical reactor in coordinates r and z may be viewed as a finite slab reactor in coordinates x, y, and z. In both cases the leakage in the z direction is simulated by the usually DB_z^2 fictitious leakage absorber. The slab problem, with composition varying as a function of x, is supplied with a chord buckling, $B_y^2(x)$, which forces $\phi(x)$ to be of the same form as the known cylindrical solution $\phi(r)$. The $B_y^2(x)$ introduces a fictitious group-dependent leakage absorber or source at each point, which simulates the dilution or concentration of the neutron population in the circumferential direction as it diffuses outward or inward radially.

The chord buckling in the reflector, $B_{y2}^2(x)$, of a reflected cylinder, considering only one group of neutrons, is

$$B_{y2}^2(x) = B_{y1}^2(x_1)\,\frac{D_1}{D_2}\,\frac{x_1}{x}\,\frac{K_0\left(\frac{ax_1}{R_c}\right)\,K_1\left(\frac{ax}{R_c}\right)}{K_0\left(\frac{ax}{R_c}\right)\,K_1\left(\frac{ax_1}{R_c}\right)}, \qquad (1)$$

where $B_{x1}^2(x_1)$ is the chord buckling for this core evaluated at the core-reflector interface at x_1; D_1 and D_2 are the core and reflector diffusion

constants, respectively; K_0 and K_1 are Bessel functions; R_c is the extrapolated bare-core radius. The quantities x_1, a, and R_c are related by the transcendental criticality equation. Equation (1) shows that the chord buckling has a discontinuous jump in value at the core-reflector interface. This jump, present in multigroup problems as well, results in continuity in the value of $DB_y^2(x)$ at the boundary.

The multigroup formulation of this method requires that

$$B_y^2 = -\frac{1}{r\phi^c}\frac{d\phi^c}{dr} \qquad (2)$$

be true for each group. Here ϕ^c is the cylindrical solution and r is the radius.

In a six-group test comparison using the MACH-1 diffusion code,* the k_{eff} of the reflected cylindrical core and its slab simulation agreed within 10^{-4}. The six-group fluxes agreed within less than one percent except very near the outer boundary. This agreement is as good as can be expected using 20 elementary slab regions.

b. Effect of ^{239}Pu Alpha Values upon Reactivity of ZPR-3 Assembly 51. Recent concern about the value of alpha of plutonium-239 has led to a calculated estimate of the reactivity effect upon Assembly 51 of increased alpha values in the energy range from 0.1 to about 25 keV. The increased alpha values for the multigroup cross-section groups in this range were roughly based upon the provisional data reported by Schomberg, Sowerby, and Evans.** The increased alpha values were assumed to affect the group cross sections through increase in the group capture cross sections for plutonium-239. The ratios of the group alpha values based on the Schomberg data to those of cross-section Set 29001 are compared in Table II.B.10. The calculations resulted in a reactivity decrease of about -3.4% k upon use of the capture cross sections corresponding to the larger alpha values.

TABLE II.B.10. Ratios of Plutonium α Values

Group J	E_J^{min} (keV)	$\alpha_J^{SSE}/\alpha_J^{29001}$ [a]	Group J	E_J^{min} (keV)	$\alpha_J^{SSE}/\alpha_J^{29001}$ [a]
12	15.03 [b]	1.85	17	1.23	1.89
13	9.11	2.24	18	0.96	1.66
14	4.31	2.27	19	0.58	2.82
15	2.61	2.12	20	0.28	1.93
16	2.03	2.06	21	0.10	2.11

[a] α_J^{SSE}: group value of α roughly based upon provisional α(E) data of Schomberg et al.**

α_J^{29001}: group value of α corresponding to group capture and fission cross sections in Set 29001.

[b] E_{12} upper energy is 24.8 keV.

*Meneley, D. A., Kvitek, L. C., and O'Shea, D. M., MACH-1, A One-dimensional Diffusion Theory Package, ANL-7223 (June 1966).

**Schomberg, M. G., Sowerby, M. G., and Evans, F. W., A New Method of Measuring Alpha (E) for Pu^{239}, Symposium on the Physics and Safety Problems of Fast Reactors. Karlsruhe, German Federal Republic, Oct. 30-Nov. 3, 1967. Paper SM-101/41.

c. Relative Reactivity Variations with S_N Order for ZPR-3 Assembly 51 Systems in Different Geometries. One-dimensional slab, cylinder, and sphere calculations in six energy groups using the Argonne one-dimensional discrete-ordinate transport code SNARG-1D were made using S_2, S_4, and S_6 approximations. The cores had the composition of Assembly 51. The slab case had the axial reflector of Assembly 51. The cylindrical case had the radial reflector composition of Assembly 51. The spherical cases were carried out with the radial reflector composition and thickness, and axial reflector composition and thickness. These one-dimensional cases were compared with S_2, S_4, and S_6 analyses using the R-Z geometry of the Argonne two-dimensional discrete-ordinate program SNARG-2D. The comparison are shown in Table II.B.11.

TABLE II.B.11. Comparative Variations of k for ZPR-3 Assembly 51 with S_N Approximations in Various Geometries

	Two-dimensional Calculation-- Cylindrical	One-dimensional Calculations			
		Spherical		Cylindrical-- Radial Reflector	Slab-- Axial Reflector
		Radial Reflector	Axial Reflector		
$k(DT)/k(S_6)$		0.990	0.987	0.993	0.999
$k(S_2)/k(S_6)$	1.007	1.010	1.013	1.001	0.999
$k(S_4)/k(S_6)$	1.000	1.001	1.001	1.001	1.000

Results indicate that the slab-geometry aspects in the axial direction would be adequately calculated by either diffusion theory or S_2, which are essentially equivalent, in slab geometry. The cylindrical-geometry aspects in the radial direction would require S_2. The two one-dimensional spherical results and also the two-dimensional cylinder results indicate instead that S_4 is needed. The simulatory spherical cases show that the correction from S_2 to S_4 is about -1.0% $\Delta k/k$, whereas the cylinder correction by two-dimensional calculation is about -0.7% $\Delta k/k$.

C. Component Development--LMFBR

1. Sodium Technology Development--Engineering Development

a. Sodium Quality Measurement (S. B. Skladzien)

Last Reported: ANL-7427, pp. 26-27 (Feb 1968).

(i) In-line Techniques. Recent large variations in the oxygen concentration of sodium samples taken by our dip-sampling and vacuum-distillation procedures (as much as 10 ppm at the 30-ppm level) prompted an investigation of the apparatus and analytical method. The possibility of distilled sodium falling or dripping from the dip rod back into the sample cup, after the distillation, was corrected by reforming the rod.

After analysis of the argon supply indicated high moisture and oxygen content, and no leaks were detected in the supply line, the supply

bottle was replaced with ultrahigh-purity agron; when the supply pressure regulator was removed, evidence of moisture was found on the high-pressure side that could only have come from the original supply bottle. Since the change in gas supply, analyses of four sodium samples show a maximum variation of 1.2 ppm oxygen at the 30-ppm level.

All recent sodium samples were taken by the dip method, so that consistent results could be achieved, and all questionable sampling and analytical procedures or problems could be corrected. This is expected to allow accurate correlation of line sampling with the dip method.

A new data-acquistion system was installed to improve accuracy and speed tabulation of the more important data from the sodium analytical loop. The unit is very versatile because it can be programmed for various ranges of ac and dc voltages and resistance.

2. Reactor Mechanisms Development--Materials Evaluation

a. Sodium Effects on Wear Properties of Materials (E. S. Sowa)

Last Reported: ANL-7427, pp. 28-29 (Feb 1968).

Additional wear tests of Clarite vee blocks in sodium and argon atmospheres with the Falex test machines were terminated after a sticking relay during startup caused the argon-atmosphere samples to be overheated to 1500°F. New blocks have been loaded into vacuum, argon, and sodium rigs for a new series of tests.

Continued operation of the CAMEL loop permitted minor circuit difficulties to be eliminated. The potential-drop interlock circuit across the main electromagnetic pump performed excellently, except that setting varied with operating time as wetting of the pump wall developed. The pump was calibrated after the wetting stabilized at 600°F; it will be calibrated further at higher temperatures.

To establish a basis for later material balances, samples of the as-received piping for the CAMEL loop were analyzed chemically and metallurgically, and the sodium was analyzed chemically prior to charging. Also, calibration curves were made for the pressure transducers at room temperature. Similar data will be taken for higher temperatures and with progressive time lapse to establish the performance characteristics of the transducers.

A modified bypass sampler has been designed for the loop so that 2.5-cm^3 specimens of sodium can be obtained periodically for analysis. To decrease the time for equilibration, the sodium will flow from an upper isolation chamber down to the sampling cup by passing through an annular

jet nozzle that will cause turbulence near the cup wall. After valves in the inlet and outlet lines are closed to trap the sodium in the cup and chamber, the sodium will freeze rapidly. With the sodium solid, the chamber and cup will be removed from the line by disconnecting a Conoseal fitting and shearing the sodium at the joint. After they are transferred to a glovebox, the chamber and cup will be separated by disconnecting a similar fitting that joins them.

b. Intermediate Range Neutron Monitor (G. F. Popper)

Last Reported: ANL-7427, p. 30 (Feb 1968).

(i) Detectors. The Westinghouse WX-31353-25 high-temperature cables have not been received because of minor fabrication problems.

A sample of Boston Insulated Wire Co. Bostrad detector extender coaxial cable has been obtained. This cable, which is equivalent to an RG-149U normal coax, is rated at 1500°F, 1×10^{13} rads, and 1×10^{22} nvt. It has a 75-ohm nominal impedance and less than 25 pf/ft. The cable will be tested with the WX-4036 fission counter up to 850°F.

The ~15-ft cables on the detectors from LASL are too short to be used in the EBR-II modified "O" thimble. The original manufacturers have been asked to estimate the cost and time required to replace these cables with new 28-ft triaxial cables.

(ii) Circuits. The EG&G Model-RM811 neutron monitor will be used with a Hewlett Packard Model 5554A charge-sensitive preamplifier, a Keithley Model-410C picoammeter, and a Power Designs Model-2K10 power supply to test the fission counters.

The selected charge-sensitive preamplifier is a low-noise general-purpose instrument for use with nuclear detectors. Noise is inevitable in any detector-amplifier system. In a charge-sensitive preamplifier, noise is strongly a function of input capacitance. This capacitance includes the detector, the cable, and the connectors. As the capacitance increases so does the system noise. Up to 2000 pf of capacitance have been added to the preamplifier input; the system noise remains well below the alpha threshold. With this preamplifier, excellent overall system performance has been achieved. Room-temperature alpha and neutron integral bias curves have been obtained with the WX-4036 detector using low-temperature RG-71U cable to connect it to the preamplifier.

Until the preamplifier is received (which may take six weeks), we plan to continue system tests with a demonstration model.

Preliminary discussions were held with Milletron on the wide-range monitor system. System designs are being developed; the estimated delivery date is mid-June.

c. Fuel-Pin Thermocouple Development (A. E. Knox)

Last Reported: ANL-7427, p. 31 (Feb 1968).

(i) Electrical Insulators. Single-crystal alumina is being tested. Hard-fired, 99.5% pure beryllia insulators have been received and will be tested after the spectrochemical analysis is received.

(ii) Materials Compatibility. The third tantalum-UO_2 compatibility sample, TU-3, evidenced a leak after 63 hr of operation at 2400°C, so the experiment was terminated. Examination revealed that the leak was in a tantalum support tube and not in the tantalum-UO_2 region of the capsule. The support tube and the capsule are being examined metallographically.

(iii) Out-of-pile Tests. The failure of thermocouples TTC5 and TTC6 is being investigated by spectrochemical and X-ray diffraction analyses.

d. Fission-Gas Pressure Transducer Development (J. R. Folkrod)

Last Reported: ANL-7427, pp. 31-32 (Feb 1968).

(i) Strain-gauge System. The Statham PA-812 thin-film strain-gauge pressure transducer has been repaired by the vendor so that it will measure absolute instead of gauge pressure. In room-temperature pretest checks, the combined effect of linearity and hystersis was less than ±1% of full-scale output. The transducer has been tested successfully to 250°C; the maximum uncorrected error was less than -6% of full scale. When the output was corrected for zero shift, the largest error was -3% of full scale. The sensitivity and zero shift at various temperatures are:

Temperature (°C)	Sensitivity (mV/psia)	Zero Shift (mV)
23	0.2482	0.00
75	0.2450	-0.57
105	0.2433	-0.65
150	0.2441	-0.64
200	0.2444	-0.58
250	0.2480	-0.61

This unit will be tested further to determine its maximum reliable operating temperature.

(ii) Null-balance System. The transducer assembled from a body (built by Metal Bellows Corp.), a probe, and a stop has been tested for one month at 900°F and up to 80 psig. After three weeks, an abrupt (overnight) change occurred in the contact electrical resistance. Good contact has become more difficult; when the simulated fission-gas pressure is increased, the contact resistance does not decrease to as low a level as before, resulting in a zero shift in the calibration curve that is 4.5 psig lower than that of an earlier calibration curve. (A calibration curve based on reference-gas pressure versus simulated-fission-gas pressure is made weekly.) If the new curve is reproduced in future calibrations, instrument accuracy will be $\pm 1/4$ psig.

The change in contact resistance makes the instrumentation sluggish. However, good readout can be achieved if the operator makes the instrument more sensitive, causes it to hunt for a time, and then desensitizes it.

A third transducer has been assembled for an experiment in the CP-5 reactor. It will measure the fission-gas pressure generated in a fuel pin during irradiation.

e. Signal Lead Connectors for Sodium Service (A. P. Grunwald)

Last Reported: ANL-7427, pp. 34-35 (Feb 1968).

(i) Test of Electrical Connectors in a Sodium-vapor Atmosphere. It has been found that the sodium-filled lower portion of the test assembly was 45°F hotter than the connector-mounted top because the lower portion was more exposed to the furnace heater. By thermally shielding this section from the heaters, we have demonstrated that the temperature difference can be controlled as desired in future tests.

When the top of the test assembly was sawed off so the connector interior could be inspected, an extensive deposit of sodium was seen at the base of the pins. This sodium deposit had caused the pins to short during the test. To learn whether such connectors can be salvaged for later use, water was applied to remove the sodium. However, the reaction between the sodium, water, and Durock-128 insulation produced a foaming, black, ink-like liquid, and three pins broke loose from the insulator. Further application of water caused more liquid to form and the insulation disintegrated rapidly. An improved insulation, Durock-208, will be used in future connectors to be tested.

f. Failed Fuel Locating Method Development (F. Verber)

Last Reported: ANL-7419, p. 34 (Jan 1968).

Further review of the flow diagram for the failed-fuel-monitoring loop indicated the need for mounting the pump in the bottom horizontal leg of

the loop instead of vertically. Although limitations of the internal pump tube supports necessitated the change, it also eliminates the need for a shutoff valve between the pump and surge tank, because the contents of the surge tank now can be drained directly to the dump tank without passing through the pump.

The design drawing for the surge tank is approximately 90% complete. Equipment and materials available for fabrication of the loop include: the ac electromagnetic pump, capacitors for a power-factor-correction capacitor bank for the pump, an electromagnetic flowmeter, a variable autotransformer for pump control, a sodium dump tank, 12-in. stainless steel pipe for the sodium surge tank, and about 70% of the electric-heater equipment.

D. Systems and Plant--LMFBR

1. 1000-MWe Plant

a. Contract Management and Technical Review (L. W. Fromm)

Last Reported: ANL-7427, pp. 35-36 (Feb 1968).

(i) The Babcock & Wilcox Co. Subcontract. Drawings for the reference concept are approximately 85% complete. Major thermal and hydraulic parameters for the reference core have been calculated.

Six trade-off studies were completed and reviewed; two were revised in response to review comments. Economic- and physics-oriented parametric studies are continuing as part of Task III.

Architectural general-arrangement drawings for the building are 70% complete.

(ii) Westinghouse Corp. Subcontract. Six of the seven Task-I topical reports have been written and edited, and nine of the eleven sections of the Task-I report have been written.

Completed Task-II work includes the design of the reactor-vessel internals, the reactivity-control system, and the core thermal-hydraulic analysis. Conceptual system-design descriptions are being written for areas that are not expected to change as a result of Task-III evaluation studies. Cost data and heat balances are being developed.

(iii) General Electric Co. Subcontract. Approximately 65% of the Task-I report has been drafted.

Nuclear analyses have been conducted for 15 variations from the basic core. The data are being used in thermal-hydraulic analysis.

Core-design mechanical drawings are being prepared for the reference reactor. Two methods of lifting the reactor shield plug are being studied. Work has begun on a pneumatic scram-actuating device. An emergency-cooling-system analysis was completed. Two cover-gas systems were developed and are being compared.

(iv) Combustion Engineering, Inc., Subcontract. The design of the reference core is essentially complete. Five conceptual design descriptions have been prepared and are being reviewed. A safety analysis on the effect of gas bubbles in the reference core was completed. Calculational problems associated with CE's version of the MC^2 multigroup cross-section code were resolved with the assistance of ANL. Preliminary results have been obtained on the Task-III parametric studies.

(v) Atomics International Subcontract. The study is approximately 35% complete. All overall system-design descriptions have been prepared and the system-selection studies have been completed. The Task-I report has been drafted and is being reviewed. Task-II system-design descriptions are about 75% complete and Task-III work has started. Early Task-III efforts include a nulcear-uncertainty analysis, a fuel-handling review, a safety and accident analysis, and an economic parameter study. Component-level system-design descriptions in Task III are being prepared.

E. EBR-II

1. Research and Development

a. EBR-II System Design Descriptions (E. Hutter)

Last Reported: ANL-7391, p. 51 (Oct 1967).

When the working outline was approved and preparation of the design descriptions was authorized, priorities were established as follows:

Vol. II--Primary System
Vol. III--Secondary System
Vol. IV--Steam System
Vol. V--Electrical System
Vol. I--General Facilities

Preparation of drafts and illustrations for Vol. II, Primary System, has begun.

b. Reactor Experimental Support--Reactor Analysis and Testing (R. R. Smith)

Last Reported: ANL-7427, pp. 37-45 (Feb 1968).

(i) Digital Data Collection. The third draft of the Digital Data Acquisition and Reduction System Proposal is being reviewed.

(ii) Nuclear Analysis

(a) Computer Programs for Analysis of Fission-product Activity. Whenever the reactor is operated intermittently it is difficult, from an inspection of the record of cover-gas activities, to conclude whether or not small increases in radioactivity are the consequences of small fission-product releases or are peculiarities of time-power history. To aid such evaluations, computer programs have been written to accept as input the complete time-power log of reactor operation and pertinent decay constants. The result of such a computer analysis is a time-dependent parameter proportional to the extent of saturation for a particular index species. Such values may be directly compared with the actual results of radiometric analyses of cover-gas and primary-coolant samples.

Two programs were written. One deals with the buildup and decay of ^{133}Xe and ^{135}Xe activities in the cover gas, and the other deals with the buildup and decay of ^{131}I, ^{133}I, and ^{135}I activities in the primary sodium. The usefulness of both programs was assured by comparing computed values of activity of ^{133}Xe, ^{135}Xe, and ^{133}I with corresponding experimentally

determined values over a three-week period which involved over 100 irradiation time increments. There was substantial agreement in all cases.

These programs will be used in future searches for failed fuel elements or capsules. Differences between computed and experimentally measured values of fission-product activities in the cover gas and primary sodium will then be indicative of failure. This approach should increase the capability for detecting small fission-product releases.

(b) Run-26 Feedback Function. An appendix on heat transfer is being developed for the report on the Run-26 feedback function. The heat-transfer information is being correlated with the system time constants derived from the rod-drop tests. The two prompt negative coefficients in the feedback function have been identified with fuel and coolant expansion, and the positive coefficient with a 2-sec time delay has been identified with bowing of the Row-7 stainless steel blanket. Rows 8 and 9 are being analyzed as possible contributors to the more delayed effects.

(c) Effect of Reduced-flow Conditions on the Power Coefficient of EBR-II. Changes in the core loading and reflectors of EBR-II have been accompanied by variations in the integrated power coefficient (power-reactivity decrement). These variations have been studied by reactivity measurements at reduced flow. The decrement P measured by the indicated position of a calibrated control rod, can be expressed as

$$P = E + D + B,$$

where

E = expansion effect of core and blanket materials, sodium density changes, and axial elongation of fuel;

D = reactivity changes due to relative displacement of core and control rods as a result of expansion of control-rod extension shafts;

B = subassembly bowing effects.

The expansion effect was calculated from the thermal and reactivity properties of clean fuel, sodium, and structural material in a generalized flow-dependent form:

$$E = [-Q(1.015 + 11{,}100\,\alpha/R] + (0.037/R^{0.4}) + [6500 + (408/k)]\,\alpha, \quad (1)$$

where

Q = power, MW;

R = fraction of full flow;

α = coefficient of linear thermal expansion of fuel, $°C^{-1}$;

k = fuel thermal conductivity, cal/sec-cm-°C.

The reactivity change D is simply proportional to Q/R for a given rod-bank position. The subassembly bowing effect B was obtained by subtracting the full-flow values of E and D from the measured values of P at full flow. The parameter B was then generalized to other flow conditions by making the assumption that the bowing is dependent only on the rise of sodium temperature through the reactor. With E, D, and B all in flow-dependent form, P can be calculated for all power and flow conditions, if effective values of k and α are available. In this study covering Runs 25 and 26, however, effective values of k and α which best fit the experimental reduced-flow data were determined by a least-squares criterion.

The fitted values of α/k, given in Table II.E.1, are a measure of the fuel-expansion component of the power coefficient. The ratio α/k shows a tendency to increase during a 1500-MWd operating period. (Some of the final values are based on interpolations within a 20-MW region of the full-flow power-reactivity curve, only the end points of which were determined experimentally. Parametric studies have shown that this interpolation does not significantly compromise the data.) Since the reduced-flow data indicate an increase in the fuel-expansion component of the power coefficient, but operating data do not reveal any corresponding increase in the total PRD to 45 MWt, this implies that the positive effects of bowing must have increased during this period. This deduction can be explained by an increase in the clearance between subassemblies at zero power and is consistent with postirradiation button-to-button measurements of the subassemblies.

TABLE II.E.1. Measured and Calculated Values of Power-reactivity Decrement (PRD) at Reduced-flow Conditions (Ih)

Run 25, Start				Run 26, Start (200 MWd)				Run 26, Middle (1000 MWd)				Run 26, End (1700 MWd)			
Q	R	P_{exp}	P_{calc}	Q	R	P_{exp}	P_{calc}	Q	R	P_{exp}	P_{calc}	Q	R	P_{exp}	P_{calc}
10.0	0.9	20.6	21.3	22.8	0.9	20.0	20.3	22.4	0.9	16.4	18.5	22.4	0.9	11.3	14.1
17.2	0.9	23.2	25.1	23.8	0.75	22.0	21.7	22.7	0.75	16.4	17.9	23.0	0.75	10.3	11.3
22.5	0.9	26.8	27.4	30.0	0.9	27.1	24.4	22.8	0.6	19.8	20.2	23.2	0.6	12.0	12.1[a]
22.5	0.75	25.2	27.6	24.1	0.6	28.8	28.1	14.9	0.36	18.4	17.2	14.9	0.36	6.5	6.3[a]
22.5	0.6	30.1	28.7	30.7	0.73	31.5	32.6	29.9	0.72	27.3	26.5	30.1	0.72	20.5	18.4[a]
22.5	0.54	31.1	31.0	24.2	0.54	32.8	33.4	22.6	0.54	21.6	22.5	23.0	0.54	12.6	13.3
42.5	0.95	40.8	40.1												
	$\alpha/k = 3.8 \times 10^{-4}$				$\alpha/k = 3.8 \times 10^{-4}$				$\alpha/k = 6.5 \times 10^{-4}$				$\alpha/k = 8.6 \times 10^{-4}$		

[a]Based on an assumed extension of the full-flow PRD curve.

The fitted values of α and k were applied Eq. (1) to yield the tabulated values of P (calculated), which agree with P (experimental) to within 2 Ih in most cases. Calculation of P over the complete field of power and flow conditions has revealed regions, particularly at low flow and high burnup, where positive power coefficients are likely to exist.

(d) Release of Fission-product Species, March 5 through 12, 1968. As indicated by radiometric analyses of samples of primary cover gas, two small fission-product gas releases occurred during reactor operation in March, the first between 1430 and 1530 on March 5, and the second between 0700 and 1030 on March 11. Both releases were verified by small, but significant, increases in the Fission Gas Monitor (FGM) recordings, but neither caused any perceptible increase in the delayed-neutron-monitor signals. Cover-gas analysis, after the reactor was shut down following the second release, also showed evidence of two very minor additional releases in the periods 0500 to 1000 and 1430 to 1530 on March 12. These were not detectable by the FGM. Cover-gas activities for ^{133}Xe and ^{135}Xe during the period February 23 through March 13 are shown in Fig. II.E.1.

(1) Background and Description of Events. Prior to Run 27, two suspect experimental subassemblies, XG05 and XA08, were removed from the core and placed in the storage basket. Run 27A began on Feb. 5 and terminated on Feb. 28 after 283 MWd of operation. During this period there was no indication of any new fission-product release. On Feb. 28 the reactor was shut down, three prototype reorificed driver subassemblies were installed in Rows 4, 5, and 6, and the suspect experimental subassembly, XG05, was installed in grid position 4C2. Fuel handling for Run 27B was completed on Feb. 29. The reactor was made critical on March 1 at 0715, and power was gradually increased to 45 MWt at 0030 on March 2.

Steady power operation at 45 MWt continued until March 5, when a reduced-flow test was begun just prior to shutdown. Criticality measurements were taken at 41.5 MWt with 100% flow, then power was reduced to 22.5 MWt. Shortly after primary-system flow was reduced to 54%, a reactor scram was caused by a perturbation of the flow in primary-coolant pump No. 2.

After the reactor was restarted, power was raised to 45 MWt, with the intention of finishing the uncompleted reduced-flow experiment. An increase in the ^{133}Xe and ^{135}Xe activity in the primary cover gas (sample manually obtained at 1545 hours) caused a change in plans. The reduced-flow experiment was deleted from the Run 27B physics program, but to verify the cover-gas activities, operation was continued at 45 MWt until 2001 hours on March 5, when the reactor was shut down. The FGM and FERD (Fuel Element Rupture Detector) systems were closely monitored, and samples of cover gas were taken and analyzed every hour. At shutdown, a total of 460 MWd of operation had been logged for Run 27 to complete Run 27B.

No perceptible increase was noted in the FERD signals. Since this system is sensitive to those species which are chemically fixed in the bond, i.e., ^{88}Br, ^{87}Br, and ^{138}I, it was tentatively concluded

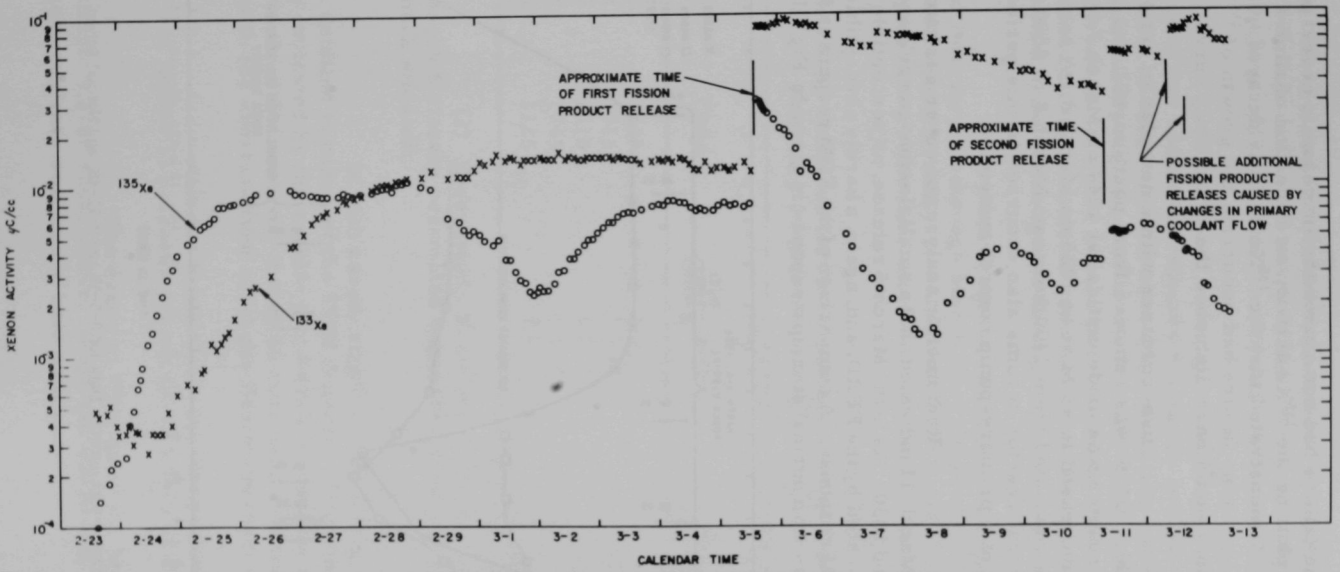

Fig. II.E.1. Xenon Activity in EBR-II Cover Gas for the Period from February 23 to March 12, 1968

that a bond-type failure had not caused the increase in cover-gas activity. The results of plotting the ^{135}Xe activity as a function of time after the indicated release demonstrated that the ^{135}Xe activity decayed with a 9.2-hr half-life. If a bond-type failure had occurred, the growth of ^{135}Xe from ^{135}I (fixed in the bond) would have disturbed the ^{135}Xe decay curve.

In accordance with a new plan of action, the suspect subassembly, XG05, was removed from position 4C2 and replaced by XA08. The reactor was made critical at 1844 on March 7, and power was gradually increased to 45 MWt at 1225 on March 8. A series of reduced-flow tests were conducted from 1400 hours on March 8 to 0800 hours on March 11. Several reactor scrams also occurred in this period because of malfunctioning of a primary-pump control system.

Radiometric analyses of cover-gas samples taken on the morning of March 11 indicated that a small fission-gas release had occurred between 0700 and 1030. As in the March 5 release, no perceptible signal increase was indicated by the FERD, and, again, a barely perceptible increase was noted in the FGM response. A comparison of the FGM responses for the March 5 and 11 releases with a normal startup response is given in Fig. II.E.2. Further

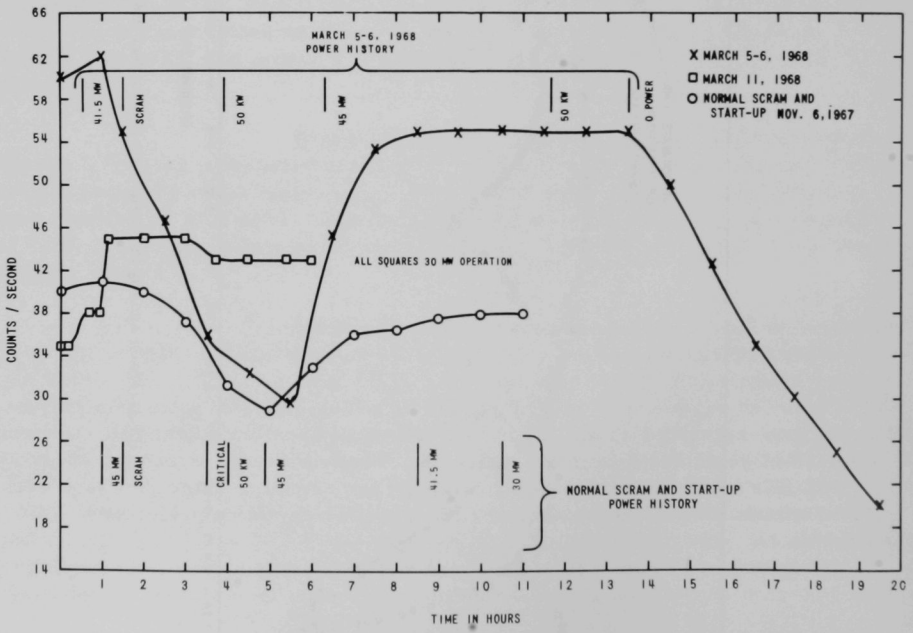

Fig. II.E.2. Charged-wire-monitor Data for 3-5-68 and 3-11-68, and Normal Scram and Startup

reduced-flow testing was deleted, and the reactor continued in operation at 30 MWt and 74% flow until 1515 to verify the cover-gas activity. Power was reduced to 50 kW at 1515, and the reactor was shut down at 1700.

Continued cover-gas analyses on March 12 indicated evidence of two additional releases during the periods 0500 to 1000 and 1430 to 1500. These releases were quite small and were not verified by the FGM. Of likely significance is the fact that pump flow was reduced to 65% at 0930 and to zero flow for the period 1300 to 1451. It was tentatively concluded that the associated reduction in primary-coolant pressure caused additional expansion of gases through the defect at these times.

A block diagram showing power operation for the entire period February 23 through March 12 is presented in Fig. II.E.3. Results of radiochemical analyses conducted for ^{131}I and ^{133}I in primary coolant samples taken before and after the indicated releases are given in Table II.E.2.

TABLE II.E.2. Analyses for Iodine Isotopes in Sodium Samples February 27 through March 11, 1968

Date	Time	^{131}I $\frac{dis}{min\text{-}g} \times 10^{-3}$	^{133}I $\frac{dis}{min\text{-}g} \times 10^{-3}$
2/27/68	1535	1.4	3.4
2/28/68	1715	2.3	4.9
3/4/68	1610	4.4	3.1
3/5/68	1745	6.1	5.2
3/11/68	1125	7.5	2.2

(2) Discussion. From the evidence available, the gas release of March 5 closely resembled that of March 11, except that the latter was much smaller.

In both cases, slight evidence of a release may be seen from a detailed scrutiny of the FGM records. Since both releases were significantly indicated by the results of cover-gas analyses and were barely perceptible in the FGM records, it may be concluded that the released gas was deficient in the shorter-lived rare-gas fission-product isotopes.

At least three items of information indicate that the March 5 and March 11 releases did not involve loss of sodium bond:

1) The decay of ^{135}Xe after the March 5 release followed a simple 9.2-hr decay curve. If sodium containing ^{135}I had been released, the decay rate would have been complex.

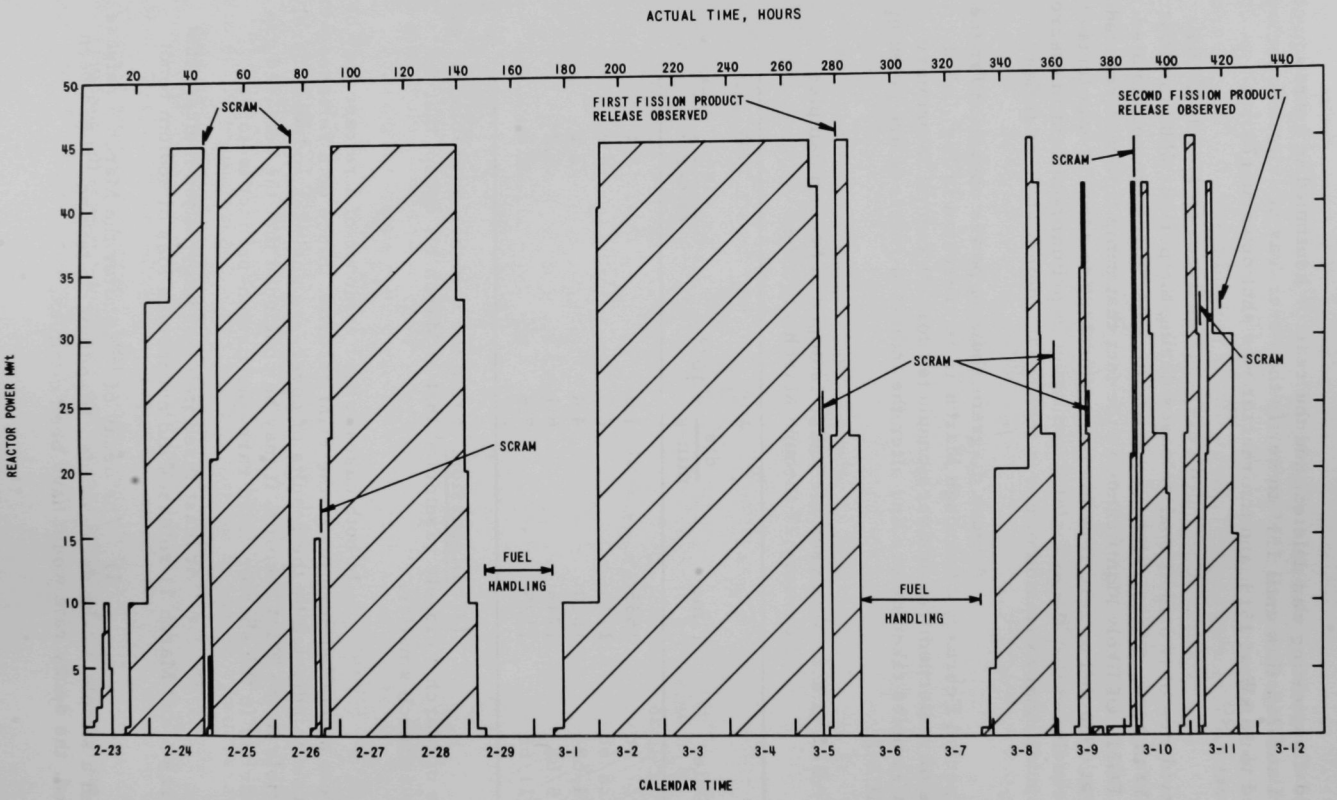

Fig. II.E.3. EBR-II Power Operation for February 23 to March 12, 1968

2) The increases in ^{133}Xe and ^{135}Xe counting rates in all cases (March 5, March 11, and two on March 12) were too sharp to identify with a buildup from ^{133}I and ^{135}I. Step changes such as those observed are characteristic of simple gas releases.

3) The slight increases in ^{131}I activity in sodium samples between 1610 March 4 and 1745 March 5, and between 1745 March 5 and 1125 March 11, are accountable in terms of normal buildup from the time-power history. A significant leak of bond sodium would have caused an increase in the ^{131}I level, which would have been unaccountable in terms of the actual time-power history.

The evidence indicates that the various releases were of the gas type and not a result of sodium bond loss. The question then arises as to whether the release was associated with a driver-fuel element or an experimental capsule.

In a driver-fuel element, iodine, bromine, and rare-gas species are continuously emitted by recoil action to the sodium bond, and the gas space above a driver element will contain short-lived species such as ^{88}Kr, ^{89}Kr, and ^{138}Xe, each of which is sensed by the FGM. Since the increase in the FGM signal was barely perceptible, however, it must be concluded that a substantial fractionation of rare-gas species (on the basis of half-life) occurred. In other words, some physical process was responsible for "holding up" fission-product gases until the shorter-lived species such as ^{88}Kr, ^{89}Kr, and ^{138}Xe preferentially decayed. Such a physical process suggests, but does not prove, a mechanism based on an intermittent or pulse-type release of a gas bubble from an experimental fuel element into the gas plenum region of the capsule. After a period of decay, the gas at some later time escapes through a defect in the gas region of the capsule. This could be caused by continued pressure buildup in the capsule, by a sudden opening of the defect, or by a reduction in pressure in the primary coolant outside the plenum. Since the fission gas decays for some time before entering the primary coolant, the shorter-lived isotopes, when compared to normal equilibrium values, will have a lower concentration than the longer-lived isotopes.

Data are still being collected and evaluated in the attempt to locate and fully understand the release. Prior to the March 5 release, it had been hypothesized that the December 7, 1967, release had been associated with one of the two experimental subassemblies, XG05 or XA08. After inserting XG05 in the core and experiencing the subsequent release, it was tentatively concluded that XG05 contained the failed capsule. After replacing XG05 with XA08 and experiencing the second release, however, this conclusion was not considered valid. Further attempts to determine the location of the failed fuel and to show a definite relationship between the December and March fission-product releases have proven inconclusive.

Two IBM-1620 computer programs were written for predicting the radioactivity levels of the primary sodium and cover gas due to normal operation, and these programs are now being used in the analysis and evaluation. Because of erratic power operation during periods of testing, and because background activity levels in the primary coolant and argon cover gas are a function of power level, it is often difficult to determine if measured values of activity are normal or abnormal. The programs just developed are capable of predicting, with an appropriate input of power-time history, the activity levels of the fission-product gases and other species fixed in the coolant at any time in power operation. These predicted values can then be compared to measure values to determine the normality of the particular activity in question.

(3) Conclusions and Summary

1) Detectable increases in the ^{133}Xe and ^{135}Xe activities from primary-coolant cover-gas samples were observed on March 5, 11, and 12. Subsequent behavior of the fission-product species is indicative of a gas-type release.

2) The small March 5 and 11 releases were verified by the FGM.

3) No significant increase was noted in the FERD signals before, during, or following the indicated times of release.

4) The two very small releases of March 12, occurring after reactor shutdown, were probably caused by a decrease in primary-coolant pressure resulting from a flow reduction.

5) The evidence indicates that the fission-product release is from an experimental capsule rather than a driver element.

6) The qualitative behavior of the indicated releases is consistent with a mechanism involving a defect in the plenum region of an experimental capsule containing a failed fuel pin. This model also theorizes a "diffusion" or "holdup" time in which the fission gas has an opportunity to decay before entering the primary coolant.

7) Attempts to show a relationship or nonrelationship between the December 7, 1967, fission-product release and the releases of March 5 to 12 are now inconclusive but are continuing.

c. Nuclear Analysis Methods Development (P. J. Persiani)

Last Reported: ANL-7427, pp. 46-51 (Feb 1968).

(i) Physics Analysis Statics

(a) Full Core-loading Representation of Run 27-1. The full representation of Run 27-1 by the SNARG 2-D code has been developed, it being intended to avoid the assumption of symmetry about an axis in that asymmetric configuration. Since this representation requires 99 compositions and 112 regions, the storage requirements of the code for the S-4 case make it necessary to use a smaller number of mesh points than appeared for the symmetric cases previously presented. The meshing is presented in Fig. II.E.4. All subassemblies appearing in Rows 1-8 are distinct, but outer rows are not fully described. It is expected that a mesh spacing equal to the width of one subassembly along the ordinate and to half this distance on the abscissa will yield acceptable accuracy in calculations confined to the core region, Rows 1-6.

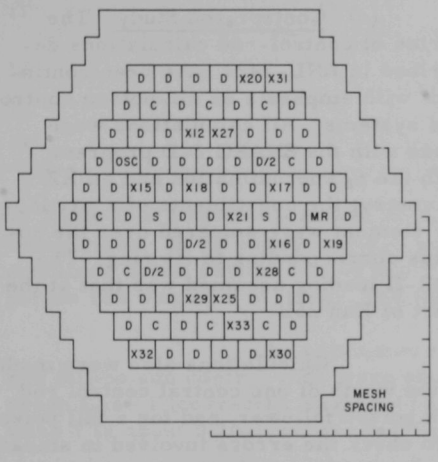

Fig. II.E.4. Run 27-1, SNARG Two-dimensional, Full Representation Meshing

(b) The Effect of Nonaxial Expanding Fuel Loadings on the Power Reactivity Curve. A series of extrapolations based on SNARG 2-D RZ calculations was performed to estimate the effect on the power coefficient due to the replacement in Runs 24, 26A, and 26C of some alloy-fuel subassemblies by oxide-fuel subassemblies, which are assumed to have a negligible axial expansion coefficient. The SNARG calculations provided row-wise expansion worths for alloy-fuel subassemblies, and these values were scaled down by the fraction of the ring replaced by oxide-fuel subassemblies. As an example, the power reactivity curves resulting from full replacement are presented in Fig. II.E.5 for Row 4, and are compared with the zero-replacement curves. Partial replacement effects are linear between the zero- and full-replacement curves. It is seen from the figure that in Run 24, which has a depleted uranium blanket, the full replacement with oxide-fuel results in a decrease of 8 Ih for the Row 4 case at 45 MW. In Run 26, which has a stainless steel reflector, the corresponding decrease is 12 Ih.

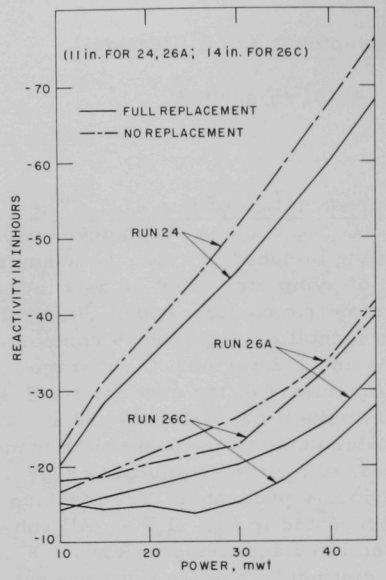

Fig. II.E.5. Total Power Reactivity Curve, Row-4 Oxide Replacement

The power reactivity curve for the uranium-blanketed system is least affected by a reduction in the fuel-expansion component. Further, the less pronounced positive bowing feedback will also allow testing a larger number of ceramic-fueled subassemblies than in a partially reflected system.

(c) Control-rod Study. The series of control-rod calculations described in ANL-7427 have been continued, with emphasis on all-poison control-rod systems. All calculations were made with the SNARG 2-D program, with the S_2 approximation and an RZ geometry; the constituents of a particular element were smeared over the annulus corresponding to its ring. The EBR-II loading assumed was that at the start of Run 26B.

Calculations also were made of the worth of one central control rod for the cases of a fuel control rod with poison follower, and for a full poison rod. These calculations can be used to check the errors involved in smearing the ten control rods in Ring 5 over an annulus, and will also be used in conjunction with the development of variational-flux-synthesis calculational methods now under study.

Tables II.E.3 and II.E.4 give results for the fuel-poison follower and full poison control rods, respectively. Cases 1-4 and 7

TABLE II.E.3. Calculated Reactivity for Movement of Fuel Control Rods with B_4C Poison Followers
(For Cases 8 and 9, Ring 5 is as in Case 1)

Case No.[a]	Core Ring	No. of Control Rods	Location of Fuel Section in Control Rod	Volume Fraction of V_4C in Follower	k
1	5	10	Completely in core	none	1.0359
2	5	10	Completely in core	0.353	1.0284
3	5	10	Lowered; bottom 5.9 in. out of core	0.353	1.0031
4	5	10	Lowered completely out of core	0.353	0.9328
7	5	10	Lowered completely out of core	0.406	0.9256
8	1	1	Completely in core	0.406	1.0342
9	1	1	Lowered completely out of core	0.406	1.0091

[a]The numbering of the cases as used in ANL-7427 has been retained; therefore some case numbers are missing.

TABLE II.E.4. Calculated Reactivity for Movement of Full Poison Control Rods with a 0.406 Volume Fraction of B_4C (For Cases 13 and 14, Ring 5 is as in Case 1 of Table II.E.3)

Case No.	Core Ring	No. of Control Rods	Location of Poison Section on Control Rod	k
10	5	10	Bottom at core top	0.9594
11	5	10	Lowered; bottom 7.8 in. from core top	0.8975
12	5	10	Bottom at core bottom	0.8637
13	1	1	Bottom at core top	1.0189
14	1	1	Bottom at core bottom	1.0028

of Table II.E.3 were contained in ANL-7427 and are included here for comparison. In all cases, the B_4C poison had a density of 2.5 g/cc and contained boron enriched to 69 a/o ^{10}B. The poison section for the full-poison rod was 13.5 in. long. The following results are of interest:

The calculated total worths of the fuel-poison follower and full-poison control rods were about the same. The difference in k between Case 2 (corrected slightly to a B_4C volume fraction of 0.406) and Case 7 is about 0.10, whereas that between Cases 10 and 12 is about 0.095.

The total worths of the control rods in the center of the reactor were 1.6 and 2.5% Δk for a full-poison and a fuel-poison follower rod, respectively. These numbers can be compared roughly with one-tenth of the values mentioned in the previous paragraph for ten control rods in Ring 5. The ratio of the total worth of one rod in Ring 1 to that in Ring 5 is roughly 1.7 and 2.5 for the cases of a full-poison and fuel-poison follower rod, respectively. Both numbers agree roughly with experimental results reported previously* for a smaller core for which the worth of a fuel subassembly in Ring 1 was about twice its worth in Ring 5.

As discussed in ANL-7427, a question of interest to users of the EBR-II as an irradiation facility is how uniform in the z-direction the flux will be with a poison control system. A good measure of the flux "tilt" is the vertical fission density distribution. Figure II.E.6 shows this distribution in the ring containing the full-poison control elements and the ring just next to it for an extreme case, No. 11 of Table II.E.4. As predicted in ANL-7427, this "tilt" is about the same as that for the fuel-poison follower extreme case, No. 9 of Table II.E.3. (Note that for both these cases, the poison section bottom is at about the middle of the core.) Except for the extreme upper section of the core, this ratio varies only several percent.

*Kirn, F. S., and Loewenstein, W. B., ANL-6864 (Oct 1964).

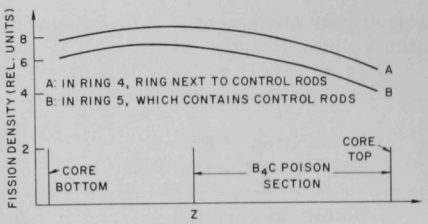

Fig. II.E.6

Fission Density Distribution for 10 Full-poison Control Rods Inserted 7.8 in. into Core (Case 13, Table II.E.4)

(d) Physics Analysis--Dynamics. During this report period a FORTRAN code has been written for use with the 160-A to aid in determining analytic coefficients in a dynamics model from reactor experimental data. At present the code can handle up to four coefficients which can be plus or minus in sign.

Some additional preliminary values for constants in the EBR-II control-rod-bank block diagram (see ANL-7427, p. 46, Fig. I.E.3) are as follows:

$$\theta_c/P = 3.6°F/MW$$

$$\theta_p/P = 2.93°F/MW$$

$$C_1 = 5.06 \times 10^{-4} \text{ in./°F}$$

$$C_2 = 1.8 \times 10^{-4} \text{ in./°F}$$

$$C_3 = 2.0 \times 10^{-4} \text{ in./°F}$$

$$C_4 = 2.0 \times 10^{-4} \text{ in./°F}$$

$$W = 2.23 \times 10^{-3} \ \delta k/k \text{ per inch.}$$

The total expansion at 45 MW is 153 mils, corresponding to 3.42×10^{-4} $\delta k/k$ or 14.7 Ih.

d. Reactor System Testing, Surveillance, and Evaluation (B. C. Cerutti)

Last Reported: ANL-7427, pp. 51-54 (Feb 1968).

(i) Fuel-handling Operations. The 70.6-in. elevation at which difficulty was encountered in placing subassemblies in reactor core positions 5D4 and 6E1 is the same elevation at which difficulty was encountered during the recent problem with a damaged control-rod thimble.

At this elevation the bottom of the subassembly hex can is passing the top of the control-rod thimble (position 5D4 is between the thimbles for control rods Nos. 2 and 3).

A special dummy subassembly (E-82), fabricated with a smooth transition between the hex can and the lower adapter, was installed in core position 5D4 with no indication of binding or hangup on the upper edge of either thimble. A force of less than 50 lb was required to insert this special dummy subassembly. The subassembly was then removed from the core, transferred to FCF, and washed. Inspection showed light scratch marks on five of the six hex-can flats, but none of the marks indicated that significant damage could have occurred to the adjacent thimbles.

Changes in assembly procedures and specifications for all EBR-II subassemblies are being made to eliminate overhanging edges which could cause interference at the lower edges of the hex cans. This change will be made to all subassemblies loaded into the primary tank in the future.

(ii) Force Settings on Main Core Gripper. Because of difficulties encountered during insertion of subassemblies into the reactor, the push-force settings on the main core gripper were decreased to prevent possible damage to components. The high and low push forces were set at 250 and 175 lb, respectively, and these settings have been retained.

(iii) Special Procedures for Fuel Handling. Assistance was given to the EBR-II Operations Group in revising the special and abnormal operating procedures for the EBR-II fuel-handling system. A comprehensive review was made of abnormal alarm conditions that might arise during fuel-handling operations, and new operating procedures were written for the operating manual. Operator training classes are planned for discussion of fuel-handling procedures and problems that might be encountered during routine fuel-handling operations.

e. Higher Power Operation (R. E. Rice)

Last Reported: ANL-7419, pp. 50-52 (Jan 1968).

Prototype reorificed driver subassemblies were installed in core positions 4F3, 5C2, and 6C4. The readings of the outlet temperature thermocouples in these locations were compared with readings when standard driver subassemblies were in these locations. The decrease in temperature was less than that predicted from the inverse flow ratio. The reason for this is being investigated, but it is suspected that thermocouple readings are being affected by mixing of coolant flow from adjacent subassemblies.

f. Fuel Swelling and Driver Surveillance

(i) Mark IA--Anomalous Fuel Swelling Investigation (F. G. Foote)

Last Reported: ANL-7427, pp. 54-58 (Feb 1968).

(a) Extended Burnup of MC-S-type Fuel Pins. The Fuel Surveillance Committee has recommended that Subassembly C-291, known to contain only low-swelling fuel, be reinserted into the core for an additional 0.1 a/o burnup.

(b) High-burnup Irradiations of Mark-IA Fuel. Subassemblies XO15 and XO17 are accumulating additional burnups. Subassembly XO17 will reach target burnup of 1.5 a/o midway through Reactor Run 28.

(c) Effect of the Change to Mark-IA Design upon Fuel Swelling. Swelling results from Subassembly C-298 are not yet available. The conclusions, drawn from the examination of fuel elements from Subassembly C-297 and reported previously (see ANL-7427, pp. 54-55), remain unchanged.

(d) Effect of Enrichment Increase from 48% (Mark I) to 52% (Mark IA). Swelling results from Subassembly C-293 are not yet available. The conclusions, drawn from examination of fuel elements from Subassembly C-283 and presented previously (see Progress Report for January 1968, ANL-7419, pp. 53-54), remain unchanged.

(e) Effect of Pressure upon Swelling of U-5 w/o Fs Alloy. All postirradiation measurements of the pins from Capsule P-3 have been made. Estimate of burnup still must be confirmed. A metallographic examination may also be made if needed for further interpretation of the results. Capsule P-3 concludes the pressurized capsule series.

Postirradiation data for P-3 appear in Table II.E.5. The data for both fuel swelling and fission gas release, plotted versus

TABLE II.E.5. Density Data for P-3 Pressure Specimens Undergoing Estimated 1.3 a/o Burnup[a]

Specimen No.	Cast Pin No.	Mean In-reactor Fuel Temp (°C)	Mean[b] In-reactor Pressure (psia)	Preirradiation Density (g/cc)	Postirradiation Density (g/cc)	$\Delta V/V^c$ (%)	Fission Gas Release (% of Theoretical)
1	54-1	591	1829	18.09	16.04	12.8	-
2	-2	618	953	18.11	14.50	24.9	-
3	-7	591	522	17.98	13.83	30.0	5.8
4	-4	618	258	18.12	11.52	57.3	23.7
5	-5	591	117	18.12	11.08	63.5	42.2
6	-6	618	84	18.12	10.27	76.4	74.8

[a]All of melt No. 409.
[b]Effects of fuel swelling and gas evolution are not included.
[c]Calculated from density change.

in-reactor pressure in Fig. II.E.7, are based on an estimated burnup of 1.3 a/o. According to the relationships shown, the release of fission gas is much more effectively restrained by the application of external pressure than is the swelling of the fuel.

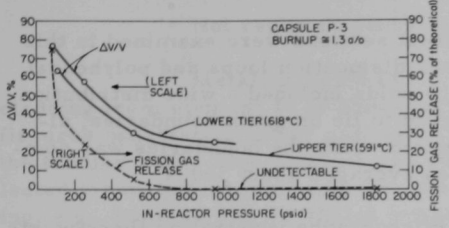

Fig. II.E.7. Effect of Pressure on Swelling and Gas Release

The existence of two separate ΔV/V versus pressure curves for the upper and lower tiers of the specimens reflects some measurable difference in burnup and temperature of irradiation.

(f) Effect of Heat Treatment upon Swelling of U-5 w/o Fs Alloy. Analysis of the pins irradiated in Capsule H-1 gave burnup values of 1.03 a/o for the lower tier and 0.96 a/o for the upper tier; estimated burnup was 1.2 a/o for both tiers.

Pins irradiated in Capsule H-2 are being cooled and have not yet been examined.

A decision has been made to omit the irradiation of Capsule H-3 because of its projected low-information yield. The tentative conclusion from the two previous capsules in this series is that swelling is independent of prior heat treatment. Any difference in heat treatment appears, at this time, to be cancelled out early in the neutron-exposure period.

(g) Hot Laboratory Examination of Irradiated Fuel

(1) Fuel Surveillance. Swelling data and calculated fuel-pin burnup are now available for 54 fuel elements from six different subassemblies that were removed from the core at the end of Reactor Run 26.

Two subassemblies (C-2132, 2133) that contained fuel elements of the Mark-IB design were inserted into the core (in reactor grid positions 3B1 and 3C1, respectively) at the beginning of Reactor Run 27. Subassembly C-2132 is scheduled for removal midway through Reactor Run 28 at approximately 0.5 a/o burnup.

(h) Analysis of Fuel-pin Swelling. The good correlation between high silicon content and low swelling remains unchanged.

(ii) Voids in Mark-IA Fuel Cladding (S. D. Harkness)

Not previously reported.

Mark-IA fuel cladding has been examined by transmission electron microscopy. The Type 304L stainless steel-cladding sections were

taken from a fuel element that exhibited high swelling (fuel $\Delta V/V > 13\%$). There was evidence that the fuel had been in contact with the cladding in this element, thereby significantly raising the cladding stress level.

Foils from two different sections were examined in this initial study. A large number of Frank dislocation loops and polyhedral voids were found in each sample. The voids included a wide distribution of sizes. Very few voids were observed to lie on grain boundaries, although the occurrence of depleted regions along the boundaries was common. The width of the depleted region averaged about 350 Å.

Two representative micrographs illustrating these points are presented in Fig. II.E.8. The average void size ($\langle D \rangle$), number density (N_v), and volume fraction (V_f) calculated from a series of micrographs are listed in Table II.E.6.

SH-7

Sample 1--Tilted to show dislocation loops

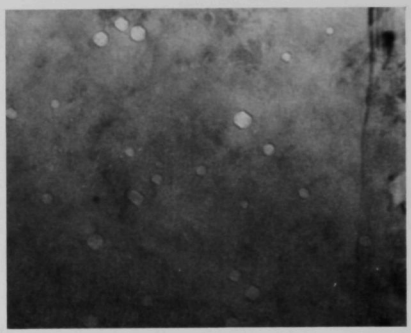

SH-10

Sample 2--Dislocation loops out of contrast. Note polyhedral shape of voids.

Fig. II.E.8. Structure of Mark-IA Fuel Cladding (Magnification 208,000X)

TABLE II.E.6. Results of Examination of Mark-IA Fuel Cladding

Sample No.	Max Cladding Temp (°C)	Approximate Fluence ($n/cm^2 \times 10^{-22}$)	$\langle D \rangle$ (Å)	N_v (No./$cm^3 \times 10^{-15}$)	V_f (%)
1	480	1.2	93	5.4	0.2
2	465	1.4	105	4.0	0.2

(iii) Cladding-integrity Investigation of Mark-IA Fuel Elements (R. A. Noland)

Not reported previously.

Metallographic sections of the Type 304L stainless steel cladding from element 16 of Subassembly C-249 were found to have axial fissures penetrating either partially or, as in one section, entirely through the tubular wall. This element was one of four Mark-IA fuel elements selected for metallographic examination because of relatively high fuel swelling, e.g., from 10.9 to 14.8%, as indicated by sodium measurements. The fuel-pin swelling in element 16 was the third highest of the group, namely, 13.5%. No fissures were found in any of the sections of the three other elements examined. All were transversely sectioned at 1.0-in. intervals that started upwards from a point 6.25 in. from the lower end of each element; thus the regions of highest burnup and maximum temperature were sampled.

A task force has been organized that will attempt to determine the cause(s) of the fissures in element C-249-16, and to establish whether the problem is unique to this element or involves other elements. A preliminary work plan has been drawn up by the task force, and action that implements this plan is now underway in Illinois and in Idaho.

Twelve additional elements that exhibited low as well as relatively high fuel swelling after irradiation are now on hand from the EBR-II site. Eleven of the group are clad with tubing from the same batch used to clad element 16. These elements, along with seven tubes from which the irradiated fuel has been removed, are being investigated.

(iv) TREAT Experiments (F. G. Foote)

Not reported previously.

(1) Fuel-motion Studies with Mark-IA Fuel Elements (C. J. Renken)

Pulsed electromagnetic test equipment has been designed that will measure the motion of the fuel inside irradiated Mark-IA fuel elements while they undergo transient irradiation in TREAT. Hopefully, the motions of the fuel and sodium can be measured separately and without interference from the drastic change in electrical resistivity of the fuel-element materials during the transient irradiation. Suppression of this resistivity transient will be accomplished by means of a differential transducer, sensitive only to the actual sodium meniscus and the end of the fuel. Differentiation between the fuel motion and the sodium motion should be

possible by means of an analysis of the reflected pulse at various sampling points. The transducer must be capable of withstanding the ambient temperature around the fuel element (approximately 150°C) and must be shielded from the heat developed in the fuel element during the transient. Construction of the electronic equipment is about 50% completed.

g. Mark-II Driver Fuel Element Development (J. H. Kittel)

Last Reported: ANL-7427, p. 59 (Feb 1968).

As of March 6, Run 27B was completed, with a total of 461 MWd of exposure for Run 27. Table II.E.7 presents the status of Mark-II fuel elements being irradiated in experimental Subassembly XO29.

TABLE II.E.7. Status of Encapsulated Mark-II Fuel Elements Irradiated in Experimental Subassembly XO29 in EBR-II

Position No.	Element No.	Enrichment (%)	Element Length (in.)	Restrainer Type and Location[a] (in.)	Max kW/ft	Max Temp at Fuel Center (°C)[b]	Temp of Cladding ID (°C)[b]	Calculated Burnup (a/o)
1	265	93.15	26	A 0.75	10.48	643	551	0.27
2	237	93.15	24	C 0.18	10.28	649	559	0.27
3	213	93.15	24	B 0.32	10.33	647	557	0.26
4	203	93.15	24	A 0.33	10.31	637	548	0.26
5	266	93.15	26	B 0.72	10.33	649	559	0.26
6	259	93.15	26	B 0.25	10.37	668	582	0.26
7	255	93.15	26	C 0.77	10.36	669	584	0.26
8	232	93.15	24	A 0.27	10.32	664	580	0.26
9	212	93.15	24	B 0.24	10.26	640	553	0.26
10	234	93.15	24	B 0.27	10.30	646	557	0.26
11	251	93.15	26	C 0.34	10.26	669	584	0.26
12	262	93.15	26	A 0.38	10.25	671	589	0.26
13	230	93.15	24	C 0.21	10.16	667	586	0.26
14	263	93.15	26	A 0.38	10.14	662	579	0.26
15	258	93.15	26	A 0.75	10.07	618	538	0.26
16	288	93.15	26	C 0.27	10.13	637	548	0.26
17	267	93.15	26	C 0.70	10.20	664	579	0.26
18	205	93.15	24	A 0.23	10.15	667	586	0.26
19	218	93.15	24	C 0.25	10.12	666	586	0.26
20	284	80.0	26	A 0.70	8.74	628	557	0.22
21	200	80.0	24	C 0.26	8.70	621	549	0.22
22	270	80.0	26	C 0.75	8.66	595	519	0.22
23	209	80.0	24	A 0.25	8.74	623	542	0.23
24	201	80.0	24	C 0.19	8.73	627	553	0.22
25	275	80.0	26	A 0.27	8.68	628	558	0.22
26	279	80.0	26	B 0.24	8.73	623	554	0.22
27	202	80.0	24	C 0.20	8.63	622	551	0.22
28	287	80.0	26	B 0.64	8.64	600	527	0.22
29	225	80.0	24	C 0.21	8.67	604	529	0.22
30	289	80.0	26	C 0.72	8.66	621	553	0.22
31	227	80.0	24	A 0.25	8.59	621	550	0.22
32	219	80.0	24	B 0.27	8.59	615	545	0.22
33	276	80.0	26	A 0.78	8.59	594	524	0.22
34	277	80.0	26	B 0.27	8.60	596	520	0.22
35	207	80.0	24	C 0.20	8.59	599	526	0.22
36	269	80.0	26	C 0.25	8.55	596	526	0.22
37	283	80.0	26	A 0.68	8.46	588	516	0.21

[a]Tube restrainer type:
A = Slotted.
B = Nonslotted.
C = Three indents equally spaced.
Location: distance of restrainer above the top of the fuel.
[b]Temperatures calculated with Hectic II Code with depleted uranium blanket.

Twenty-five replacement capsules were shipped to Idaho early in February. These were to replace capsules scheduled for removal at intervals of burnup from 1 through 5 a/o. Upon receipt, the closure welds

were inspected by X-ray techniques, and 22 out of 25 capsules were rejected because of weld-metal thinning below the tube-wall thickness. The fault lay in the joint design because acceptable welds were difficult to obtain consistently even with utilization of fully automatic welding procedures.

The capsules will be returned to Illinois for repair or re-encapsulation in the event repairs cannot be made. In the past, repairs were not possible in areas where sodium was present. In the event the welds cannot be repaired, two joint-designs have been proposed that would result in acceptable welds not sensitive to small changes in welding procedure. Test samples have been prepared and sent to Idaho for review.

h. Equipment--Fuel Related (E. Hutter)

(i) Improved Gripper and Holddown Force-limit Device

Last Reported: ANL-7427, pp. 59-60 (Feb 1968).

The electronic control system was connected to the other components of the test rig. Then the entire prototype improved gripper and holddown force-limit device was operated to evaluate performance. The control system functioned satisfactorily in stopping the drive motor when preset force limits were reached; the tripping, checking, and force-remembering functions also operated properly.

Calibration procedures were conducted to obtain qualitative results, and a certified calibrated force gauge was used to measure the forces applied by the mechanism. (Previously, the force gauge was found to be in error and was returned to the factory for correction and certification of its accuracy. When returned, it was checked briefly in tension and appeared to be satisfactory.) Anomalous results were obtained during calibration of the applied push forces. The spring constant of the force-limit assembly appeared to differ for push forces and pull forces. For example, for equal spring displacement, the push force was 2250 lb and the pull force was 1750 lb. Some hysteresis and nonlinearity also were indicated. Investigation revealed that the calibration constant for the force gauge was different in compression and tension, and would account for most of the discrepancy noted. The force gauge is being recalibrated again on a tensile-testing machine. Initial tests indicate that the calibration constant and hysteresis of the gauge depend considerably on the mounting arrangement.

Although the initial tests of the force-limiting device indicate that the design is sound and major design changes are not necessary, qualitative and quantitative tests will continue. Electronic parts are being obtained for the final unit.

(ii) Oscillator Rod Mark II

Last Reported: ANL-7427, pp. 60-61 (Feb 1968).

Drawings for the Mark-IIB Type-IV oscillator rod have been checked and are being reviewed by the plant modification committee.

Fabrication of the oscillator-rod special thimble, storage-basket adapter sleeve, and adapter-sleeve handling tool has started.

i. Equipment--Reactor and Primary Coolant System (B. C. Cerutti)

Last Reported: ANL-7427, pp. 61-62 (Feb 1968).

(i) General Improvements

(a) Instrumentation for Argon Cooling System (ACS) of Fuel-unloading Machine. The design of an auxiliary source of power for the dc turbine motor in the ACS was approved. This new power supply will prevent inadvertent use of the batteries which are the source of emergency power.

(b) One-hundred-point Data-acquisition System. Following a series of tests using plant parameters as input to the one-hundred-point data-acquisition system, a standard input filter was designed to reduce electronic noise. The filter network was packaged with a mating quick-disconnect plug to permit inserting the filter directly to the input line. The filter is effective for noise reduction to a level of $\pm 20\ \mu V$.

(c) Spare Control-rod Drives. The reworked gripper jaws for the two new spare control-rod drives were returned to ANL-ID from ANL-Central Shops, where they had been remachined to the latest cam contour design and rechromed as requested by the EBR-II Engineering Group. The grippers were reassembled and the drives are essentially ready for use.

(d) Control Rods. A proposal to add a special collar to existing control-rod subassemblies to prevent damage to thimbles during fuel-handling operations was approved by the Plant Modification Committee. This collar will permit the core holddown to move the control-rod thimble out of the way when subassemblies are installed adjacent to the control-rod position.

(ii) Sodium Sampling Pump and Filter. Tests of the modified pump-drive mechanism using a Formsprag reverse-locking clutch were not satisfactory, so the clutch was removed. Further investigation indicates that the electrical modifications, employing a timing relay and ammeter, will satisfactorily provide a positive indication of pump malfunction. These electrical modifications are being accomplished.

(iii) Seal Intermediate Heat Exchanger. Working drawings of the single continuous-strip baffle have been completed. The baffle is being fabricated. A test rig to accommodate the baffle will be constructed of Type 304 stainless steel. The test rig, with the baffle mounted in place, will be soaked in 700°F sodium to determine whether the spring characteristics of the baffle are affected.

j. Secondary Sodium and Power Systems (B. C. Cerutti)

Last Reported: ANL-7427, pp. 62-64 (Feb 1968).

(i) Sampling Systems for Secondary Sodium. The fire-damaged instrumentation and control systems for the secondary-sodium sampling system are being restored. Line heaters were reinstalled on the sampling loop piping outside the control panel, and each heater circuit was temporarily connected to a variable transformer. Temperature sensors were permanently mounted on the piping and were temporarily connected to the read-out instrument.

(ii) General Improvements--Power Plant

(a) pH Control Failure Alarm. In the case of a control failure, the pH indicator-controller used for programming acid injection into the main-condenser cooling-water system continues to add acid to the water. An alarm and actuating circuit has been designed to alarm on a control failure.

(b) Automatic Trip for Turbine-driven Condensate and Feedwater Pumps and for Blowdown Valve. A design modification was approved for providing an automatic trip for the turbine-driven condensate and feedwater pumps and the blowdown valve upon occurrence of a reactor scram.

(c) Wide-range Temperature Monitor for Steam Header. The design work on a wide-range temperature monitor for the steam header was completed. This monitor will be located on the turbine-generator gauge panel to provide the turbine operators with local indication for heat-up of the turbine during startup.

(d) Relocation of Steam Controller for No. 2 Feedwater Heater. The design work to provide control from the control room of the steam to No. 2 feedwater heater was completed.

k. Instrumented Subassembly (E. Hutter)

(i) Design (E. Hutter)

Last Reported: ANL-7419, p. 65 (Jan 1968).

(a) Drywell Concept. The sheathed instrument leads will be fastened and sealed to the bulkhead in the sodium-free dry well that will be between the extension tube and an inner hexagonal tube. Termination at

the bulkhead will permit the use of normal ceramic-bead insulation on lead wires from this point to the recording instrument on the reactor operating floor.

Methods are being developed for brazing 22 sensor leads, such as 62-mil-dia sheathed thermocouples, into the dry-well bulkhead. All the components involved in the braze joint are made of Type 304 stainless steel. A high-temperature nickel-base brazing alloy (GE No. 81) has been selected; a 30-kVA 10,000-cycle induction heater is being used. To minimize the temperature differences across the braze joints, which are of nonuniform thickness, heat is supplied to the work by radiation from a steel susceptor.

Originally, it seemed that a nonexplosive mixture of 95 v/o helium and 5 v/o hydrogen would be a suitable atmosphere for brazing simulated samples at 1160°C. This atmosphere, which was purified by passing it through a platinum catalyst and molecular sieves, maintained the surface in a bright condition. However, it did not activate the surfaces in the joint areas sufficiently to accomplish complete wetting. Figure II.E.9, which shows a typical microstructure in a joint brazed with this gas mixture, reveals considerable porosity and two large nonwetted areas. These deficiencies were overcome by using tank hydrogen (that had been purified in the same manner) to pretreat the braze joint without any brazing alloy at 1160-1180°C to activate the surface, then cooling the work to room temperature, adding the braze material as a powder, and reheating the assembly to 1160°C in hydrogen. Figure II.E.10 shows a typical microstructure obtained using this procedure.

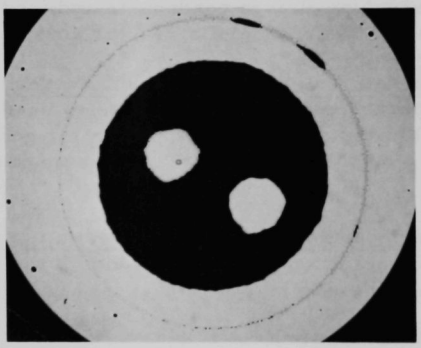

Fig. II.E.9. Considerable Porosity and Two Large Nonwetted Areas Are Evident in Brazed Joint Where the Thermocouple Sheath Passes through Bulkhead. This joint was brazed in helium-hydrogen mixture and pieces were not pretreated.

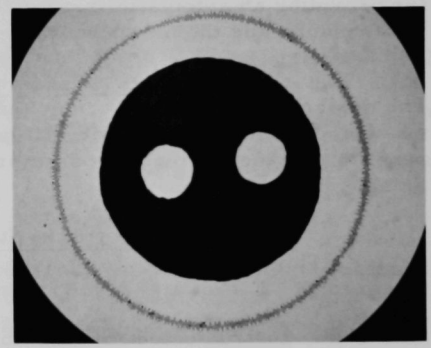

Fig. II.E.10. Sound Joint Was Made in 100% Hydrogen Atmosphere after Surfaces Were Activated by Pretreatment. In both cases, surfaces were Type 304 stainless steel, brazing alloy was GE No. 81, and brazing temperature was 1160°C.

Two full-scale simulated samples, such as shown in Fig. II.E.11 were brazed using the same procedures. Both samples appear to be properly brazed and are leaktight as determined by a helium mass spectrometer leak detector.

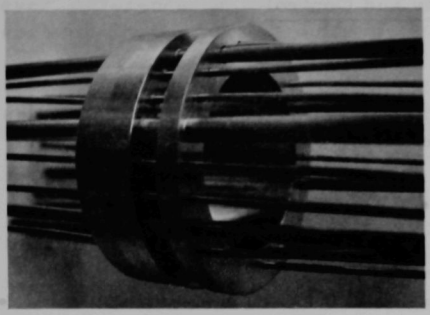

Fig. II.E.11. Full-scale Simulated Sample Brazed with Method Used for Fig. II.E.10. Leaktight joints were made where 22 instrument sheaths pass through bulkhead.

A full-scale fixture is being built for brazing the bulkhead in the subassembly structure, which will be 12 ft long at this stage of construction.

(b) Fuel-pin Thermocouples. The design of the fuel-pin thermocouple is final except for details of the hermetic seal.

All the materials, except for the hermetic seals, are available. Construction procedures being developed will be used to build thermocouples for test and, possibly, for use in the instrumented subassembly.

The hermetic seal desired for the fuel-pin thermocouples would have a 0.160-0.220-in. diameter and would employ an alumina insulator that is brazed into place. A prime objective in the design of the seal is to develop a configuration that can be purchased quickly.

The hermetic seal for the sheathed leads and low-temperature thermocouples must not increase the sheath diameters. Available ceramic seal materials that could be melted into the open end of a sheath are being investigated.

A number of sheathed leads, some dried and sealed and others unsealed, have been brazed into a bulkhead to determine the effect of moisture on brazing. Measurements of insulation resistance at high temperature will be used to evaluate the effects of the brazing.

1. Packaged Loop (B. C. Cerutti)

Last Reported: ANL-7419, p. 65 (Jan 1968).

The feasibility study for the packaged loop is in progress. Increased effort is being devoted to the removal coffin, and to insertion and removal problems of the in-reactor tube. Auxiliary components such as the surge tank and the purification system are being studied in greater detail.

m. Process Chemistry (D. W. Cissel)

Last Reported: ANL-7427, pp. 64-70 (Feb 1968).

(i) Sodium Coolant Quality and Control

(a) Primary Sodium

(1) Sampling. Table II.E.8 lists the sodium samples taken from the primary system for the period 2/16/68 through 3/15/68.

TABLE II.E.8. Primary Sodium Samples

Date	Container	Analysis
2/23/68	two 10-ml Pyrex beakers	Trace metals
2/27/68	10-ml Pyrex beaker	Activity
2/28/68	10-ml Pyrex beaker	Activity
2/28/68	1-in. aluminum tube	Historical
3/4/68	10-ml Pyrex beaker	Activity
3/5/68	10-ml Pyrex beaker	Activity
3/5/68	1/2-in. stainless steel tube	O_2, H_2
3/7/68	two 10-ml quartz beakers	Trace metals
3/11/68	10-ml Pyrex beaker	Activity
3/15/68	1-in. aluminum tube	Historical
3/15/68	two 10-ml quartz beakers	Cyanide ion method development

(2) Radionuclides. Five primary-sodium samples were analyzed by gamma spectrometry for radionuclides with the results listed in Table II.E.9. (See Sect. II.E.1.b for detailed information concerning fission-product releases.)

TABLE II.E.9. Activity in Primary Sodium

Sample Date	Isotope, Ci/g		
	^{137}Cs	^{131}I	^{133}I
2/27/68		6.6×10^{-4}	1.6×10^{-3}
2/28/68		1.1×10^{-3}	2.3×10^{-3}
3/4/68		2.1×10^{-3}	1.5×10^{-3}
3/5/68	1.7×10^{-2}	2.9×10^{-3}	2.5×10^{-3}
3/11/68		3.5×10^{-3}	1.0×10^{-3}

(3) Trace Metals. One sample of primary sodium taken in a quartz beaker has been analyzed for trace metals by atomic

absorption. Results are listed in Table II.E.10. Results from samples taken in Pyrex beakers were reported in ANL-7427, p. 64. Impurities in the Pyrex were apparently dissolved during the dissolution step. Especially noticeable is the lower nickel values for the quartz-beaker samples; however, differences in nickel content might be due to particulate matter in the sodium. Further samples are required to provide more information.

TABLE II.E.10. Trace-metal Impurities in Primary Sodium

(Sample taken 3/7/68)

Impurity	Concentration (ppm)	Impurity	Concentration (ppm)
Bi	<2	Mg	<0.3
Co	<0.2	Mn	<0.1
Cu	0.2	Ni	<0.4
Fe	1.0	Sn	19

(b) Sodium Analytical Methods

(1) Carbon in Sodium. As part of the program for developing analytical methods for determining the amount of carbon in sodium, the recovery tests on carbon species in sodium are continuing by the oxyacidic flux method. A series of tests on hexahydroxy benzene, a carbon species identified in sodium by English workers, gave the results shown in Table II.E.11.

TABLE II.E.11. Carbon Recovery Tests for Hexahydroxy Benzene

Run No.	Carbon Added (μg)	Carbon Recovered (μg)	Percent Recovery
1	134.4	129.8	96.6
2	134.4	135.0	100.4
3	134.4	130.6	97.2
4	134.4	130.6	96.7
5	134.4	135.6	100.9
		Average Recovery, %	98.4

A previous series of tests with the sodium salt of ethylene diamine tetraacetic acid (EDTA) gave somewhat erratic results. A series of three repeat runs with a greater amount of carbon (as EDTA) added to the reaction vessel gave results shown in Table II.E.12.

TABLE II.E.12. Carbon Recovery Tests for EDTA

Run No.	Carbon Added (μg)	Carbon Recovered (μg)	Percent Recovery
1	128.8	130.0	100.9
2	128.8	129.8	100.9
3	128.8	134.0	104.0
		Average Recovery, %	101.8

The purpose of using EDTA is to prove the recovery of carbon from compounds containing the $\geqslant C-N\leqslant$ bond system.

Cyanuric acid recovery tests in which most of the carbon is bonded as $\rangle C{=}N-$ are in process. Library work to determine a suitable nitrile (in which the carbon is bonded as $-C{\equiv}N$) for recovery tests is progressing.

Work on the determination of CN^- in sodium using the commercially available "Orion" CN^- specific electrode has demonstrated that this method is adequately sensitive and has promise. If the CN^- ion can be quantitatively transferred to the 0.1M NaOH from the sodium sample, this method will be both fast and simple. Efforts to achieve these conditions are in progress. The "Orion" electrode crystal has already shown signs of dissolution and may have too short a useful lifetime to be practical when weighed against its cost (~$100).

n. Experimental Irradiations and Testing (D. W. Cissel)

Last Reported: ANL-7427, pp. 70-75 (Feb 1968).

(i) Experimental Irradiations

(a) Status of Experiments in EBR-II. The status of experimental irradiations in EBR-II as of March 31 is shown in Table II.E.13.

Individual suspect experimental Subassemblies XG05 and XA08 were temporarily reinserted in the reactor for Runs 27B and 27C, respectively, and then removed again after each of these runs resulted in increased fission-gas activity in the primary cover gas (see Sect. II.E.1.b).

Experimental Subassembly XO30 was removed from grid position 6E1 at the sponsor's request and transferred to the FCF for disassembly. The six capsules from Pacific Northwest Laboratory (PNL) were transferred from the FCF to the TAN (Test Area North) Hot Shop to be

TABLE II.E.13. Status of EBR-II Experimental Irradiations

Subassembly (Position)	Date Charged	Capsule Content and Number of Capsules ( )	Experimenter	Accum Exposure (MWd) 3/31/68[a]	Estimated Goal Exposure (MWd)
XG02 (7A1)	7/16/65	UO_2-20 w/o PuO_2 (1) Stainless Dummies (18)	GE	13,616	16,700
XG03 (7D1)	7/16/65	UO_2-20 w/o PuO_2 (2) Stainless Dummies (17)	GE	13,616	22,500
XG04 (7B1)	7/16/65	UO_2-20 w/o PuO_2 (2) Stainless Dummies (17)	GE	13,616	42,050
XG05[b] (4C2)	9/3/65	UO_2-20 w/o PuO_2 (9) U-15 w/o Pu-10 w/o Zr (1) U-15 w/o Pu-10 w/o Ti (1) UC-20 w/o PuC (3) Structural (5)	GE ANL ANL ANL GE	12,640	13,750
XA08[c] (4F2)	12/13/65	UC-20 w/o PuC (8) Structural (11)	ANL ANL	10,703	19,800
XO10 (7F3)	3/24/66	UO_2-20 w/o PuO_2 (4) Structural (11) Structural (4)	GE ANL PNL	10,547	19,600
XO12 (4B2)	8/10/66	UO_2-20 w/o PuO (19)	NUMEC	6,847	20,100
XO15 (4A2)	11/15/66	UO_2-20 w/o PuO_2 (11) UO_2-20 w/o PuO_2 (2) UC-20 w/o PuC (4) U-Fs (Mk-1A) (2)	NUMEC GE ANL ANL	5,192	11,000
XO16 (4D2)	1/13/67	Structural (9) Structural (10)	ANL GE	3,872	7,400[d]
XO17 (4C3)	11/15/66	UO_2-20 w/o PuO_2 (11) UC-20 w/o PuC (3) U-Fs (Mk-1A) (5)	NUMEC UNC ANL	5,192	6,500
XO18 (2B1)	12/6/66	Structural (3) Structural (1) Structural (2) Structural and Heavy Metal Fission Yield Sample (1)	GE PNL ANL ANL	4,502	21,300
XO19 (6D2)	1/13/67	UO_2-20 w/o PuO_2 (7) $(U_{0.8}Pu_{0.2})C$ (3) Structural (8) Graphite (1)	GE UNC PNL PNL	3,872	7,500[e]
XO20 (6B5)	1/13/67	UO_2-PuO_2 (9) $(U_{0.8}Pu_{0.2})C$ (3) Structural (4) Structural (2) Graphite (1)	GE UNC PNL ANL PNL	3,872	7,500[e]
XO21 (2D1)	2/27/67	Structural (7)	PNL	3,872	21,500
XO22 (7C4)	2/27/67	Structural (7)	PNL	3,872	5,000
XO25 (4E2)	10/10/67	Structural (19)	GE	2,224	7,400[d]
XO26 (7D5)	10/11/67	Structural (7)	NRL	2,224	3,000
XO27 (4B3)	11/22/67	UO_2-25 w/o PuO_2 (18) Structural (1)	GE PNL	1,195	7,200
XO28 (4D3)	11/22/67	U-15 w/o Pu-10 w/o Zr (15) U-Fs (4)	ANL ANL	1,195	9,200
XO29 (4E3)	12/22/67	U-Fs (Mk-II) (37)	ANL	576	5,100
XO30[f] (6E1)	10/10/67	Thermocouple Material (2) Graphite (3) Structural (1) Stainless Dummies (13)	PNL PNL PNL	2,108	No Limit
XO31 (6C1)	11/22/67	UO_2-25 w/o PuO_2 (19)	PNL	1,195	2,200
XO32 (6F1)	11/22/67	UO_2-25 w/o PuO_2 (19)	PNL	1,195	11,000
XO33 (5E2)	12/22/67	$(U_{0.8}Pu_{0.2})C$ (19)	UNC	576	10,000

[a] Accumulated exposure during March was 293 MWd for all subassemblies except as noted.
[b] Irradiated during Run 27B only.
[c] Irradiated during Run 27C only.
[d] New goal as defined by experimenter.
[e] Being considered for further exposure.
[f] Terminated at end of Run 27B.

loaded into a cask for shipment to PNL. The entire transfer operation to the TAN Hot Shop was performed within 44 hr after reactor shutdown to permit PNL to meet its schedule for recovery and monitoring of short-life flux dosimeters.

(b) Status of Irradiation Experiments Given Administrative Approval-in-principle (AIP). The present status of all irradiation experiments which have been approved in principle but which have not been inserted in the reactor remains the same as given in ANL-7427, p. 72, Table I.E.20.

(c) New Experimental Subassembly Design. After the General Electric Company (GE) concurred in the design of the new Mark-F-37 subassembly to accommodate 37 fuel elements having a 0.250-in.-dia cladding and wrapped with a 0.0625-in.-dia spacer wire, fabrication was started on the initial six sets of hardware.

Analysis and testing are being performed to determine the most feasible subassembly design to accommodate an irradiation with capsule surface temperature approaching 1200°F. This experiment must conform with the criterion that the subassembly effluent temperature must remain within 100°F of the average for the six adjacent EBR-II subassemblies. This work was initiated to provide an irradiation subassembly for the GE Group 5 experiments.

(d) Other Work

(1) Melt-wire Temperature Monitors. In order to measure the coolant outlet temperatures, two inner-blanket and four outer-blanket subassemblies of depleted uranium have been assembled with melt-wire temperature-monitor capsules installed in the top adapters. These capsules have tantalum liner cups to contain the melt wires. The two inner-blanket subassemblies will be installed on opposite sides of the core in Row 7, and the four outer-blanket subassemblies will be installed in Rows 8, 9, 12, and 16 in Sector E. All except the Row-8 subassembly will be under outlet-thermocouple positions. The melting points of the wires in Rows 8 and 9 are 845, 813, 788, and 720°F. Those in Rows 12 and 16 melt at 813, 788, and 720°F.

The four outer-blanket capsules were examined by neutron radiography after assembly. Two melt wires in edge positions were found to have been overheated by assembly welding operations. One was an 845°F wire in a Row 8 or 9 subassembly, and the other was an 813°F wire in a Row 12 or 16 subassembly. Duplicate melt wires are present in each capsule, so the range of temperatures is still covered.

Tests of melt-wire and capsule compatibility were continued. A Type 304 stainless steel capsule containing seven melt wires was heated for five days at 1000°F, sectioned, and examined metallographically. The reaction of the melt-wire alloys with the stainless steel was markedly reduced as compared with a similar capsule heated for five days at 1100°F.

A stainless steel capsule with tantalum liner cups to contain the melt-wire alloys was heated for five days at 1100°F. Metallographic examination showed attack by a zinc vapor on stainless steel external to the tantalum liner, but this reaction apparently did not penetrate the capsule wall.

(2) Equilibration--Internal Friction Techniques for Analysis of Oxygen in Sodium. The EBR-II Experimental Procedure for Equilibration--Internal Friction Techniques for the Analysis of Oxygen (and other interstitial elements) in the EBR-II Primary Sodium was completed, and distributed for review and approval. Prototype hardware has been prepared for flow tests for measurement of the effect of the equilibration capsules upon the subassembly outlet flow.

(3) Miscellaneous. Temperature distributions in EBR-II Mark-II prototype-element irradiation capsules in experimental Subassembly XO29 were calculated by use of the HECTIC II code, and the data were tabulated for use in experiment evaluation.

(4) Utilization of Radiation-induced Changes in Silicon Carbide to Measure Temperatures in EBR-II. A proposal is being prepared for an experiment to test the silicon carbide-change method of subassembly temperature measurements in EBR-II. The use of this method has been reported in

> Martin, W. H., and Price, A. M., Determination of Irradiation Temperature in Graphite Irradiation Experiments in the Dounreay Fast Reactor, UKAEA, TRG Report 1117(C) (1966).
>
> Thorne, R. P., Howard, V. C., and Hope, B., Radiation-induced Changes in Porous Cubic Silicon Carbide, UKAEA, TRG Report 1024(C) (1965).

The degree to which annealing causes silicon carbide to recover from irradiation-induced changes (in dimensions, thermal conductivity, and electrical conductivity) is linear with annealing temperature above the irradiation temperature. No recovery takes place below the irradiation temperature. By plotting measurements of a physical property (e.g., dimension) against annealing temperature, the irradiation temperature may be determined at the intersection of the recovery curve and the constant physical property curve.

Work at Oak Ridge National Laboratory (ORNL) has shown that irradiation temperatures deduced from dimensional changes in irradiated silicon carbide correspond to actual measurements of irradiation temperature within 5°C. The coming ORNL materials irradiations in experimental Subassemblies XO34 and XO35 will utilize silicon carbide monitors within the irradiation capsules.

(ii) Nondestructive Testing

(a) Capsule Examination. Twenty-five Mark-B-37-type encapsulated Mark-II driver-fuel replacement capsules for experimental Subassembly XO29 were X-rayed, and 22 were rejected for insufficient wall thickness on capsule closure welds. The sponsor has proposed a design change for the closure weld that should assure a uniform wall thickness.

Idaho Nuclear Corp. delivered seven Mark-B-7 structural-type capsules to be irradiated for materials fatigue studies in experimental Subassembly XO37.

One Mark-A-19 fuel capsule intended for inclusion in the reconstituted experimental Subassembly XO11 was received from Los Alamos Scientific Laboratory. Tungsten inclusions were identified in the closure weld by X-ray examination. The capsule will be returned to the sponsor for repair.

Pacific Northwest Laboratory delivered five Mark-A-19 fuel capsules for inclusion in reconstituted experimental Subassembly XO11.

Numerous X rays have been taken of the lower ends of driver-fuel elements from cold-line production to study the statistical occurrence of clad swelling in the vicinity of the lower spade.

(b) Neutron Radiography. Neutron radiographs of unirradiated driver-fuel elements were taken at TREAT to develop the proper technique for radiographing radioactive elements.

(c) Antimony-Beryllium Neutron Source for Neutron Radiography in FCF. A freshly irradiated antimony metal source was obtained from MTR on March 25. With this source, tests were made of the antimony-beryllium neutron source in the EBR-I maintenance cell. The objectives of these tests were to determine the effectiveness of different collimator designs in promoting image sharpness, to select the collimator for initial use in the FCF, and to make neutron radiographs of actual experimental capsules (unirradiated) for demonstration purposes, simulating as closely as possible the conditions for radiography in the FCF argon cell.

(iii) Handling and Examination

(a) Irradiated Capsules from Experimental Subassembly XO11. Leak testing of capsules from experimental Subassembly XO11 by ANL and GE (HOV-4 and F4F, respectively) was delayed. GE expects to complete the testing of Capsule F4F during April; however, ANL cannot continue work on Capsule HOV-4 until hot-cell renovations are completed.

The remaining capsules from Subassembly XO11, which have been inspected and are awaiting return to the reactor to complete their exposure, are stored in the FCF Air Cell. ANL Capsule SOV-7 was recently bent; the cause is unknown. A new storage container which completely encloses the experimental capsules was fabricated and now contains the capsules in the Air Cell. Arrangements are in progress to return SOV-3 from ANL-MET to replace the damaged SOV-7 which will be returned for examination.

(b) Testing of Subassembly Sodium-removal Procedure

(1) Cyclical Testing of Stressed Capsules of Type 304 Stainless Steel. Experimental Subassembly X900, containing the pressure-stressed tubing samples, received safety and operational approval for a position in Row 7 and an exposure of about 0.5×10^{22} nvt.

Metallurgical examination of sample tubes following the fourth cycle of sodium exposure and cleaning is in progress. Preliminary results indicate no changes in the Type 304 material in any of the exposure-cleaning cycles.

(2) EBR-II Subassembly Recycle Test. A spent driver-fuel subassembly, C-278, is being subjected to a special recycle test in which it is taken from the primary sodium through the washing procedure and back into the primary sodium. The subassembly has completed two cycles and has been returned to the primary sodium for the third time. Five cycles are planned. Data from examination of the element cladding will complement information from the X900 test.

(3) Electromagnetic Equipment for the In-cell Testing of Sodium Bonds in Irradiated Capsules. The mechanical design of the in-cell equipment was completed. The electronic components for the Mark-A capsule design are essentially complete (see ANL-7427, p. 75). Work is in progress on the electronic components for inspection of Mark-B-37 capsules (or elements).

(c) Equipment for FCF In-cell Neutron Radiography. The mechanisms for capsule and foil positioning to be used in conjunction with the Sb-Be neutron source were received from the vendor. They were assembled in the FCF mockup area for testing prior to installation in the cell.

(iv) Safety Review of Experiments. The EBR-II Irradiation Review Committee (IRC) acted on the following experiments:

(1) Experimental Subassemblies XO34 and XO35, both containing structural materials from ORNL, were recommended for reactor safety and operational approval.

(2) A single capsule from GE, containing mixed-oxide fuel from Group E1H, was judged unacceptable for irradiation because of a section of reduced thickness in the capsule wall.

(3) Experimental Subassembly X900, containing pressurized Mark-B-37 tubes for investigation of possible deleterious effects due to sodium removal by water washing, was recommended for reactor safety and operational approval.

(4) Experimental Subassembly XO36, containing 19 mixed-oxide fuel capsules of GE's Group 8B, was recommended for reactor safety and operational approval.

(5) A group of replacement capsules for experimental Subassembly XO29 was reviewed with regard to weld-thickness acceptability below the normal limit of 90%. The IRC judged the capsules to be unacceptable.

(6) Driver-fuel Subassembly C-291 was requested to be extended in burnup from the present 1.2 a/o to a maximum of 1.3 a/o in light of the supporting information available. The IRC recommended that C-291 be extended in burnup as requested.

o. FCF Process Analysis and Testing (M. J. Feldman)

Last Reported: ANL-7427, p. 76 (Feb 1968).

(i) Test and Analytical Methods. Two heated vacuum chambers are being built to leak test irradiated fuel elements or experimental capsules inside the shielded cells. These will be utilized for leak testing suspect elements or capsules as described in the Progress Report for December 1967, ANL-7403, p. 76. The driver-fuel test chamber is ready for installation. Out-of-cell wiring and piping are being installed. Design of the experimental capsule test chamber is complete.

Criticality approval has been obtained for the use of the neutron radiography system in the argon cell.

p. FCF Experimental Support--Hot Fuel Examination Facility (HFEF)--Feasibility and Cost Study (N. J. Swanson)

Last Reported: ANL-7399, p. 85 (Nov 1967).

A summary of the HFEF conceptual equipment components, design criteria, and development items was prepared to enable a comparison of HFEF with the Fast Flux Test Facility (FFTF) inert-gas hot-cell complex, as requested by DRDT. A meeting was held with Pacific Northwest Laboratory personnel at Richland to review the summary and establish a common list for comparison purposes at the next HFEF-FFTF coordination meeting, scheduled for April 2 and 3.

The main efforts of HFEF personnel have been directed toward refining the conceptual design in order to assure a strong technical base for initiating Title-I activities. Efforts have also been directed toward the establishment of the HFEF/FCF interface and the defining of the functional requirements including those to be provided by FCF.

q. Superheater and EM Pump Study and Test (R. A. Jaross)

(i) Superheater Vibration Study

Last Reported: ANL-7427, pp. 76-78 (Feb 1968).

Operational cycling (e.g., startup and shutdown) of the superheater is considered significant in that long-term creep effects might alter the vibrational characteristics of the tubes. For example, at the ~800°F operating temperature, creep relaxation of the tensile stresses would decrease the axial load, which would decrease the natural frequency of the tube.

Creep data* for a 2.5% Cr-1% Mo steel (Croloy) at 1112°F, as characterized by the secondary creep rate, can be represented by

$$\tau \frac{d\epsilon}{dt} = \left(\frac{\sigma}{30.9}\right)^{7.6}, \quad (\tau \equiv 1 \text{ hr}), \tag{1}$$

where $d\epsilon/dt$ is creep rate in strain/hr and σ is stress in tons/in.^{2}

At design operating conditions (~60°F temperature difference between shell and tube) and 1/16-in. upset of the shell, the tensile stress in the tubes is 2240 psi. The creep rate at the design stress from Eq. (1) (assuming this law holds also at ~800°F) is 1.12×10^{-11} strains/hr. Even at a constant stress of 2240 psi, the strain per 10,000 hr (~1 yr) is only 0.00001%. Therefore, within the limits of this study using the available creep data, we can conclude that creep will have a negligible effect on the vibrational characteristics of the tubes.

r. Reactor Improvements, Nuclear Instrument Test Facility Study (B. C. Cerutti)

Last Reported: ANL-7419, p. 73 (Jan 1968).

Because of a physics test program during the beginning of Run 27, gamma-flux mapping of the 01 instrument thimble was possible only at a reactor power of 30 MWt. Figure II.E.12 is a plot of the data taken. The reactor had been at 30 MWt for approximately two days. The maximum gamma reading was 2.44×10^4 R/hr. The thimble temperature was 120°F. The figure also shows data taken in the thimble five days previously when the reactor was shut down.

s. Feasibility Study of Fuel Failure Detection--Chemical and Mechanical Methods

(i) Trace Elements Analytical Techniques (C. E. Crouthamel)

Last Reported: ANL-7427, pp. 78-79 (Feb 1968).

An adsorption technique is being considered as a method for identification of tagged elements. A scouting experiment was performed to test the use of alumina as a substrate material for adsorption of tagged elements from liquid sodium. The objective of the experiment was to obtain qualitative information on the distribution of selected tagged elements between sodium and the alumina substrate.

Irradiated samples of high-purity gold and antimony were dissolved in liquid sodium to a concentration level of about 10^{-6} a/o for

*Edmunds, H. G., Repeated Cyclic Strains, Proc. Instn. Mech. Engrs., 1965-66, 180, pt. 31; pp. 373-379.

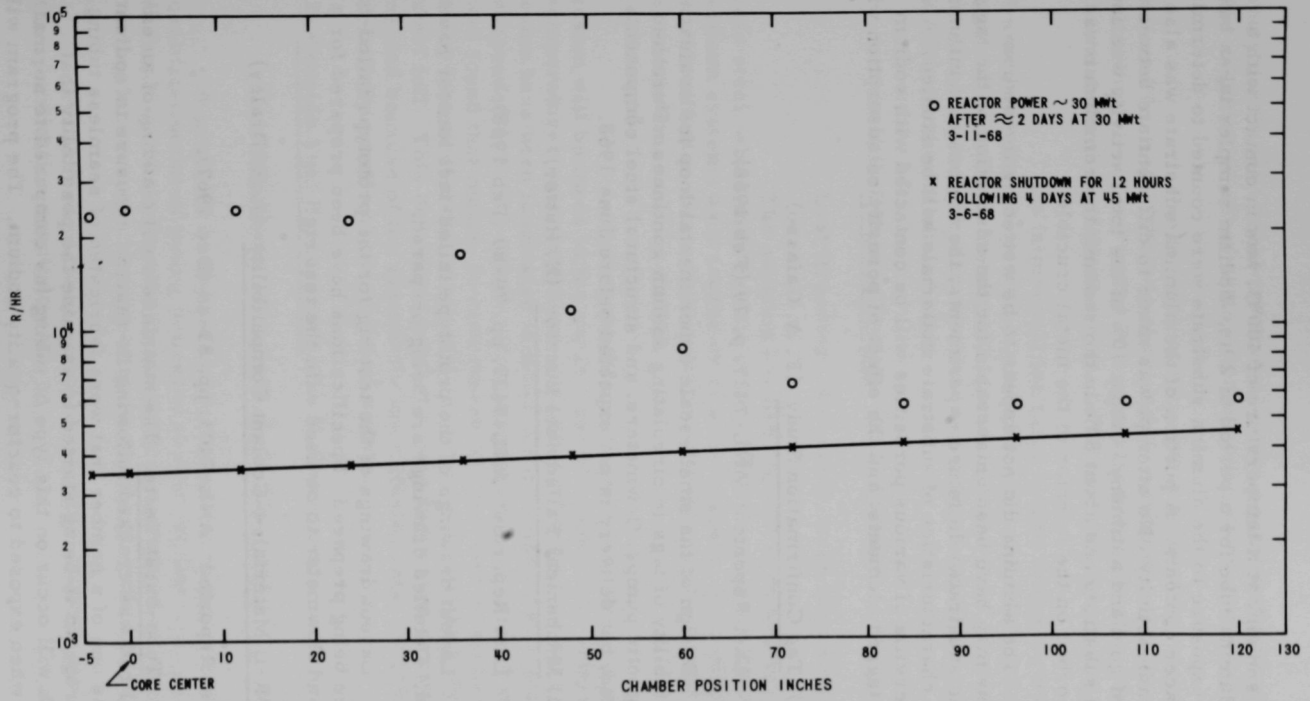

Fig. II.E.12. Gamma Flux vs. Chamber Position

each tag. The sodium, at a temperature of 400°C, was in contact with a high-density alumina tube for a period of 2 hr. Sodium samples taken before and after exposure to the alumina substrate were counted to determine the relative tracer contents. A portion of the alumina substrate was also surveyed for radioactivity. No attempt was made to differentiate between the activities of gold and antimony. About 10% of the total activity was found on the alumina substrate and about 80% in the sodium; the remainder was apparently adsorbed on the interior of the metal crucible.

The alumina did not appear to be wetted by the sodium. Thus, conditions may have been unfavorable for the adsorption of the tagged elements on the substrate. In future experiments, the factors that influence the adsorption characteristics of substrate materials will be studied. Alumina and/or beryllia of various porosities will be contacted with sodium containing the tagged elements, and the effect of porosity on adsorption will be evaluated.

(ii) Tag Confirmation Study (F. A. Cafasso)

Last Reported: ANL-7427, p. 79 (Feb 1968).

Design of the small-scale experimental loop for evaluating the chemical stability of tags in circulating sodium continues. Purchase orders for magnetic pumps, flowmeters, and structural steel components have been placed, but delivery is not expected before June 1968.

(iii) Mechanical Failed-fuel Locator (E. Hutter)

Last Reported: ANL-7427, pp. 79-80 (Feb 1968).

Layout drawings of the prototype failed-fuel locator have been completed. Detailed drawings are being prepared.

Layout drawings of the test rig for the prototype failed-fuel locator also are being prepared. Specifications have been prepared for a sodium pump and flowmeter to be used with the test rig.

t. EBR-II Materials--Coolant Compatibility (J. E. Draley)

Last Reported: ANL-7403, pp. 83-84 (Dec 1967).

(i) Tube-burst Tests. The stainless steel cladding of an experimental fuel rod was cracked following in-reactor exposure to sodium. This cladding is one of a number that were fabricated of seamless tubing. A laboratory program is being started to examine the possibility that localized attack will occur on this type of tubing (as compared to normal welded tubing) when exposed to reactor-quality sodium. The program will

study conditions of heat treatment, surface preparation, and deformation that might be in effect during and following reactor exposure.

Preliminary to tube-burst tests of the irradiated tubes recovered from the SURV-I subassembly, specimens of unirradiated blanket-rod tubing have been tested in a specially prepared rig. The tests indicate that at least three different heats of blanket-rod tubing are in stock.

At failure, all the tubes bulged to approximately 150% of the original diameter in the ruptured region. All tubes failed by splitting longitudinally for a distance of approximately 2 tube diameters. The split tubes were photographed, and data are being retained for comparison with failures in the irradiated tubes.

(ii) Diffusion Studies (F. A. Cafasso)

Last Reported: ANL-7403, p. 84 (Dec 1967).

The question has been raised as to whether Type 304 stainless steel, which may contain up to 0.5% tramp copper, behaves in liquid sodium systems as a source or sink for copper. Accordingly, information on the diffusion rate and distribution of copper in liquid sodium-stainless steel systems is being sought.

Initially, rough measurements of the rate of copper diffusion will be made in the range from 500 to 800°C to determine at what temperatures equilibrium measurements may be practical. Tantalum capsules have been fabricated in which a coil of stainless steel foil can be suspended in liquid sodium. In a test experiment carried out at 650°C, it was found that molten sodium flowed into the narrow spaces between the many layers of a coil made of 2-in.-wide by 1-mil-thick Type 304 stainless steel foil. This demonstrated that a very large area of stainless steel, needed because of the expectedly low diffusion rate, could be bathed in a relatively small volume of liquid sodium.

2. Outside Fuel Procurement (C. E. Stevenson)

Last Reported: ANL-7419, p. 76 (Jan 1968).

A group of 20 samples of fuel-element tubing, secured from the third qualification lot of tubing delivered to Aerojet-General Corp. by the Matthey-Bishop Co., was subjected to mechanical-property testing by a commercial testing laboratory. Results of these tests are summarized in Table II.E.14.

Properties of these samples are quite uniform, and are well within the specification requirements.

TABLE II.E.14. Mechanical Properties of EBR-II Fuel-element Tubing
(Type 304L Stainless Steel, Welded, 0.174-in. OD x 0.009-in. Wall)

Type of Test	Test Results		Specification Requirements
	Average	Range	
Tensile (ASTM A370-65)			
a) At 0.02 in./min Strain Rate:			
Yield Strength, psi,[a] 0.2% Offset	40,900	39,700-48,400	30,000 min
Ultimate Strength, psi[a]	97,300	95,800-99,500	75,000-105,000
Elongation, %	60	56.0-63.5	50 min
b) At 0.2 in./min Strain Rate to Yield, 0.5 in./min above Yield:			
Yield Strength, psi,[a] 0.2% Offset	41,800	40,700-47,400	-
Ultimate Strength, psi[a]	96,200	95,000-97,500	-
Elongation, %	56.5	53.5-61.0	-
Burst Pressure, psi	8,420	8,200-8,600	7,500 min
Hardness, Vickers, 0.5-kg load	148	143-152	168 max
Flaring Test (ASTM A450-66)	All pass		Pass
Reverse Flattening Test (ASTM A450-66)	All pass		Pass

[a]Calculated for nominal tubing cross section.

3. Operations--Reactor Plant (G. E. Deegan)

Last Reported: ANL-7427, pp. 82-83 (Feb 1968).

a. Operations. The reactor was operated for 293 MWdt in Runs 27B and 27C during March. Each run was terminated after the detection of an increase in fission gas activity in the primary cover gas (see Sect. II.E.1.b). Two previously suspected experimental subassemblies had been reinserted in the reactor for these runs: XG05 was present during Run 27B, and XA08 during Run 27C. A positive identification of the source(s) of the fission gas has not yet been made. The cumulated total of EBR-II operation is 16,117 MWdt.

Following reactor startup for Run 27B on March 1, the power-reactivity decrement was measured as 41.2 Ih at 45 MWt with control rods banked at 12.00 in. Steady power operation at that level continued until March 5, when one of the above-mentioned fission gas releases was detected during a test with reduced power and normal outlet coolant temperature (constant-ΔT test). Run 27B was terminated, and experimental Subassembly XG05 was removed and replaced by XA08.

Other loading changes for Run 27C proceeded normally until binding was encountered at the 70.6-in. elevation while loading a surveillance subassembly in core position 5-D-4. This position is between control rods

Nos. 2 and 3. A special dummy subassembly with a smooth contour at the bottom edge of the hex can was fabricated and then inserted in core position 5-D-4 without difficulty. This dummy subassembly was then successfully replaced with a standard driver subassembly. A subsequent attempt to insert a half-worth driver subassembly in position 6-E-1 also met with binding at the 70.6-in. elevation, and a depleted-uranium blanket subassembly which had been reworked to smooth the bottom edge of the hex can was then inserted normally into this position. Control rods Nos. 2 and 3 were lifted clear of their thimbles and reinserted with no indication of interference.

Before the startup of Run 27C, timed rod drops were conducted on control rods Nos. 2 and 3 both with and without the scram air assist. The results of these tests were normal and indicated no significant thimble deformation or interference.

After the startup of Run 27C on March 7, the power-reactivity decrement at 45 MWt was measured as 37.3 Ih with control rods banked at 12.5 in. Reduced-flow, constant-ΔT experiments were begun on the afternoon of March 8. During the ensuing 64-hr period, six reactor scrams occurred at varying reactor power levels and primary system flows. Each was initiated by a high rate of change of primary-system-flow interlock which resulted from rapid flow perturbations. During this time an attempt was made to complete the physics experiments, and the pump system and controls were under constant surveillance. On the morning of March 11, while the reactor was operating at a power level of 30 MWt, radiometric analyses of primary-cover-gas samples indicated that a very small fission-product gas release had occurred. The reactor was operated for several more hours to confirm the release, and then Run 27C was terminated.

The primary-pump-control circuitry was checked with the assistance of a field service engineer from the manufacturer of the pump-control equipment. The eddy-current clutch-current controller which appeared to be malfunctioning for pump No. 2 was removed and replaced by a modified controller which was available. Primary-pump operation since that time has been relatively stable, with no sign of a controller malfunction.

Loading changes for Run 27D were completed on March 29. Table II.E.15 summarizes loading changes during March.

b. Operational Support and Maintenance

(i) Repair of Fire Damage and Cleanup in Sodium Boiler Plant. The piping in the secondary-sodium sampling system which was exposed to the fire was washed with 5% acetic acid and rinsed with demineralized water. Sections of pipe and tubing that were covered with deposits of

TABLE II.E.15. Loading Changes in EBR-II during March 1968

Date	Grid Position	Removed	Installed[a]	Comment
3/1/68	4-C-2	C-2003	XG05	Installed for leakage test
3/1/68	4-F-3	C-2064	C-2127	
3/1/68	5-C-2	C-2038	C-2128	
3/1/68	6-C-4	B-382	B-389	
3/1/68	14-D-8	U-1455	U-1146	
3/1/68	6-A-1	B-3000	B-372	
3/6/68	4-A-1	C-2036	C-2134	
3/6/68	4-E-1	C-2027	C-2135	
3/6/68	5-D-4	C-295	E-82	
3/7/68	6-E-1	XO30	A-788	Irradiation completed
3/7/68	5-D-4	E-82	C-2061	
3/7/68	4-C-2	XG05	C-2003	Removed because of suspected leakage
3/7/68	4-F-2	C-2007	XA08	Installed for leakage test
3/20/68	4-F-2	XA08	C-2007	Removed because of suspected leakage
3/20/68	2-F-1	C-2005	C-2009	
3/21/68	3-B-2	C-2007	C-2124	
3/21/68	3-F-1	C-2031	C-2121	
3/21/68	7-A-4	A-812	X900	
3/28/68	6-D-4	B-354	B-377	
3/28/68	6-A-3	B-356	B-382	
3/28/68	6-C-2	B-357	B-383	
3/29/68	5-A-1	L-447	L-454	Removed subassemblies were suspected of leakage because they may contain elements with seamless-tube cladding
3/29/68	6-C-3	B-358	B-378	
3/29/68	6-E-2	B-359	B-379	
3/29/68	6-A-5	B-360	B-380	
3/29/68	4-C-2	C-2003	C-2006	
3/29/68	6-A-2	B-352	B-381	
3/29/68	6-B-4	B-355	B-388	

[a]A--Depleted-uranium inner-blanket subassembly.
B--Row-6-type driver fuel subassembly.
C--Driver-fuel subassembly.
E--Special dummy subassembly.
L--Control-rod subassembly.
X--Experimental subassembly.
U--Depleted-uranium outer-blanket subassembly.

sodium oxide were checked with dye penetrant for cracks or other damage. There was no indication of any damage. Tubing between the plugging valve and economizer in the plugging meter system was replaced, and the tubing was sent to ANL-MET for inspection. The tubing was found to be satisfactory without any indication of corrosion or other abnormalities.

(ii) Fuel Unloading Machine (FUM). The argon line between the FUM vapor trap and the FUM gas outlet nozzle was removed and cleaned to remove sodium deposits. The sodium drip catcher was removed from the rotating port and cleaned.

(iii) Secondary Sodium System Valve, SN-17. The bellows whose failure required replacement of the valve SN-17 on February 9, 1968, was removed from the valve body, cleaned, and inspected. A pin hole was found near the top of the bellows. The bellows was sent to ANL-CEN for further inspection and failure evaluation.

(iv) Secondary Sodium Sampling System. The supply valve to the secondary-sodium sampling station was replaced with a new 1/2-in. Nepro bellows-sealed valve with backup packing. The original valve did not contain backup packing and was not considered to be satisfactory for this application.

c. Operator Training. Two technicians were qualified, and one final written examination and one final examination for requalification were successfully completed.

Lectures and films on the properties and hazards of sodium were prepared and presented to operations maintenance and other selected personnel. Prepared printed material on sodium which summarizes the lecture was given to each person. Books of photos of plant incidents were prepared and made available to operating personnel.

d. Operating Procedures. Revisions to the Makeup Water Demineralizers, Blowdown Demineralizers, and Emergency Procedures sections of the Operating Manual were completed. Reviews of the Unrestricted Operation and Abnormal Conditions sections of the Fuel Handling Division, the Argon Purification System, and the Special Procedures section of Division II are in progress.

A revision to the Operating Information Book which covers operation of the heater controllers for the large and small rotating seal plugs was issued. Drafts of procedures for operation of the emergency argon manifold in the reactor building and for manual control of the primary-tank argon-blanket pressure were completed.

The secondary sodium system drawing, showing induction and resistance heating locations and thermocouple control and readout points,

and the secondary sodium purification system flow diagram, including the cooling water and Dowtherm systems, were reviewed and updated. Power plant, reactor auxiliary systems, and argon cooling system diagrams were also reviewed and updated.

Preparation of on-station posted operating procedures continues.

4. Operations--Fuel Cycle Facility (M. J. Feldman)

Last Reported: ANL-7427, pp. 83-91 (Feb 1968).

a. Hot Line Operation. Production activities in the hot line have been resumed. Some of the operational steps had been previously suspended as a result of measurements which showed deformation of the element jacket at the lower end (see ANL-7427, p. 84). A new inspection step has been added to measure the diameter of the jackets at the junction of the fuel and the lower tip. A temporary maximum diameter of 0.177 in. has been set as the upper limit for acceptability. This diameter is the maximum that would be obtained if the largest acceptable jacket diameter, jacket wall thickness, and tip diameter were combined. Initial results from inspection of hot-line-produced elements indicate that less than 4% of the elements will be rejected as a result of being oversize. Metallographic examinations show that there is very minor wall thinning of the jackets at this maximum diameter. It is recognized that this limit (0.177 in.) is on the conservative side and experiments are continuing to help define a more realistic, and possibly larger, acceptable diameter at this point [see item f. (iii) below].

Additional runs were being made to produce 70% enriched fissium elements for use in the experimental programs. Chopped pins of 70% enriched fissium were blended by melting with a uranium-2 w/o silicon alloy to increase the silicon content of this alloy to about 300 ppm. The resultant alloy was then processed into acceptable elements. Table II.E.16 summarizes the productive activities for the report period.

b. Cold Line Operation. A summary of the month's production data is given in Table II.E.17.

Normal production activities in the cold line are continuing. A new inspection step has been added to measure the diameter of the jackets at the junction of the fuel and the lower tip. A temporary maximum diameter of 0.177 in. has been set as the upper limit for acceptability. This diameter is the maximum that would be obtained if the largest acceptable jacket diameter, jacket wall thickness, and tip diameter were combined. Initial results from inspection of cold-line-produced elements indicate that approximately 8% of the elements are expected to be rejected as a result of being oversize. Metallographic examinations show that there is very minor wall thinning of the jackets at this maximum diameter. It is

TABLE II.E.16. Production Summary for Hot Line

	3/1/68 through 3/31/68	Total This Year
1. Subassemblies received:		
Core, Control, Safety	6	31
Other	4	5
2. Subassemblies Dismantled (for processing)	4	31
3. Subassemblies Dismantled (for examination, etc.)	2	3
4. Subassemblies Fabricated	6	10
5. Subassemblies Transferred to Reactor:	10[a]	12
Subassemblies Stored in L&O Vault and Interbuilding Corridor	0	0
6. Elements Decanned:		
From Irradiated Subassemblies	319	1,996
Rejects	0	122
Other	78	78
Total Decanned	397	2,196

Melt Refining

	Irradiated Fuel	Recycle Material	New Fuel
7. Number of Runs	3	1	1 (70%)
8. Average Pour Yield, %	91.3	90.1	94.9
1968 to Date (Total)	14	7	1

Processing

	3/1/68 through 3/31/68	Total This Year
9. Injection-casting Runs (Total Number)	4	22
10. Elements Processed:		
Accepted	425	1,195
Rejected	71	177
11. Elements Welded:	360	919
Rewelded	0	0
12. Elements Leak-tested:		
Accepted	377	1,087
Rejected	10	18
13. Elements Bonded (including recycle)	523	1,477
14. Elements Bond-tested:		
Accepted	393	1,164
Rejected	22	77
15. Elements to Surveillance	0	681
Number of Subassemblies	0	22

Waste Shipments

16. Cans to Burial Ground	2	16
17. Oxide and Glass Scrap to ICPP	1	18

[a] Includes 5 from L&O vault and 1 from passageway storage pits.

TABLE II.E.17. Production Summary for Cold Line

	3/1/68 through 3/29/68	Total This Year
1. Alloy Preparation Run:		
New Fuel	2	6
Remelts	3	12
Total	5	18
2. Injection-casting Runs	10	32
3. Pins Processed:		
Accepted	805	2,655
Rejected	40	160
4. Elements Welded	360	1,953
Elements Rewelded	0	13
5. Elements Leak-tested:		
Accepted	444	2,064
Rejected	22	40
6. Elements Bond-tested:		
Accepted	628	4,116
Rejected	52	130
7. Subassemblies Fabricated	8	17
8. Subassemblies Sent to Reactor	3	3

recognized that this limit (0.177 in.) is on the conservative side and experiments are continuing to help define a more realistic, and possibly larger, acceptable diameter at this point [see item f. (iii) below].

Addition of silicon to the vendor-produced ingots continues. The silicon was added in the form of a uranium-2 w/o silicon alloy or by blending of heels from previous injection-casting runs with the ingots. The heels contain higher concentration of silicon as a result of small pieces of Vycor that become entrapped in the heels at the conclusion of previous injection-casting runs. Because this silicon is not homogeneously mixed in the heel, a representative sample cannot be obtained. Analytical results obtained from castings in which heels were used indicate a silicon content 10 to 15% (30 to 50 ppm) above that calculated on the basis of samples of the charge material including heel.

The results of previous experiments involving the addition of silicon metal (as powder or granules) to the charge material in an alloy-preparation run have shown that with liquation periods of 1 to 4 hr at 1350 ± 50°C the percentage of charged silicon that is found in the product is ~86 ± 2%. The desired silicon content for these experiments ranged from 400 ppm to 2 w/o.

Experiments are continuing to determine the yield of silicon in the product when the silicon is added as a uranium alloy containing 1 to 2 w/o silicon.

Transfer of irradiated EBR-II subassemblies to the Idaho Chemical Processing Plant (ICPP) will be accomplished by means of a top-loading and -unloading cask which employs water to cool the contained subassembly convectively. A heat test of the cask was conducted with a low-thermal-output subassembly (total fission-product decay heat of about 275 W). The test consisted of filling the cask with demineralized water, loading the subassembly into the cask from the air cell, and reading the temperature of the water at four points along the length of the cask. The test results showed that temperature equilibrium was reached at about 24 hr after insertion of the subassembly into the water-filled cask and that natural circulation of the water coolant had occurred. At equilibrium the temperature of the coolant was about 81°F near the bottom portion of the subassembly and about 89°F toward the top portion of the subassembly (initial temperature of the coolant was about 68°F). When irradiated subassemblies having higher fission-product decay heat outputs (outputs of 600 to 700 W and outputs of the order of 1000 W) become available, further heat tests will be made. Until these tests at higher heat outputs are completed, the cask will not be approved for subassembly transfers to the ICPP.

c. Maintenance and Repair. Two operating manipulators were removed from the argon cell for replacement of broken pins in the carriage drive gear train.

A problem with loss of power to the air-cell crane has recurred. This problem results from a loss of electrical contact of the bridge pick-up brushes with the overhead bus bars (see Progress Report for September 1967, ANL-7382, p. 8). Coating of the brushes with a conductive lubricant provided a temporary solution. A more permanent solution to this problem is being sought.

d. Operator Training. Rotation of personnel to new work assignments was carried out to provide on-the-job training.

e. Operating Manuals and Reports. During the past month, two revised sections of the manual were submitted for review and acceptance. Seven sections or parts of sections which are approved for issuance are in various stages of preparation. Eleven modifications or changes to approved sections were issued.

f. Analyses

(i) Chemical Analyses. The number of fuel-product analyses on hot-line, cold-line, and vendor fuel samples, together with the average value and range, are tabulated below.

Analyzed for	Number	Average Value	Range
U (total and isotopic)	28		
U (total)		94.57 w/o	94.02-95.33
^{235}U (% of total U)		52.13 w/o	51.58-52.47
Pu (total and isotopic)	7		
Pu (total)		1125 μg/g	386-1575
Mo	30	2.53 w/o	2.44-2.65
Ru	28	1.90 w/o	1.82-2.10
Rh	21	0.268 w/o	0.250-0.284
Pd	21	0.189 w/o	0.167-0.205
Zr	23	0.086 w/o	0.051-0.156
Nb	23	0.014 w/o	0.007-0.017
Fe	34	356 ppm	72-1040
Al	6	180 ppm	135-205
Si	44	350 ppm	55-790
C	5	275 ppm	240-320
Ni	21	145 ppm	38-213
Cr	18	<28	<16-79
Total Analyses:	337		

Analyses for surveillance of irradiated pins from the reactor are tabulated below.

Analyzed for	Number	Average Value (ppm)	Range (ppm)
Fe	8	358	110-700
Al	7	180	60-390
Si	28	205	55-420
C	7	245	150-475
Tc	13	350	195-600
Total Analyses:	63		

(ii) Postirradiation Analysis of EBR-II Fuel. All the fuel elements from Subassemblies C-2111 and C-2113 which were suspected of containing a leak have undergone low-power irradiation leak checks in TREAT.

No leaks were found; however, the background from external surface uranium contamination would mask the results of an extremely small leak. An effort was made to decontaminate the surface of one group of the elements by use of demineralized water. This method of decontamination did not remove enough of the surface contamination to affect the results when these elements were retested in TREAT. A more reactive decontamination solution was not used because of the possibility of damage to the jacket surface which would preclude the possibility of reinserting these elements in EBR-II for leak test purposes.

As mentioned in ANL-7427, a silicon surveillance program has been formulated for EBR-II driver fuel. This proposed program, which is currently being scrutinized by appropriate ANL review committees, is intended to evaluate the irradiation performance (specifically, irradiation swelling) of U-5 w/o Fs alloy containing silicon to a maximum content of 920 ppm. Included in the program is fuel alloy in which silicon is not intentionally added. Approximately 7 subassemblies of a total of 11 proposed are now available for irradiation, and the remainder are currently being fabricated. Surveillance examinations will be conducted on these subassemblies following EBR-II irradiation to the range of 0.9-1.2 a/o maximum burnup.

Five subassemblies which were manufactured in the cold line have been proposed for inclusion in a fuel-surveillance program intended to evaluate the irradiation performance of driver fuel produced in the cold line. Postirradiation examinations would be conducted following fuel-burnup increments of approximately 0.6, 0.95, 1.0, 1.1, and 1.2 a/o, respectively. The proposed program is currently being reviewed before being initiated. The subassemblies are now available for irradiation.

As a part of the EBR-II Driver Fuel Anomalous Swelling Program, a single subassembly, C-291, has been recommended for irradiation to a maximum burnup of 1.3 a/o (0.1 a/o beyond the presently established burnup limit of 1.2 a/o). The fuel elements in this subassembly were fabricated from injection-casting batches 4137 (silicon content 271 ppm) and 4142 (silicon 243 ppm), respectively. Postirradiation surveillance examinations of elements containing fuel from these two batches were conducted previously when spent Subassembly C-292 was examined. Elements using batches 4137 and 4142, respectively, in C-292 (companion Subassembly to C-291) were found to have an irradiation swelling ranging from 4.1% to 5.7% following varying burnups to a maximum of 1.185 a/o. This low swelling shown in C-292 indicated that additional burnup could be

safely accommodated by elements in Subassembly C-291. This appears to be reasonable, especially since irradiation swelling approaching a maximum of approximately 15-16% has been observed in the past for other elements which have performed satisfactorily in all respects. Complete postirradiation examinations will be conducted of the fuel elements from this subassembly following this increased irradiation if approved in order to extend the evaluation of irradiation performance of the U-5 w/o Fs fuel.

Four of the five subassemblies containing fuel elements of Mark-IB design are now undergoing irradiation in EBR-II. Irradiation of two of these subassemblies, C-2132 and C-2133, began at the start of Run 27, while irradiation of two others, C-2134 and C-2135, began at approximately midway through Run 27. These subassemblies will be irradiated to burnup levels ranging from 0.5 to 1.2 a/o in order to evaluate the irradiation performance of this element design. The fifth subassembly of this program, C-2136, is in the reactor storage basket awaiting insertion in the core in the near future. Postirradiation examinations will be conducted on all elements following their prescribed irradiation.

(iii) Production Analysis. Measurements have been made on elements from the hot line and cold line to determine the diameter of the element jackets at the junction of the fuel and the lower plug. Deformation of the jackets in this area is a result of the impact that the fuel pin imparts to the lower plug during bonding (see ANL-7427). A number of jackets from each diameter range were sectioned and measured to determine the amount of wall thinning as a function of wall deformation. The results of these measurements and the results of measurements of jacket diameter in the deformation area are shown in Fig. II.E.13. The nominal jacket wall

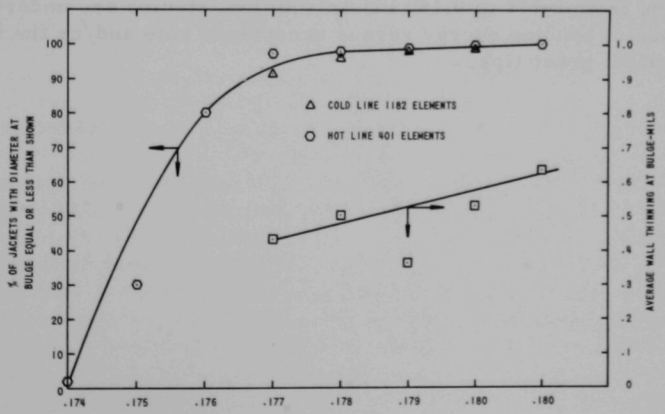

Fig. II.E.13. Jacket Diameters

thickness is 9 ± 0.5 mils, and the nominal jacket diameter in the region of the lower plug is 0.1750 ± 0.0015 in.

An analysis has been made of the mechanical-strength properties of the element jacket as a function of the wall thinning resulting from this deformation. Two factors contribute to the hoop stress in the jacket wall. The first is the stress due to internal pressure which results from thermal expansion of the fuel and sodium from expansion of the fuel due to irradiation swelling, and from any release of fission gases within the jacket. The second factor is the thermal stress induced in the jacket wall as a result of the difference in temperature between the inside and outside of the jacket wall. These two stresses and their combination were compared for areas of the jacket at the deformation region and for areas of the jacket where the fuel reaches the highest temperature. These calculations show that even with a combination of the maximum deformation observed in production of fuel in the hot line (0.1825-in. jacket diameter and 0.00065-in. decrease in jacket wall thickness) the total hoop stress is less in the deformed region than in the hottest region of the fuel (approximately midlength). This occurs because the temperature differential across the jacket wall is lower (28°F) in the region of the lower tip, where very little power is generated, than in the midlength of the fuel element, where maximum power is generated and the temperature differential across the jacket wall is the highest (42°F). The internal pressure is assumed to be uniform over the entire length of the jacket. Based on these calculations, the jacket deformation (as seen to date) is not the determining factor in assessing the capability of the element.

A technical report is being prepared which recommends increasing the maximum acceptable diameter of the jacket in the region of the spade from 0.177 to 0.180 in. In addition, studies are underway on limitation of bonding energy versus acceptance rate and/or the use of harder (unannealed) lower tips.

PUBLICATIONS

LIQUID-METAL FAST BREEDER REACTOR--CIVILIAN

In-Reactor Sodium Corrosion of Vanadium and Vanadium-Titanium Alloys
S. Greenberg, C. F. Cheng, and W. E. Ruther
Nucl. Appl. 4, 170-172 (Mar 1968)

Summary Review of Flowmeters Suitable for Measuring Sodium Flow at Temperatures Up to 1200°F in the Fast Flux Test Facility (FFTF)
G. F. Popper, D. E. Wiegand, and M. C. Glass
ANL-7340 (Dec 1967)

Problems and Precautions in Spectral-Index Measurements
G. S. Stanford
Neutron Thermalization and Reactor Spectra, Proc. IAEA Symp., Ann Arbor, July 17-21, 1967. Intern. Atomic Energy Agency, Vienna, 1968, pp. 37-47

III. GENERAL REACTOR TECHNOLOGY

A. Applied and Reactor Physics Development--Research and Development

1. Reactor Code Center (M. Butler)

Last Reported: ANL-7427, p. 93 (Feb 1968).

New programs assimilated into the Center library include HWOCR-SAFE from Atomics International, PERT4 from Battelle's Pacific Northwest Laboratory, CINDER from the Bettis Atomic Power Laboratory, BURNUP from General Electric's Nuclear Technology Department, GGC3 from Gulf General Atomic, JUPITOR1 from Oak Ridge National Laboratory, and KAK and RAM from the ENEA Computer Programme Library. These programs are now available for distribution upon request.

2. Theoretical Reactor Physics

a. Cross Section Data Evaluation (C. N. Kelber)

Last Reported: ANL-7427, p. 93 (Feb 1968).

A Fortran program was written to calculate the parameters $\bar{\mu}_L$, ξ, and γ from the Legendre expansion coefficients for elastic-scattering angular distributions. The series given by Amster* were used in the program. It was found that, even for highly peaked angular distributions, the first 4 or 5 coefficients yield quite accurate values for these parameters. However, many more coefficients may be required in order to give positive angular distributions over the complete range of the scattering angle.

A study is being made of unresolved resonance parameters for ^{235}U. A Fortran program was written to calculate capture and fission cross sections from average resonance parameters by integrating over the appropriate statistical distributions. The fission and reduced neutron widths are being varied with energy in order to give cross sections in agreement with experimental averages over various energy ranges.

Several more ENDF/B materials have been processed through ETØE and merged with the current MC^2 library tape. Also, a few materials have been processed which differ from ENDF/B in certain respects, such as a version of ^{238}U with smaller smooth capture cross sections.

---

*Amster, H., Evaluation of the Cross Section Transformation Matrices of Zweifel and Hurwitz, J. Appl. Phys. 27, 307 (1956); Heavy Moderator Approximations in Neutron Transport Theory, ibid., 29, 623 (1958).

The conversion of CURVEPLØT to OS-360 has been completed.

A preliminary analysis of ^{239}Pu data using CODILLI and CURVEPLØT has been attempted. The data analyzed were the Saclay fission data in the energy range from 20 to 45 eV. The main purpose of the analysis was to test the various input and output options of CODILLI, and to acquire experience with the program. In the process, one option of the subroutine WEIGHT had to be modified somewhat in order to improve the fit. Since this energy range has been analyzed by F. T. Adler and D. B. Adler using the same program and the Bollinger data, and since the Saclay data are rather poor in the range from 30 to 40 eV, no attempt to determine resonance parameters has been made. Instead, an analysis of the data in the relatively unexplored higher energy range has been initiated.

The resolution function for the Petrel data has been obtained and is being studied. The analysis of the Petrel data will commence as soon as a practical form for the resolution function has been decided upon.

3. Nuclear Data

a. Cross Section Measurements (C. E Crouthamel and N. D. Dudey)

Last Reported: ANL-7403, pp. 103-105 (Dec 1967).

(i) Monoenergetic Neutron Cross-section Measurements. Neutron radiative capture cross sections are being measured as a function of neutron energy between 100 keV and about 2 MeV. Monoenergetic neutrons are produced by bombarding lithium targets with protons from a Van de Graaff accelerator. Capture cross sections are required to evaluate (1) the behavior of materials proposed for structural or control use and (2) the effects of fission-product buildup upon the neutron worth in fast reactors. The data are also useful in testing and evaluating theories of nuclear reactions.

Targets of interest are irradiated in the form of pressed pellets or metal foils. These targets usually weigh about 0.5 g, and are 1 cm in diameter and 0.1 to 3 mm thick. The target is irradiated with a gold monitor in front and in back of the target, and with a ^{235}U fission counter behind the back gold foil. The average neutron flux and average neutron energy are calculated from the amount of activity induced in the monitors, the size of the target, and the size of the neutron beam.

A computer code is being written which will calculate the average flux and energy in the following manner. The activity induced in the two gold foils is determined from the counting data by a least-squares method. The solid angles intercepted by the front gold foil, the back gold

foil, and the fission counter are calculated from the geometry of the experiment, considering the dimensions of the neutron source. The number of incident neutrons determined from each of the three monitors is corrected to the effective center of the target by calculating the average solid angle presented by the target. The difference in the value of the flux calculated from the three monitors reflects relative errors in the values used for the ^{197}Au and ^{235}U cross sections, all errors associated with radioactivity measurements, and errors resulting from calculated solid angles. The total error, which was determined by averaging over many targets for the neutron energy range from 100 keV to 2 MeV, was calculated to be ±7.4% for a given target. This error is largely due to a systematic difference of nearly 10% between the ^{235}U monitor and the adjacent gold monitor, and may be the result of uncertainties in the values used for the cross sections. An attempt will be made to resolve this difference by checking against the (n,α) reaction of ^{10}B and the (n,p) reaction of ^{1}H, whose cross sections are more accurately known.

Van de Graaff irradiations at neutron energies between 100 keV and 1.8 MeV were reported in ANL-7403 for the $^{89}Y(n,\gamma)^{90m}Y$, $^{51}V(n,\gamma)^{52}V$, and $^{85}Rb(n,\gamma)^{86}Rb$ reactions. Because the irradiations of vanadium did not include gold monitors, additional irradiations have been performed using both gold and ^{235}U monitors. Irradiations to measure the $^{87}Rb(n,\gamma)^{88}Rb$, $^{50}Ti(n,\gamma)^{51}Ti$, $^{84}Sr(n,\gamma)^{85}Sr$, and $^{86}Sr(n,\gamma)^{87m}Sr$ reactions have also been completed, with the exception of a few irradiations that will serve as an independent check of the data.

Most of the cross sections for the above measurements have been hand calculated, and final values will be reported when calculations utilizing the computer code have been completed and when error assessments have been made.

(ii) Integral Cross-section Measurements. In evaluating the long-term behavior of reactors, it is necessary to know fission and capture cross sections of the uranium and plutonium isotopes which build up through successive captures in the primary fuel isotopes. A program is currently being carried out to determine these ratios as a function of position in the core and blankets of EBR-II. The behavior of structural and fuel-cladding materials is also of interest and is being examined by determination of long-lived (n,p) and (n,α) reaction products.

The 65 samples from the first EBR-II irradiation have been declad and analysis has begun. Four stainless steel spacers used in the subassemblies have been dissolved, and are being analyzed for ^{63}Ni, ^{58}Co, ^{60}Co, ^{55}Fe, ^{59}Fe, ^{54}Mn, and ^{51}Cr. The expected yields of these reaction products were previously calculated from differential cross-section data and from the assumed flux and energy distribution of EBR-II. Preliminary measurements indicate good agreement between calculated and measured

values for the $^{60}Ni(n,p)^{60}Co$ and $^{54}Fe(n,p)^{54}Mn$ reactions; however, it appears that the calculated value for the $^{58}Ni(n,p)^{58}Co$ reaction is larger than the measured value by a factor of ~3. A considerable variation in neutron intensity as a function of position in EBR-II is observed, but conclusions concerning the relative "hardness" of the neutron energy spectrum as a function of position must wait until further analyses are completed.

(iii) Low-mass Fast-neutron Fission Yields. Information concerning the yields of low-mass particles released in fission is of considerable importance to the development of fast reactors. Tritium represents a bioradiological disposal problem which must be handled by the fuel-reprocessing scheme. Hydrogen and helium isotopes are important because of their interaction with the fuel matrix and fuel-cladding materials. The emission of light particles in fission is also of fundamental interest to nuclear theory.

An experiment to measure the yields of these particles by means of particle identification and counting of each emitted particle is being set up. The experimental design has been completed, electronic diagrams drawn, specifications of electronic equipment prepared, and the detectors and electronic equipment ordered. Initial measurements will involve evaluation of the method and a few survey experiments. For this purpose, a scattering tube, which consists of a simple target, a detector, and a neutron monitor holder, is being designed. This scattering tube will enable a determination of ^{3}H, ^{1}H, and ^{4}He yields per incident neutron on ^{235}U or ^{239}Pu targets. A sample of ^{252}Cf will be incorporated in the scattering tube to serve as a means of calibrating and checking out the operation of the system.

b. Burnup Analysis and Fission Yields for Fast Reactors (R. P. Larsen)

(i) Development of Analytical Procedures for Fission-product Burnup Monitors

Last Reported: ANL-7419, pp. 95-98 (Jan 1968).

(a) X-ray Spectrometric Determination of Rare Earth Fission Products. Measurement of burnup in fast reactor fuels by an X-ray spectrometric assay of the rare earth fission products is under development. The basic steps in the procedure are (1) addition of terbium (a rare earth not produced in fission) as an internal standard, (2) separation of the rare earths from interferences, (3) mounting of the rare earths on a metal plate, and (4) assaying of the fission product rare earths and the internal standard by X-ray spectrometry. The effectiveness of the internal standard technique in achieving increased precision was reported in ANL-7419. For fixed amounts of rare earths and terbium, the individual

rare earth-to-terbium line-intensity ratios were sufficiently constant to warrant preparation of calibration curves.

Calibration curves have now been prepared using a series of 12 plates. Each plate contained 8 μg of terbium (internal standard) and a total of 15 to 90 μg of five inactive fission product rare earths: lanthanum, cerium, praseodymium, neodymium, and samarium. The $LaL\alpha_1$, $CeL\alpha_1$, $PrL\alpha_1$, $NdL\alpha_1$, $SmL\alpha_1$, $NdL\beta_1$, and $TbL\beta_1$ line intensities were measured, and line-intensity ratios (rare earth to internal standard) were calculated from the line-intensity data. Calibration curves (line ratio versus composition) were then derived from a least-squares data analysis.

To evaluate the calibration curves prepared from this data, the actual concentration of each rare earth on each plate was compared with that calculated using the measured line intensity and the calibration curve. The average relative error calculated for each rare earth in the range from 30 to 90 μg is as follows: lanthanum, 1.9%; cerium, 1.6%; praseodymium, 1.1%; neodymium, 1.1%; and samarium, 1.1%. Below 30 μg the errors were somewhat larger due to low line intensities.

Typical results were as follows:

	Amount (μg)	
Rare Earth	Present	Found
Lanthanum	11.6	11.8
Cerium	21.5	21.9
Praseodymium	9.7	9.8
Neodymium	37.8	37.9
Samarium	7.0	7.1

The reproducibility of the data from these calibration studies is a further indication that the method is capable of providing data of the requisite precision for burnup analysis. Future plans include testing of procedures for the separation of fission product rare earths from other fuel constituents.

c. Cross Section Measurements (A. B. Smith)

Last Reported: ANL-7427, pp. 93-97 (Feb 1968).

(i) Fast Neutron Cross Sections

(a) Elastic and Inelastic Neutron Scattering from Even-Even Deformed Nuclei. More than four-hundred angular distributions of neutrons scattered from Hf, Gd, and Sm were measured during the period.

The region of incident neutron energy extends from 0.8 to 1.5 MeV, with good definition of both incident and emitted neutron energies. The results are now being processed. When these procedures are completed and the values combined with the previous results at lower energies, a good description of scattering from these deformed nuclei will be available entirely consistent with prior commitment to the RDT program of cross-section measurement. The analysis of the experimental data in terms of nuclear models has been initiated with the intent of interpolating and extrapolating the available experimental information to provide the greatest possible information for the reactor physicist.

(b) Inelastic Scattering from Nuclei near Mass 50. The inelastic-scattering cross sections of titanium were carefully determined at a number of incident neutron energies up to 1.5 MeV. An inspection of the raw data indicates that the results are of good quality. The data are being processed, including corrections for multiple scattering and other experimental perturbations.

The study of inelastic scattering from iron has been completed some time ago. The results are now being prepared for publication and the numerical values transmitted to the National Nuclear Cross Section Center (NNCSC) at BNL. The formal report is a proper cooperative effort between this group and the South African Pelindaba Laboratory, which has obtained complementary information. The composite results substantially contribute to the RDT requests for such information on iron.

(c) Scattering Standards. The accuracy of requested cross sections and the precision of measurement techniques are now often such as to make the precision of the standards employed in the work a matter of appreciable concern. This is particularly true of the differential elastic-scattering cross sections of carbon, which are normally employed as the reference standard. A careful evaluation of this standard cross section is now called for and is in progress. Pending the outcome of this analysis, careful measurements may be necessary.

(d) Fast-neutron Activation Cross Section of ^{236}U. Activations are to be made for neutron energies of 30 and 550 keV. The integrated neutron flux of the forthcoming absolute measurement of 30-keV activation will be greater than that of the past run at the expense of energy resolution, as counting rate versus background has been a problem. The 2-foil fission chamber to be used for the relative measurements has been checked and found satisfactory. The $4\pi\ \beta$-γ coincidence apparatus has been tested satisfactorily; it will be further checked against 4π counters used by DeVolpi.

(e) Total Neutron Cross Sections

(1) Calcium. Measurements of the neutron total cross section for calcium, using the automated monoenergetic transmission method, were made from 100 to 650 keV in 1-keV intervals. The sample used was potted in a mass container which presented for transmission 1.12 in. of calcium sandwiched between 0.005 in. of brass. The "no sample" run was conducted with a similar empty container. The data for these measurements have not yet been fully processed.

(2) Natural Iron. Similar measurements also were made with iron at several selected intervals from 500 keV to 1.45 MeV. Although the absolute values of these measurements were in error above 650 keV due to contamination by a second neutron group, they were useful in correlating resonance locations in the time-of-flight data for the same element. The resonance locations for both sets of data were identical within the expected error at 500 keV, and at 1.45 MeV (point of maximum difference) were about 12 keV apart.

(f) The $^{7}Li(p,n)^{7}Be$ Reaction. The angular distribution of product neutrons has been analyzed in terms of Legendre polynomial expansion in the center-of-mass system and found to compare reasonably well with previous work. There seems to be a discrepancy of about 10% in the shape of the total cross section obtained from this analysis in the region $1.93 < E_p < 2.15$ MeV between this work and three previous investigations. An attempt will be made to recheck this shape with a grey neutron detector.

(ii) Fission Process Data. The data from the measurements for 150- and 500-keV-neutron-induced fission of ^{235}U has been partially processed. Table III.A.1 lists the average mass and energies of the light and heavy fragments, and the variance of their distributions. Similar quantities are shown for thermal-neutron fission of ^{235}U obtained during the same period with the same experimental arrangement.

TABLE III.A.1. Summary of Mass-Angle-Energy Results for Neutron-induced Fission of ^{235}U at Thermal, 150-keV, and 500-keV Energies

	E_n (keV)								
	Thermal			150			500		
Angle	0°	45°	90°	0°	45°	90°	0°	45°	90°
$\langle M_L \rangle$	97.1	97.2	97.2	97.3	97.5	96.8	97.2	97.5	97.0
$\langle M_H \rangle$	139.0	138.8	139.0	138.9	138.6	138.7	138.8	138.4	138.6
$\sigma^2(M)$	34.5	32.8	34.3	35.1	33.3	35.0	35.7	33.6	35.4
$\langle E_L \rangle$	100.2	100.2	100.2	99.8	99.8	100.2	99.8	99.8	99.7
$\langle E_H \rangle$	70.2	70.4	70.2	70.2	70.4	70.3	70.2	70.4	70.2
$\langle E_{KT} \rangle$	170.4	170.7	170.3	170.0	170.3	170.5	169.9	170.4	170.1
$\sigma^2(E)$	114.6	111.7	115.3	117.0	112.6	117.5	116.8	110.8	117.2

(iii) Instrumentation and Digital Techniques

(a) (n;n'gamma) Measurement Apparatus. This device, development of which was previously reported, has been tested and found to exceed the original performance expectations. Resolution of the system was 9% for a gamma ray of 800 keV; judged very satisfactory. The unit shortly will be put into research use with first attention to the excitation of the 320-keV state of vanadium. The experimental procedure should be particularly rewarding at and near the reaction thresholds.

(b) Modular Computer Interfacing. Development of improved modular interfacing for the existing on-line computers has been initiated. The intent is to provide an extended scope of laboratory automation, improved reliability through interchangeability, and a modular interfacing system capability to new digital machines and basic nuclear equipment as it becomes available. The initial work is in the area of overall planning and concepts.

(c) Liquid Scintillation Detection. The design of a large liquid scintillation detector for determinations of fission cross section, $\bar{\nu}$, and capture processes has been completed. The instrumentation is to be employed at the coming Fast Neutron Generator, and only test procedures will be pursued at the existing small installation. This particular instrument is representative of the scheduled effort intended to make productive research tools available to the program coincident with the delivery of the new Generator.

(d) Total Neutron Cross Section Detector. The liquid scintillator and γ-ray-discriminated system for measurements of neutron total cross sections at energies above 650 keV was tested using accelerator-produced neutrons in the target-area environment. The detector was located in the same large shield used in the low-energy measurements. However, the water in the tank was saturated with borax. Initial measurements indicate the configuration will perform quite efficiently for the measurements at higher energy. However, a minor modification in the shielding is being made for additional γ-ray isolation. An extensive modification in the computer program also is being made to provide additional γ-ray discrimination in the data processing. When these changes are completed, a more detailed test will be made with accelerator-produced neutrons.

B. Reactor Fuels and Materials Development

1. Fuels and Claddings--Behavior of Reactor Materials

a. Irradiation Behavior of Advanced Ceramic Materials (L. C. Michels)

Last Reported: ANL-7419, pp. 102-103 (Jan 1968).

Neutron radiography of the specimens in Capsule ANL-56-11, which was removed from the MTR at the end of Cycle 270, has been com-

TABLE III.B.1. Irradiation Data for Capsule ANL-56-11[a]

Specimen No.	Design Parameters: Fuel Composition	Design Parameters: Effective Density (%)	Operating Conditions: Max Cladding Temp (°C)	Operating Conditions: Estimated Burnup to Date: a/o (U+Pu)	Operating Conditions: Estimated Burnup to Date: fiss/cc x 10^{-20}[b]
MV-2	UC-20 w/o PuC[c]	79	470	9.3	25
MV-6	UC-20 w/o PuC[c]	80	480	9.8	25
S-15	US	82[d]	380	6.7	13
S-16	US	90	510	9.1	20
S-17	US	88	500	7.6	17
S-18	US	77	610	9.6	18

[a]All cladding of fuel is Nb-1 w/o Zr alloy of 0.281-in. OD and 0.012-in. thickness.
[b]Based on effective density.
[c]Vibratorily compacted mixed UC and PuC powders.
[d]Partially annular pellets with center thermocouple.

In Specimen MV-2, the fuel ruptured the cladding in the top one-fourth of the pin. There appears to be a density variation over the length of the pin, with no apparent increase in cladding diameter in the bottom three-quarters of the pin. Specimen MV-6 also showed a density variation along the length of the pin, but there appeared to be an increase in the cladding diameter in the bottom three-quarters of the pin.

Specimens S-15, S-16, and S-17 appeared to be intact, with no detectable increase in cladding diameters and no appreciable variation in fuel density along the pins. Specimen S-18 appeared to be intact with a density variation along the length of the pin and an increase in cladding diameter in the midsection of the pin.

The causes of what appeared to be variations in fuel density in Specimens MV-2, MV-6, and S-18 are unknown.

b. Structures and Properties of Advanced Fuel Materials
(J. H. Handwerk)

(i) Thermodynamic Properties: Heat Capacity of PuO_2
(O. L. Kruger)

Not reported previously.

This investigation was undertaken to provide high-temperature heat capacity data for PuO_2, which are needed for thermodynamic calculations and the interpretation of fission-product behavior in irradiated fuels. The plutonium dioxide used in this study was obtained as a calcined-oxalate powder from Hanford Laboratories. Most of the impurity elements were below the limits of detection by spectrographic analysis, but iron was present to the extent of 0.0050 w/o. The as-received material was calcined in air at 1300°K for approximately 8 hr to assure complete conversion of the

powder to the stoichiometric compound. Further characterization showed that the powder had an average O/Pu ratio of 2.008 ± 0.007 and a lattice constant of 5.3946 ± 0.0001 Å.

Changes in heat content of a 30-g sample of this material were measured in a copper-block drop calorimeter.* The overall calibration of the apparatus was checked by measurements from 400 to 1400°K with calorimetry-conference sapphire obtained from the National Bureau of Standards. These measurements had a maximum deviation of less than 0.75% from the NBS data on similar material.

The molar enthalpy changes for the various drop temperatures are listed in Table III.B.2. These results are expressed in terms of the "defined gram-calorie," equivalent to 4.184 absolute joules. The atomic weight of plutonium was assumed to be 239.18 for these calculations. The enthalpy of the capsule was subtracted from the total observed value to obtain the enthalpy of the specimen. Since the heat content of the capsule amounted to only 17% of the total, the error associated with this correction was extremely small. The enthalpy changes of PuO_2 are shown as a function of temperature in Fig. III.B.1. The good agreement between heat contents obtained from heating and cooling cycles indicates that the specimen did not change composition or structure during the measurement. A maximum heat content of 23.2 kcal/mole was found at 1404°K, the highest temperature investigated in this study. Data reported for higher temperatures were obtained by extrapolation of the enthalpy curve.

TABLE III.B.2. Measured and Calculated Heat Contents of PuO_2 for Various Drop Temperatures

Temp (°K)	$H_T - H_{298}$ (cal/mole)		Deviation	Temp (°K)	$H_T - H_{298}$ (cal/mole)		Deviation
	Observed	Calculated			Observed	Calculated	
192	-1795.21	-1634.82	160.39	971.2	13548.15	13680.55	132.40
298.16	0.00	-189.84	-189.84	989.7	14193.56	14085.17	-108.39
435.1	2437.91	2337.12	-100.79	1010.5	14681.69	14540.59	-141.10
481.2	3251.45	3255.38	3.93	1060.0	15817.93	15626.39	-191.54
484.9	3408.73	3330.00	-78.73	1144.5	17653.82	17485.69	-168.15
503.3	3571.44	3702.81	131.37	1228.5	19554.79	19340.10	-214.69
511.3	3750.42	3865.76	115.34	1236.3	19232.09	19512.58	280.49
598.2	5605.29	5663.08	57.79	1317.8	21160.17	21317.27	157.10
654.1	6820.18	6839.76	19.58	1318.5	21366.27	21332.79	-33.48
655.5	6828.31	6869.40	41.09	1397.9	23188.60	23095.18	-93.48
727.7	8200.48	8406.54	206.06	1404.2	23218.43	23235.11	16.68
745.9	8737.42	8796.47	59.05	1500.0[a]	25370.00	25366.52	-3.48
801.2	9830.27	9986.30	156.03	1600.0[a]	27600.00	27596.27	-3.72
839.0	10825.51	10803.43	-22.08	1700.0[a]	29810.00	29830.53	20.53
922.5	12674.95	12617.58	-57.37	1800.0[a]	32030.00	32068.88	38.88

[a]Extrapolated.

*Savage, H., Rev. Sci. Inst. 37, 1062 (1966).

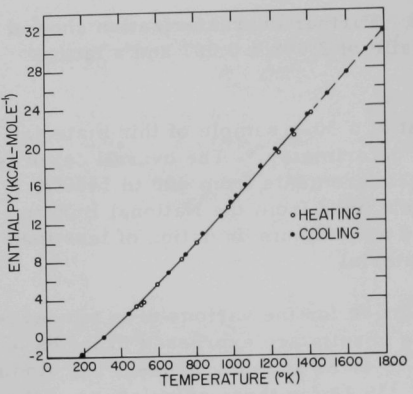

Fig. III.B.1. Enthalpy of PuO_2 as a Function of Temperature

All enthalpy measurements were corrected for the self-heating of plutonium from radioactive decay.* The procedure consisted of adding the self-heating rate of plutonium to the initial time period of the emf (temperature) curve. Since the self-heating rate displaces the curve from the time the specimen is dropped into the calorimeter, the addition of this correction to the initial monitoring period when the calorimeter is empty makes the rate uniform for the entire run. The self-heating rate effectively becomes a colorimeter constant that is subtracted from the total heat content of the specimen. This correction ranged from 0.08 to 1.2% of the enthalpy values. The greater correction applied at the low temperatures, for which there was a longer period from drop-time to midtime and the total enthalpy was comparatively small. The estimated error in the enthalpy measurement was less than 1% at temperatures above 400°K. The low-temperature point (192°K), however, is known to have a considerably larger error, which may be as much as 5%. This value at the end of the enthalpy curve extended the heat capacity calculations to room temperature, and had little effect on the more accurate high-temperature data.

Equations of the type suggested by Maier and Kelley were used to represent the measured values of enthalpy and heat capacity. These equations:

$$H_T - H_{298} = -8468 + 22.18T + 1.040 \times 10^{-4}T^2 + 4.935 \times 10^5 T^{-1}; \quad (1)$$

$$C_p = 22.18 + 2.080 \times 10^{-4}T - 4.935 \times 10^5 T^{-2}, \quad (2)$$

were derived with a computer program by a least-squares analysis of the data.

The heat-capacity relation is the first derivative of the enthalpy equation. Heat contents calculated from Eq. (1) and the deviations between the calculated and measured values for various experimental temperatures are listed in Table III.B.2. Equation (1) fits the data with a standard deviation of 136 cal/mole. Values of C_p, $S_T - S_{298}$, and $H_T - H_{298}$ at temperature intervals of 100°K are given in Table III.B.3. These values were calculated to 1800°K by extrapolation of the enthalpy curve.

*Kruger, O. L., and Savage, H., J. Chem. Phys. 40, 3324 (1964).

TABLE III.B.3. Thermodynamic Properties of PuO_2

Temp (°K)	C_p (cal mole^{-1} deg^{-1})	$S_T - S_{298}$ (cal mole^{-1} deg^{-1})	$H_T - H_{298}$ (cal mole^{-1})
298.16	16.69	0.00	0
300	16.76	0.10	31
400	19.18	5.31	1845
500	20.31	9.72	3825
600	20.93	13.48	5890
700	21.32	16.74	8004
800	21.58	19.61	10150
900	21.76	22.16	12317
1000	21.89	24.46	14500
1100	22.00	26.55	16695
1200	22.09	28.47	18899
1300	22.16	30.24	21112
1400	22.22	31.88	23331
1500	22.27	33.42	25555
1600	22.32	34.86	27785
1700	22.36	36.21	30019
1800	22.40	37.49	32258

2. Fuels and Claddings--Chemistry of Irradiated Materials

a. Development of Analytical Facilities, Microstructure Sampling Techniques, and Analytical Procedures for Analysis of Irradiated Fuels (C. E. Crouthamel)

Last Reported: ANL-7427, pp. 101-102 (Feb 1968).

(i) Shielded Fuel Evaluation Facility. Construction of a shielded fuel-evaluation facility is proceeding. Installation of a vacuum-jacketed liquid-nitrogen line has begun; installation of manifolds for the helium purification system adsorbers has been completed. Testing of the operation of the transfer locks revealed several minor operating difficulties, which are being corrected. Construction of the enclosure and shielding for the metallograph by Central Shops is underway.

(ii) Fuel-specimen Preparation. Procedures are being developed for the preparation of ceramic fuels for metallographic examination. A method to reveal grain structure is being tested. This method involves the development of interference films on uranium carbide. Preliminary test results were reported previously (see Progress Report for April 1967, ANL-7329, pp. 59-61).

In current tests, specimens of arc-melted UC, which were polished in a helium-atmosphere box and cleaned ultrasonically with benzene, developed interference films of brilliant colors. Apparently the

films are formed by reaction of the fuel surface with an impurity in the benzene (probably H_2O), and colors are produced that vary with orientation of the grains. One specimen was photographed, repolished lightly, and then etched by the vacuum cathodic-etching technique. The grain boundaries revealed by cathodic etching coincided precisely with those marked by the interference color patterns.

The arc-cast material used for these experiments was single-phase UC. An attempt will be made to develop interference patterns on other, less ideal specimens. If this technique proves to give reproducible results, it will be a useful complement to the cathodic-etching technique. Although the interference colors deteriorate within a relatively short time (hours to days), surface structures can be delineated more rapidly and with a higher contrast by this technique than by cathodic etching.

3. Fuels and Claddings--Thermodynamics of Fuel Materials

a. Vapor Species Partial Pressures in the Ternary U-Pu-C System (P. E. Blackburn and J. W. Reishus)

Last Reported: ANL-7403, p. 110 (Dec 1967).

Mass-spectrometric Knudsen effusion studies are planned for the Pu-C and U-Pu-C systems. Initial work will be centered on the Pu-C system and, in particular, the higher temperature two-phase fields, Pu_2C_3-PuC_2 and PuC_2-C, of that system.

Samples of Pu-C with compositions ranging from PuC to PuC_2 are being prepared. Some difficulty has been encountered in preparing Pu_2C_3, but this difficulty is not considered to be insoluble. Initial experiments will be carried out with two-phase samples of PuC_2-C.

4. Techniques of Fabrication and Testing--Basic Fabricability--Research and Development

a. Development of Nondestructive Testing Techniques (H. Berger)

Last Reported: ANL-7427, pp. 105-107 (Feb 1968).

(i) Neutron Techniques. Studies of neutron radiography techniques continue with a small ^{241}Am-^{242}Cm-Be source (yield* of 1.15×10^9 neutrons/sec).

A result of particular interest is that the activation-transfer method of neutron radiography has proved to be possible using this small source. The moderator and collimator parameters were the same as given

*Yield valid for Nov. 20, 1967; ^{242}Cm half-life (T 1/2) is 163 days.

for direct-exposure results (see ANL-7427, p. 106). The quality of radiography, however, is impressively superior. Dysprosium foil (125 μ thick) gave good results with exposure to saturation (half-life of ^{165}Dy is 2.32 hr) and transfer to KK film. Gold foil (250 μ thick) even with much longer irradiations ($2\frac{1}{2}$ days) gave results of inferior quality.

Films have been obtained that give a measure of the radiographic quality obtainable, i.e., inherent unsharpness, geometric unsharpness, contrast, etc. Further work is planned.

The gamma-radiation intensity at the exposure position for the Am-Cm-Be source (1.15×10^9 neutrons/sec) BeO moderator stack, and cadmium collimator (12 by 12 by 120 cm) has been measured as 2 R/hr with no filters in the beam. Lead filters of up to 1.5 mm in thickness do not change this reading; 3- and 6-mm filters yield a reading of 0.7 R/hr.

The gamma intensity of 2 R/hr corresponds to that reported for the decayed Am-Cm-Be (1.16×10^7 neutrons/sec) source, measured at 50 cm from the source, emerged in a water moderator. This calculated agreement assumes that both moderators give the same gamma background, and that the neutron-to-gamma ratio remains the same for the new and decayed Am-Cm-Be sources.

(ii) Passive Ultrasonic Techniques. Additional lithium niobate elements were received and evaluated. A comparison of the relative sensitivities of three different cuts reveals that a Y-cut element is the most sensitive to longitudinal wave motion.

(iii) Scatter Radiography. Scatter radiography studies are being made with 1.27-cm-diameter aluminum rod samples that contain longitudinal cracks opened to the surface. The cracks are introduced into the rod samples by heating in an open flame to about 600°C and immediately quenching in cold water. Samples that contain voids of this type are being investigated because they present a more realistic void than the drilled-hole samples. The ultimate objective of the program is to detect internal voids in the specimens being investigated. Scatter results obtained from the cracked specimens are poor. The X-ray energy that enters the specimen is being increased in an attempt to improve the probability of obtaining an image of the voids on the film.

C. Engineering Development--Research and Development

1. Development of Master-Slave Manipulator Systems (R. C. Goertz)

Last Reported: ANL-7427, pp. 111-112 (Feb 1968).

a. Development of Manipulator Systems

(i) Electric Master-Slave Manipulator, Mark E4A. A servo drive unit is being irradiated in the Argonne Chemistry Division's ^{60}Co gamma facility at a rate of 1×10^6 R/hr and at a temperature of 38°C. This temperature closely approximates the maximum design ambient cell temperature for most hot laboratories. To date the unit has received an exposure dose of about 6.6×10^7 R.

With the exception of the synchro, materials and components used throughout the servo drive unit have been carefully selected for good radiation resistance, commensurate with availability. The drive-unit synchro being tested is an unmodified commercial device with only the "lead-in" insulation having questionable radiation resistance.

Performance tests of components used in the servo drive unit will be started at an initial exposure dose of 1.3×10^8 R; subsequently higher doses, up to 1.3×10^9 R, will be employed. Some parameters measured include: 1) motor power, current, resistance, and torque; 2) tachometer power, current, and output voltage; 3) brake solenoid pull-in voltage; 4) gearbox friction, and 5) the motors will be heat cycled by turning full power on and off a large number of times. These tests will provide data for a systems operation evaluation. After the 1.3×10^9 R dose has been reached, and if the unit is still functioning reasonably well, continuing tests will be run.

b. Study of Remote Handling for LMFBR Facilities. We have continued studying remote handling problems in the present and future aspects of Liquid Metal Fast Breeder Reactors. As we talk to people, we find, as we have in the past, that it is often quite difficult to explain some aspects of remote handling thoroughly enough to convey good understanding. Consequently, we are taking additional steps to try to have a number of engineers from various organizations come to ANL (Illinois) and try the Mark E4A and Slave-Television (Mark TV1). Since we have only one of the Mark E4A, we are refurbishing and setting up a Model E3 arm to make up a pair.* Master-slave manipulators really need to work as a pair rather than one arm at a time.

*Two pairs of the Model E3's were used in the Chemical Engineering Senior Cave at ANL for about seven years. They have recently been retired because they were wearing out, because they gave too much service trouble, and because they were a bit large for the relatively small cells they were in. We were able to salvage all four master arms and the amplifiers. One of the master arms is being converted to a slave arm by changing some of the parts. This can be done at very modest cost because many of the parts were on hand. The load capacity of the E3 and the E4A is nominally 50 lb, and the general performance is close enough for the two to be used as a pair for demonstrations and experiments in the cold lab.

2. Heat Transfer, Fluid Flow, and Mechanics of Materials

a. High-temperature Boiling Sodium Experiment (J. V. Tokar)

Last Reported: ANL-7427, pp. 113-114 (Feb 1968).

(i) Niobium-1% Zirconium Loop. To date, 41 boiling runs have been made in the following ranges of variables for sodium: boiling inlet velocity, 1-4 ft/sec; saturation pressure at initiation of boiling, 13-47 psia; temperature 1600-2010°F; heat flux, 1.5-4.5 x 10^5 Btu/hr-ft^2. In all cases, the approach to boiling was made by decreasing loop pressure until boiling occurred. Although the data have not been thoroughly analyzed, the following conclusions are evident:

1. In 34 of the 41 runs, no stable boiling was achieved, with or without isolation of the two-phase flow from the dump-tank free surface area.

2. In the seven remaining runs, the flow could be termed "metastable," because a slight disturbance of any independent variable caused a return to the "chugging" flow found in all runs.

3. Superheat required to start boiling for each run was initially low, increased with time, and eventually was completely unpredictable. For the last 24 runs, initial boiling occurred either in the boiler or in the adiabatic riser above the boiler, under subcooled, saturated, and superheated liquid conditions, corresponding to local superheats of 5-100°F.

During these runs the helical induction pump has not performed to specifications; a performance test showed that the pump is producing only 30% of the 120-psi rated head at 1.2-gpm flow. Thus the available pressure head and flow rate are far too low to allow either orificing (the next experimental step) or the testing of the thermal-radiation heater in the 20-48-kW range (i.e., heat fluxes up to 10^6 Btu/hr-ft^2). To correct this problem would require the purchase and installation of a new pump, a major modification.

b. Heat Transfer to Liquid Metal Heat Exchangers (R. P. Stein)

Last Reported: ANL-7427, pp. 114-115 (Feb 1968).

(i) Nonsymmetrical-duct Heat Exchangers. Experimental data have been obtained with counterflowing sodium in the variable-eccentricity double-pipe heat exchanger. Typical results are shown in Figs. III.C.1 and III.C.2.

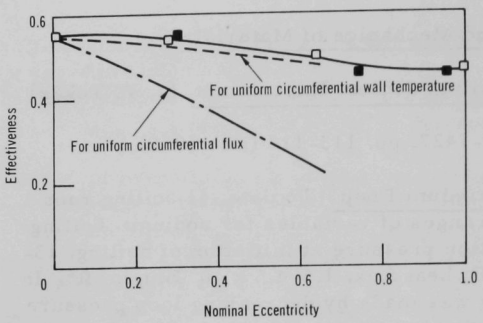

Fig. III.C.1

How Heat Transfer Effectiveness between Counterflowing Sodium in a Double-pipe Heat Exchanger Varies with Eccentricity--Comparing Calculations Based on Two Different Axially Uniform Annulus Nusselt Numbers (broken lines) with Experiment Data (solid data points represent displacement opposite to that of open data points). Sodium mass flow rates were equal in this Test Section No. 1; Peclet numbers were 668-682 on the tube side and 245-250 on the annulus side.

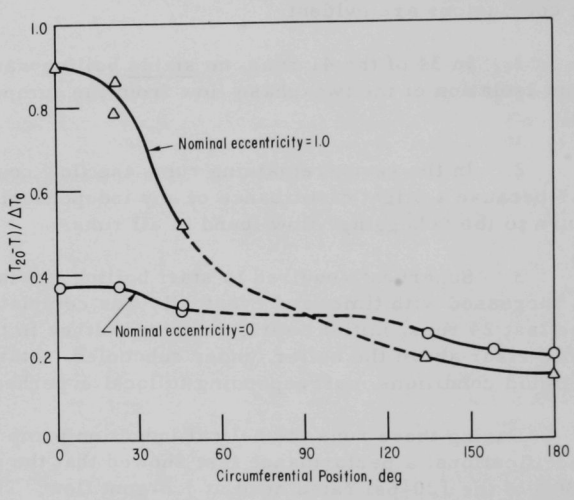

Fig. III.C.2. Temperatures around Circumference of Outer Wall of Annular Space for Two Eccentricities at Axial Position 16 Tube Diameters from Tube Inlet, Where Conditions Correspond to Those of Fig. III.C.1, and T = Outer-wall Temperature, T_{20} = Annulus Inlet Temperature, and ΔT_0 = Inlet Temperature Difference (annulus side minus tube side)

The calculated effectiveness values in Fig. III.C.1 were obtained by using (a) a current version of the Lyon-Martinelli equation,* $Nu = 5.0 + 0.025\,(Pe)^{0.8}$, for tube-side film coefficients, (b) a thermal conductivity of 27.0 Btu/hr-ft-°F for the 0.378-in.-OD x 0.012-in.-wall, 70-30 cupronickel tube, and (c) Yu-Dwyer** values for fully developed annulus-side coefficients with the heat flux uniform in the axial direction. The results

*Subbotin, V. I., et al., A Study of Heat Transfer to Molten Sodium in Tubes, At. Energ. (USSR) 13, 380-382 (1962).

**Yu, W. S., and Dwyer, O. E., Heat Transfer to Liquid Metals Flowing Turbulently in Eccentric Annuli-I, Nucl. Sci. Eng. 24, 105-117 (1966); 27, 1-9 (1967).

indicate that use of the Yu-Dwyer values based on circumferentially uniform inner-wall temperature gives good agreement with experiment, whereas use of values based on circumferentially uniform heat flux results in predicted effectivenesses that are much too low.

No effort was made to modify the calculations, which are based on "fully developed" conditions, to account for entrance effects. According to the analysis for the concentric case, the influence of such effects is expected to be weak for the operating conditions of Figs. III.C.1 and III.C.2. In Fig. III.C.1, no calculated values are given for eccentricities greater than 0.7 because that is the upper limit of the Yu-Dwyer data. Figure III.C.2 shows how the temperatures around the circumference of the outer wall of the annular space changed with eccentricity. Note that measurements of the tube position that was thought to give concentric placement actually indicated placement that was slightly eccentric. For this reason, the eccentricities on the graphs are referred to as "nominal." Additional data collection and analysis continues with the first test section.

In ANL-7427, it was noted that circumferential temperature measurements like those in Fig. III.C.2 indicated that the tube-locating devices were not operating correctly. Temperature distributions as nearly symmetrical as those shown in Fig. III.C.2 were not obtained. The problem has been solved only partially. For example, when the tube is displaced in the direction opposite to that of Fig. III.C.2, the temperature distributions, although improved, still are not satisfactorily symmetrical.

(ii) Liquid-metal-heated Steam Generators. Construction of the loop continues. The stainless steel piping to handle the mercury is approximately 90% assembled.

The computer program to provide "engineering" predictions of vaporization rates for comparison with actual data and other methods of calculation has been completed and successfully tested. This program is based on a design procedure that, in addition to assuming that a liquid-metal heat-transfer coefficient is known and independent of length, accounts for steam-side heat transfer by a Rohsenow-type empirical correlation.* To test the accuracy of this type of prediction method, it will be compared with the results of calculations based on a model that eliminates the use of heat-transfer coefficients on the liquid-metal side but retains the same Rohsenow-type empirical correlation for the steam side. The latter method results in a highly nonlinear mathematical problem because of the form of the steam-side heat-transfer relationship. The problem is further complicated by the necessity to account for the liquid-metal-side heat transfer by "first principles" rather than by the use of heat-transfer coefficients.

*Rohsenow, W. H., and Choi, H., Heat, Mass, and Momentum Transfer, Prentice-Hall, New Jersey (1961) pp. 226-228.

The essence of the difficulties, together with the basis of the present iterative method of solution, can be illustrated as follows.

Let $F_k(z)$ represent the kth approximation of the heat flux as a function of axial length z. Then, from "first principles," the $(k+1)$th approximation of the liquid-metal-side heat-transfer surface-temperature distribution is given by

$$\xi_{w1(k+1)} = \int_0^z [1 + G(z - s)]\, F_K(s)\, ds, \tag{1}$$

where G(z) represents a known function of axial distance that depends on Peclet and Prandtl numbers as well as duct geometry. With steam-side pressure drop assumed to be negligible, the Rohsenow-type correlation relates the local flux to the steam-side heat-transfer surface temperature, ξ_{w2}, by

$$F = A\xi_{w2} + B\xi_{w2}^3, \tag{2}$$

where A and B are constants. This equation allows the $(k+1)$th approximation of the steam-side surface temperature to be related to $\xi_{w1(k+1)}$ by

$$\xi_{w1(k+1)} = (A+C)\, \xi_{w2(k+1)} + B\xi_{w2(k+1)}^3, \tag{3}$$

where C is a constant determined by simple heat conduction through the heat-transfer wall. Thus, $\xi_{w2(k+1)}$ is determined from $\xi_{w1(k+1)}$ by solution of a cubic equation which, it so happens, has only one real root for a physically "real" situation. With $\xi_{w2(k+1)}$ known as a function of z, Eq. (2) gives $F_{(k+1)}(z)$, which is then applied to Eq. (1) for the next iteration. Does the basic method of solution converge, and how does it depend on the method of determining the "zeroth" approximation of the flux distribution? The initial test of the procedure by actual computation resulted in apparent instabilities after the second or third iteration. It is not known, however, whether the instabilities are a property of the method of solution or simply the usual difficulties experienced during initial debugging of a relatively complicated computer program.

c. Heat Transfer to Liquid Metal Cooled Reactor Channels (R. P. Stein)

Last Reported: ANL-7419, p. 117 (Jan 1968).

The engineering-type relationships to account for forced-convection heat transfer during flux transients (see Progress Report for July 1967, ANL-7357, pp. 116-117) have been applied to cases in which the heat flux to the fluid is assumed to be known and is represented by

$$q = q_m e^{\alpha\tau} \sin\pi(\ell/L), \qquad (1)$$

where q = heat flux density to fluid in Btu/hr-ft^2, q_m = maximum value of q, α = exponential inverse period in sec^{-1}, τ = time in second, ℓ = axial position along channel measured from inlet in feet, and L = channel length in feet. With the heat flux known, the channel heat-transfer surface and fluid bulk temperatures, as functions of both time and position, can be calculated "exactly." This allows a meaningful comparison of various approximate methods of computation. Figure III.C.3 shows such comparisons for

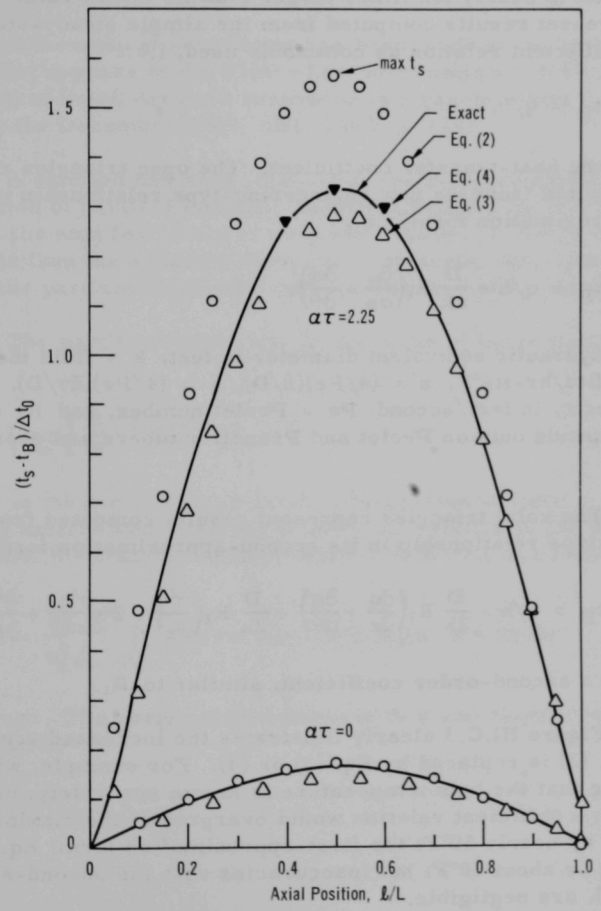

Fig. III.C.3. Comparative Computations for Flux Transient, $q = e^{\alpha\tau}\sin\pi(\ell/L)$ (Reynolds No. 100,000, Prandtl No. 0.003, Channel L/D = 200, $\alpha L/\bar{u}$ = 10)

a very rapid transient whose value of α is one-tenth of the fluid residence time in a parallel-plane channel. The system is imagined to be operating under steady-state conditions at time zero with an overall temperature rise (outlet minus inlet) equal to Δt_0 in °F. The ordinate of the graph is the difference in temperature between the channel heat-transfer surface t_s and the fluid bulk t_B, divided by Δt_0.

The graph shows exact calculations (solid lines) for the initial steady state and for a later time equal to 2.25 exponential periods when the maximum flux is nearly ten times larger than its initial value. The open circles represent results computed from the simple steady-state heat-transfer-coefficient relation as commonly used, i.e.,

$$t_s - t_B = q/h, \tag{2}$$

where h is the heat-transfer coefficient. The open triangles represent results computed from the new engineering-type relationship in its simplest or first-approximation form, i.e.,

$$t_s - t_B = q/h + \frac{D}{2k} R_1\left(\frac{\partial q}{\partial z} + \frac{\partial q}{\partial \theta}\right), \tag{3}$$

where D = hydraulic equivalent diameter in feet, k = fluid thermal conductivity in Btu/hr-ft-°F, $z = (4/Pe)(\ell/D)$, $\theta = (4/Pe)(\bar{u}\tau/D)$, $\bar{u}$ = fluid average velocity in feet/second, Pe = Peclet number, and R_1 = a coefficient that depends only on Peclet and Prandtl numbers and geometrical shape.

The solid triangles represent results computed from the new engineering-type relationship in its second-approximation form, i.e.,

$$t_s - t_B = q/h + \frac{D}{2k} R_1\left(\frac{\partial q}{\partial z} + \frac{\partial q}{\partial \theta}\right) + \frac{D}{2k} R_2\left(\frac{\partial^2 q}{\partial z^2} + 2\frac{\partial^2 q}{\partial z \partial \theta} + \frac{\partial^2 q}{\partial \theta^2}\right), \tag{4}$$

where R_2 is a second-order coefficient, similar to R_1.

Figure III.C.3 clearly illustrates the increased accuracy possible when Eq. (2) is replaced by Eq. (3) or (4). For example, with Δt_0 ~200°F, and assuming that the bulk temperature is known accurately, use of the usual heat-transfer-coefficient relation would overpredict the maximum surface temperature by nearly 50°F; the first-approximation form, Eq. (3), would underpredict by about 10°F; but inaccuracies with the second-approximation form, Eq. (4), are negligible.

Further studies in progress emphasize more realistic transients for LMFBR applications. Most, if not all, existing computer codes for fast reactor safety analyses use Eq. (2). Would replacement of Eq. (2) in these

codes with Eq. (3), or possibly even Eq. (4), offer significant and meaningful improvements in predicting, for example, the incipience of coolant vaporization?

d. Fog Flow Heat Transfer and Fluid Flow (R. P. Stein)

Last Reported: ANL-7419, p. 118 (Jan 1968).

Materials procurement problems have delayed completion of the fog-flow experimental apparatus.

A theoretical calculation has been made of the turbulent particle diffusivity that appears in the Fick's Law formulation describing the turbulent diffusion of liquid droplets suspended in a gaseous duct flow (see Progress Report for December 1967, ANL-7403, p. 115).

A solution has been obtained to the modified Basset-Boussinesq-Oseen equation of particle motion,* assuming that (1) the particle diameter is less than the smallest scale of turbulent motion, (2) the particle "response time" is less than the smallest turbulent time scale, and (3) the terminal velocity of the particle is greater than the rms turbulent velocity of the gas.

The particle diffusivity, for the case of large diffusion times, is defined by

$$\epsilon = \lim_{t\to\infty} \frac{1}{2} \frac{d}{dt} \overline{\sigma^2(t)}, \tag{1}$$

where $\overline{\sigma^2(t)}$ is the mean-square particle dispersion at time t. For a particle moving axially with terminal velocity u_t relative to the surrounding turbulent fluid, the transverse particulate dispersion was found to be

$$\overline{\sigma^2(x)} = \frac{\overline{v^2}}{u_t^2} \int_0^x \int_0^x g(x - x')\, g(x - x'')\, R_{22}(x', x'')\, dx'dx'', \tag{2}$$

where $x = u_t t$. The response of a particle to a unit impulsive force at $t = 0$ is given by

$$g(t) = 1 - \exp\left(-\frac{t}{t_p}\right). \tag{3}$$

*Corrsin, S., and Lumley, J. L., On the Equation of Motion for a Particle in a Turbulent Fluid, Appl. Sci. Res. Sec. A6 (1956).

In Eq. (2), $R_{22}(x', x'')$ is the Eulerian radial correlation function defined by

$$R_{22}(x', x'') = \frac{\overline{v(x')\, v(x'')}}{\sqrt{\overline{v^2(x')}}\sqrt{\overline{v^2(x'')}}}, \tag{4}$$

where $v(x)$ is the radial turbulent velocity at the axial location x.

It is further assumed that

(1) $R_{22}(x', x'') = \exp[-|x' - x''|/L]$, (5)

where L, the turbulent integral scale, is defined by

$$L = \int_0^\infty R_{22}(r)\, dr; \tag{6}$$

(2) the fluid is in motion with axial velocity U.

Under these assumptions, the diffusivity defined by Eq. (1) was found to be

$$\epsilon = L \frac{\overline{v^2}}{u_t} U, \tag{7}$$

where $\overline{v^2}$ is the mean-square transverse turbulent velocity.

The validity of this result will be tested experimentally.

3. Engineering Mechanics

a. Core Structural Dynamic Studies (M. W. Wambsganss)

Last Reported: ANL-7427, pp. 116-119 (Feb 1968).

Transducers are being developed to measure the random fluctuations of coolant pressure on the surface of a simulated fuel rod and to measure the rod displacement.

A stacked configuration and a more rigid mounting have improved the sensitivity and frequency response of miniature pressure transducers. The welded base plate has improved the frequency response of the transducer without introducing excessive strain sensitivity.

Stacked-configuration transducers are now constructed routinely. Both commercially available Bimorph stacks and individually stacked elements have approximately the same sensitivity. Preliminary measurements

of transducer characteristics indicate that they are adequate for our experiments. A test rod with seven transducers will be evaluated in a flowing fluid. With the transducers mounted longitudinally and circumferentially on the rod, we will make cross-correlation measurements so as to develop a characterization of the random forcing function.

To measure the displacement of a tubular specimen without disturbing the flow field, we are considering a technique involving an instrumented rod rigidly mounted within the tube and isolated from it. This technique will be particularly valuable in measuring cylinder displacement within a bundle of simulated fuel tubes. The internal displacement transducer was constructed with a 0.32-in.-dia ceramic rod. Sensing coils, which were wound on coil forms with different numbers of turns to allow the transducers to operate at frequencies sufficiently different to minimize any coupling or crosstalk, were glued to two flats ground in the midpoint of the rod at 90° to each other. The coil wires were soldered to shielded wires that were routed through the center holes in the rod. After the instrumented rod was inserted in a tubular test specimen and supported at nodal points for the vibration modes of the tube, the displacement transducers were calibrated by mounting the tube-rod assembly in the test section and using a micrometer to deflect the tube a measured amount while recording the output from the transducing system. Redesigned mounting fixtures are being fabricated for use in flowtests.

A topical report is being written to describe the theoretical-experimental approach and the results of the flowtests already performed.

D. Chemistry and Chemical Separations

1. Aqueous and Volatility Processes--Research and Development--Fluoride Volatility Process

a. Fluorination Chemistry and Procedures (M. J. Steindler)

Last Reported: ANL-7403, pp. 117-118 (Dec 1967).

A statistically designed series of five experiments simulating the fluoride volatility processing of fast breeder reactor fuels is underway, using the 2-in.-dia fluid-bed reactor. The reaction steps in the current work consisted of oxidation with 20 v/o oxygen, fluorination with 10 v/o fluorine, and a subsequent recycle-fluorination with 90 v/o fluorine.

In these experiments, effects on plutonium retention in the final bed are being studied for two ratios of fuel to alumina (0.3 and 0.6), for two fluorination temperatures (350 and 450°C) in the fluorination step, and for two recycle-fluorination times (10 and 20 hr). One run (FF-A1) has been

completed using 20% PuO_2-UO_2 powders and representative amounts of nonradioactive fission products. Run FF-Al utilized a fuel-to-alumina ratio of 0.6, temperatures of 450°C for the oxidation step and 350°C for the fluorination step, and a 20-hr recycle-fluorination sequence which consisted of 4 hr at 300°C, 3 hr each at 350, 400, 450, and 500°C, and 4 hr at 550°C.

Results for Run FF-Al are not complete. However, results obtained thus far indicate that the final bed contains <0.05 w/o Pu and <0.018 w/o U, which correspond to retention in the alumina bed of 0.5% of the 115 g of plutonium charged and 0.04% of the 459 g of uranium charged.

b. PuF_6 Chemistry and Purification Processes (M. J. Steindler)

Last Reported: ANL-7427, pp. 119-120 (Feb 1968).

In one step of the fluid-bed fluoride volatility process, oxidized fuel is reacted with fluorine, producing the hexafluorides of uranium and plutonium, and other volatile fluorides. The UF_6 and PuF_6, which are transported away from the fuel residue in a gas stream, must be separated from fission product fluorides in the gas mixture. One procedure being considered to achieve partial decontamination of PuF_6 is to pass the gas stream through a fixed bed of granulated LiF. Ruthenium fluoride is retained in the bed (see Progress Reports for January and February 1968, ANL-7419, pp. 119-120; ANL-7427, pp. 119-120). In the first stages of fuel fluorination (when the gas stream is a mixture of fluorine, actinide fluorides, and fission product fluorides), part of the plutonium is sorbed by LiF, but in the final stage of fluorination most of this plutonium is removed from the LiF by reaction with nearly pure fluorine that is then the gas stream.

One objective of current work is to identify the complexes formed in the reaction of PuF_6-fluorine mixtures with solid LiF at 300°C. Another objective, necessitated by the requirement for an adequate plutonium throughput rate, is to determine the rate of plutonium recovery obtained by passing fluorine over the complexes at 400°C.

In the present work, a PuF_6-fluorine mixture was reacted with LiF at 300°C until the total composition of the complex formed was 29.4 m/o PuF_4. X-ray powder diffraction analysis of the solid showed the presence of only $LiF \cdot PuF_4$, although it is presumed that LiF was also present. To recover plutonium from this complex, a sample was heated to 400°C and then fluorinated at 400°C with pure fluorine at a flow rate of 100 ml/min. At the end of successive 1- to 2-hr fluorination periods, the sample was weighed. The rate of weight loss during the plutonium-recovery step changed abruptly after 300-400 min of reaction time. The observed change in reaction rate suggests that two different plutonium-containing complexes participated in the recovery reaction. The X-ray powder pattern showed that the second solid phase was $4LiF \cdot PuF_4$. Apparently, some $4LiF \cdot PuF_4$

formed from $LiF \cdot PuF_4$ and LiF when the complex was heated to 400°C. In the first part of the plutonium-recovery step at 400°C, the remaining $LiF \cdot PuF_4$ is believed to have reacted with fluorine to form $4LiF \cdot PuF_4$ and PuF_6. In the second part of the plutonium-recovery step, $4LiF \cdot PuF_4$ reacted with fluorine at a lower rate than in the first part to form LiF and PuF_6.

The rate constant for the fluorination of the $4LiF \cdot PuF_4$ complex at 400°C was compared with the rate constant for the fluorination at 350-375°C of plutonium from simulated nuclear fuel. The former rate was only slightly lower, indicating that plutonium recovery from LiF beds may be practical.

c. Fission Product Fluoride Chemistry (R. L. Jarry)

Last Reported: ANL-7427, pp. 120-121 (Feb 1968).

(i) Chemistry of Ruthenium. The experimental study of the transpiration of mixtures of ruthenium fluorides and UF_6 (a stand-in for PuF_6), using fluorine as the carrier gas, has been continued. Experiments 1 to 4 were performed to evaluate absorption of ruthenium fluorides on LiF as a means of removing ruthenium from process gas streams. The ruthenium used was tagged with ^{106}Ru to allow the movement of ruthenium to be monitored by gamma counting. In these experiments, a mixture of ruthenium fluorides and UF_6 prepared in a fluorination step was trapped in a cold trap at -78°C, and then the uranium and ruthenium species were transpired in a stream of fluorine by raising the cold-trap temperature to 0, 50, 100, and 150°C. The gas stream from the cold trap flowed through a LiF trap at 300-400°C and then through a NaF trap at 100°C.

Experiment 5, similar to Experiment 4 reported in ANL-7427, was performed. A RuO_2-UF_4 mixture was fluorinated at 550°C (instead of at 600°C as in Experiment 4) with a 3:1 fluorine-oxygen mixture. The volatile products were cold trapped, and then transpirations were performed.

In Experiment 5, as in Experiment 4, the counting data indicated little transport of ruthenium during the 0 and 50°C transpiration periods. When the cold-trap temperature was increased to 100°C in Experiment 5, the quantities of ruthenium sorbed on the LiF at 350°C and on NaF at 100°C were similar to those obtained in earlier experiments. In the early stages of transpiration, the transpired ruthenium was all sorbed on the LiF. Ruthenium which broke through the LiF trap when 80% of the LiF capacity for ruthenium was reached was retained in the NaF trap. Similar sorption behavior was noted in previous experiments.

The data obtained in Experiments 1 to 5 were reviewed to determine whether sublimation of PuF_6 from the cold trap at 0°C might be a feasible technique for separating plutonium from ruthenium. Estimates

were made by comparing the background count of the LiF trap with the counting data accumulated during the fluorination period and the 0 and 50°C transpiration periods. The calculations resulted in maximum values of ruthenium transpired (95% confidence level) of 1.2, 0.8, 1.7, and 1.2 mg for Experiments 1, 2, 3, and 5, respectively, representing 0.08 and 0.17 percent of the ruthenium charged. (The corresponding value for Experiment 4 is not listed since the maximum counts per minute value was less than the background count.)

Decontamination factors were calculated (see Table III.D.1), using the values for maximum ruthenium transported at cold-trap temperatures of 50°C and less. These calculated DF values are minimum values; the actual values at 0°C are probably much higher than the values given. For comparison, theoretical DF's based on vapor pressure data for RuF_5 are provided.

TABLE III.D.1. Ruthenium Decontamination Factors[a] (DF) Obtained in Various Experiments

Temp (°C)	Theoretical[b] DF	DF, Expt. 1	DF, Expt. 2	DF, Expt. 3	DF, Expt. 5[c]
0	5×10^5	$>8.3 \times 10^2$	$>1.3 \times 10^3$	-	$>8.3 \times 10^2$
50	6×10^2	-	-	$>5.9 \times 10^2$	

[a]It was assumed that RuF_5 was the transpired species. There were 1000 mg ruthenium in each charge.

[b]For this calculation, the vapor pressure of RuF_5 at 50°C was taken from an equation by H. A. Bernhardt et al., AECD-2390 (1948). The 0°C vapor pressure value was an extrapolated value.

[c]This is the combined value for 0 and 50°C transpiration periods.

d. Neptunium Fluoride Chemistry (L. E. Trevorrow)

Last Reported: ANL-7419, pp. 121-122 (Jan 1968).

In the fluid-bed fluoride volatility process, a gas stream containing UF_6, PuF_6, NpF_6, and other volatile fluorides may be passed through a fixed bed of NaF (which would be operated at various temperatures between 100 and 400°C in various steps of the process). The NpF_6 would be removed from the gas stream by the following reaction with NaF:

$$3NaF(s) + NpF_6(g) \rightleftarrows 3NaF \cdot NpF_5(s) + \tfrac{1}{2}F_2(g). \quad (1)$$

For subsequent recovery of the neptunium from the complex as NpF_6, the $3NaF \cdot NpF_5$ may be fluorinated with fluorine.

Information on the equilibrium constant for the reaction would permit quantitative prediction of the extent to which NpF_6 would be taken up or released by a bed of NaF. The equilibrium constant

$$K_p = (P_{NpF_6})/(P_{F_2})^{1/2}$$

for the fluorination of $3NaF \cdot NpF_5$ by fluorine has been determined at a pressure of 700 Torr and temperatures of 250 to 400°C. The procedure used was to circulate fluorine gas over a sample of the complex for about 15 hr. Then a sample of the gas phase (a mixture of NpF_6 and fluorine) was trapped in a 5-cm spectrometer cell, and the total absorbance of the gaseous sample was measured at 2210 Å. In all samples, the partial pressure of NpF_6 was small compared to that of fluorine, whereas the ultraviolet absorbance of fluorine was small compared to that of NpF_6. The pressure of fluorine in a sample was assumed to be equal to the total pressure, which was measured with a nickel Bourdon gauge. The measured absorbance at 2210 Å was used in calculating the partial pressure of NpF_6.

It was determined that the equilibrium constant can be expressed as a function of temperature by the equation

$$\log K_p(atm^{1/2}) = \frac{-3.147 \times 10^3}{T(°K)} + 2.784.$$

Several measurements, made at 350°C with fluorine pressures varying from 150 to 1500 Torr, showed that $\log P_{NpF_6}$ was a linear function of $\log P_{F_2}$ with a proportionality coefficient of 0.49, which is comparable to the value of 1/2 expected for Reaction 1. The value of K_p at 350°C was 5.52×10^{-3} $atm^{1/2}$.

From the values of the equilibrium constant, the following values for thermodynamic functions for the fluorination of $3NaF \cdot NpF_5$ have been calculated over the range 250-400°C: mean enthalpy change, 14.4 kcal/mole NpF_6; mean entropy change, 12.7 cal/(mole NpF_6)(°K). The standard free energy change at 298°K was 10.6 kcal/mole NpF_6.

The results obtained in this study will be useful in devising a method for separation of NpF_6 from UF_6 by selective sorption and desorption on sodium fluoride.

e. Engineering-scale Development for UO_2-PuO_2 Fuel
(N. M. Levitz)

Last Reported: ANL-7427, pp. 121-122 (Feb 1968).

Flowsheet concepts for processing fast breeder fuels by fluoride volatility methods are being designed. A low-decontamination process

scaled for the plutonium-uranium oxide fuel load discharged from a 3000-MWe utility complex is being considered initially. The scheme selected as a reference flowsheet includes a sequence of batch operations selected for the most part on the basis of past studies on light water reactor fuels. Chemical requirements, process flows, and heat loads are being calculated, equipment is being sized, and an engineering (equipment) flowsheet is being prepared.

The proposed process steps are (1) mechanical separation of the fuel elements from some of the associated hardware, (2) decladding with a gas mixture such as 80% HF-20% O_2, (3) fuel pulverization by reaction with oxygen, (4) treatment of the particulate mixture with 100% HF to convert certain compounds to a form compatible with the process scheme, (5) fluorination with fluorine to convert the mixture to volatile UF_6, volatile PuF_6, and other fluorides (some volatile and some not), (6) steps to purify UF_6 and PuF_6 (i.e., to separate them from the bulk of the volatile fission product fluorides and cladding fluorides), and (7) conversion of the UF_6-PuF_6 mixture to mixed oxide particulate by reaction with a steam-hydrogen mixture.

2. Closed Cycle Processes--Research and Development--Compact Pyrochemical Processes

a. Process Chemistry of Molten Salt Systems (I. Johnson)

Last Reported: ANL-7419, pp. 123-124 (Jan 1968).

The solubility of calcium oxide in a $CaCl_2$-20 m/o CaF_2 salt mixture was measured to determine the limits of oxide loading in the $CaCl_2$-CaF_2/Cu-Mg-Ca reduction system specified for the current pyrochemical flowsheet.

Two experiments were performed in which calcium oxide in excess of the estimated solubility was mixed with purified $CaCl_2$-20 m/o CaF_2 in a baffled tantalum crucible at 900 to 950°C. Filtered samples were taken on both rising and falling temperature cycles after the salt had been equilibrated by stirring at each temperature for at least 2 hr.

The solubility of calcium oxide in the $CaCl_2$-20 m/o CaF_2 mixture as determined by analyses of the samples is plotted as a function of temperature in Fig. III.D.1. The data from both experiments are in excellent agreement. A break occurs in the curve at about 735°C, and a change in the ratio of fluoride to chloride in samples taken above and below the break indicates that a solid phase containing chloride precipitates below 735°C. The nature of this solid phase will be investigated in future experiments.

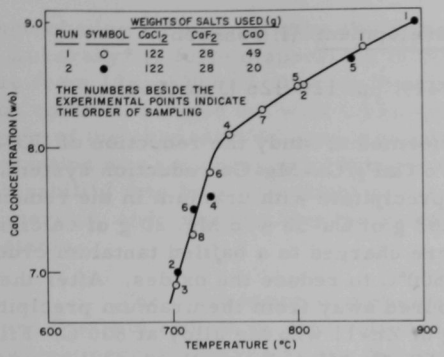

Fig. III.D.1
Solubility of CaO in $CaCl_2$-20 m/o CaF_2

b. Mass Transfer in Salt-Metal Systems (R. D. Pierce)

Last Reported: ANL-7419, p. 125 (Jan 1968).

Measurements of the distribution coefficient of cerium between Mg-Cd alloys and a 55 m/o $MgCl_2$-27 m/o NaCl-18 m/o KCl salt mixture have been completed. The measurements were made at 441, 500, 527, 578, and 636°C with magnesium concentrations ranging from 10 to 60 a/o. This work is part of a program to investigate mass-transfer rates in salt-metal systems, and is directly related to the salt-metal extraction operations used in pyrochemical processes (see Progress Report for October 1967, ANL-7391, pp. 151-152).

The results of the distribution measurements are plotted in Fig. III.D.2. The equation for the reaction of cerium transferring between the metal and salt phase is

$$Ce + 3/2\ MgCl_2 \rightleftarrows CeCl_3 + 3/2\ Mg.$$

A correlation is being developed based on equilibrium data for the reaction.

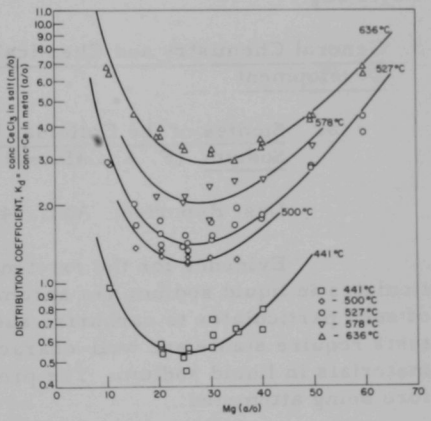

Fig. III.D.2
Cerium Distribution between Magnesium-Cadmium Alloys and 55 m/o $MgCl_2$-27 m/o NaCl-18 m/o KCl Salt

Design work has begun on the next phase of the program in which the kinetics of solute transport in salt-metal systems will be studied using single metal drops falling in a continuous salt phase. Preliminary work is being done with mercury at room temperature to devise a method of forming and releasing single metal drops.

c. Laboratory Process Development (I. Johnson)

Last Reported: ANL-7419, pp. 125-126 (Jan 1968).

An experiment was performed to study the reduction of UO_2-PuO_2 solid solution with the $CaCl_2$-20 m/o CaF_2/Cu-Mg-Ca reduction system, and to determine if plutonium would coprecipitate with uranium in the reduction. Fifty grams of UO_2-20 w/o PuO_2, 263 g of Cu-38 w/o Mg, 20 g of calcium, and 150 g of $CaCl_2$-20 m/o CaF_2 were charged to a baffled tantalum crucible and stirred at 800 rpm for 6 hr at 800°C to reduce the oxides. After the salt and the supernatant Cu-Mg were poured away from the uranium precipitate, the uranium was dissolved in 800 g of Zn-11 w/o Mg alloy at 800°C. Filtered samples were taken of both the Cu-Mg-Ca alloy during the reduction and the Zn-Mg alloy after the dissolution of the uranium precipitate. The reduction salt was also crushed and sampled.

Analyses of the samples showed that the plutonium-to-copper ratio in the Zn-Mg alloy was the same as that in the Cu-Mg-Ca reduction alloy. This result indicates that none of the plutonium (within ±0.5% analytical error) coprecipitated with the uranium, since any coprecipitation of plutonium would have resulted in a higher plutonium-to-copper ratio in the Zn-Mg alloy. The analyses also indicated complete reduction of the UO_2-PuO_2.

3. General Chemistry and Chemical Engineering--Research and Development

a. Studies of the Colloidal Behavior of Carbon-bearing Species in Sodium (F. A. Cafasso)

Last Reported: ANL-7403, p. 124 (Dec 1967).

Evidence for the existence of dispersed, carbon-bearing particulates in liquid sodium has accumulated in recent years, but the tendency of such particulates to carburize austenitic steels has not been tested. The tests require stable and well-characterized dispersions of carbon-bearing materials in liquid sodium. The preparation of such dispersions is therefore being attempted.

Stable colloids have been created in mercury, but in no other liquid metal.*,** To gain experience in preparing colloids in liquid metals and to determine the reliability of filtration for detecting such dispersions, preliminary experiments are being made with iron-in-mercury sols. Accordingly, a sol containing ~3600 ppm iron in mercury was prepared by

*Luborsky, F. E., J. Phys. Chem. 61, 1336 (1957).
**Warf, J. M. C., Karol, W. L., and Hardcastle, K. I., Inorg. Chem. 5, 1726 (1966).

electrolyzing a $FeCl_2$ solution above mercury. The procedure was that used by Luborsky* to form dispersions in mercury of iron particles ranging in size from 10 to 5000 Å. Despite the size of the particles, the bulk of the iron could be filtered out with a 15 μ-porosity tantalum frit, leaving only 5 ppm of the original 3600 ppm iron in the filtrate.** Moreover, this concentration was not changed by subsequent filtration. It thus appears that filterability may be a convenient criterion for the existence of colloidal iron in mercury and, possibly, for the existence of colloids in other liquid metal systems.

The preparation of dispersed carbon-bearing substances (e.g., C and Fe_3C) in sodium by electrolysis is not feasible. Hence, other methods in which mercury serves as the dispersant are being explored. One such method now under study is mechanical agitation. Fine particles (0.05-0.5 μ) of elemental iron were successfully dispersed in mercury at room temperature by agitation in a Wig-L-Bug† mixer. Analysis of unfiltered and filtered (15 μ-porosity tantalum frit) samples of the mixture showed the presence of 17 and 3 ppm iron in mercury, respectively. An attempt is now being made to prepare a dispersion of elemental carbon (90 Å particles) in liquid sodium by this method.

---

*Ibid, see p. 114.

**The solubility of iron in mercury is reported as <1 ppm in Hansen's "Constitution of Binary Alloys," McGraw-Hill, New York, N. Y. (1958).

†Crescent Dental Manufacturing Co., Chicago, Ill.

PUBLICATIONS

GENERAL REACTOR TECHNOLOGY

Fluorination of Uranium, Plutonium, and Neptunium from a Fluidized Bed of Alumina

L. J. Anastasia and M. J. Steindler

Abstracts of Papers Presented at 155th National Mtg., Am. Chem. Soc., San Francisco, March 31-April 5, 1968, 0-145

Studies on TTA Complexes with Metal Ions. IV. Investigations of Some Crystalline Forms of Uranyl-TTA Complex

Y. Baskin and J. R. Ferraro

J. Inorg. Nucl. Chem. 30, 241-251 (Jan 1968)

The Determination of Strain Distribution across the Interior of a Specimen from Measurements of Local Changes in Grain Shape

J. E. Flinn and E. M. Philofsky

Trans. ASM 61, 37-41 (March 1968)

Neutron Radiography of Lead

I. R. Kraska

Materials Eval. 26, 45-48 (March 1968)

Condensed Phase Equilibria in the Molybdenum Hexafluoride-Uranium Hexafluoride System

L. E. Trevorrow, M. J. Steindler, D. V. Steidl, and J. T. Savage

Advan. Chem. Ser. 71, 308-319 (1967)

Steady-State Thermal Stresses in Circular Cylinders due to Abrupt Axial Variations in Internal Heat Generation

R. A. Valentin

Nucl. Eng. Design 7, 59-72 (1968)

IV. ADVANCED SYSTEMS RESEARCH AND DEVELOPMENT

A. Argonne Advanced Research Reactor (AARR)-- Research and Development

1. Core Research and Development

a. Heat-transfer Analysis (R. R. Rohde)

Last Reported: ANL-7419, pp. 134-137 (Jan 1968).

(i) Analysis of Core Structures. New estimates of the steady-state temperature have been calculated in the analysis of temperatures in the reflector shroud and pedestal. These calculations were made for the long gusset only, because previous calculations indicate that this is a conservative case (see ANL-7419).

The previous model was changed to incorporate the upper support ring as shown in Fig. IV.A.1. Depicted there are the node numbers and the basic dimensions of the upper support ring, which, although actually circular, was approximated in these calculations by rectangular geometry.

The upper support ring is attached to the gussets by welding at Nodes 162, 163, and 164; therefore, a metallurgical bond was assumed at these locations. Table IV.A.1 lists the boundary conditions. In these calculations, more realistic (though still conservative) values of the heat-transfer coefficients were used than were employed in the previous study. Figure IV.A.2 shows the major portion of the heat-transfer boundary conditions for the structure. Faces 1 and 4 of Node 175, Face 1 of Nodes 169 and 170, and Face 2 of Node 179 were considered to be insulated. The portion of the reflector shroud and pedestal that does not include the gusset or the support ring was considered to be insulated on Faces 5 and 6. Faces 1, 2, 3, and 5 of each node of the gusset having a water boundary were assigned the Face-6 coefficients designated in Fig. IV.A.2. For example, Faces 1, 5, and 6 of Node 160 had a film coefficient of 200 Btu/hr-ft^2-°F, and Faces 2, 3, 5, and 6 of Node 40 had a film coefficient of 100 Btu/hr-ft^2-°F.

Faces 2 and 4 between Nodes 16-17, 25-26, 31-32, 66-67, and 74-75 were assumed to be insulated; for Nodes 126-127, 141-142, and 156-157, these faces were assumed to be joined by a good metallurgical bond. A film coefficient of 50 Btu/hr-ft^2-°F was assumed for the same faces of the other nodes at the interface of the gusset and the reactor shroud and pedestal proper.

The outline of the beryllium is shown in Fig. IV.A.2. The temperature of the water was assumed to be 160°F below the beryllium and 120°F on the lateral surface of the beryllium. The aluminum thermal conductivity was assigned a value of 80 Btu/hr-ft-°F, which is considered to be conservative.

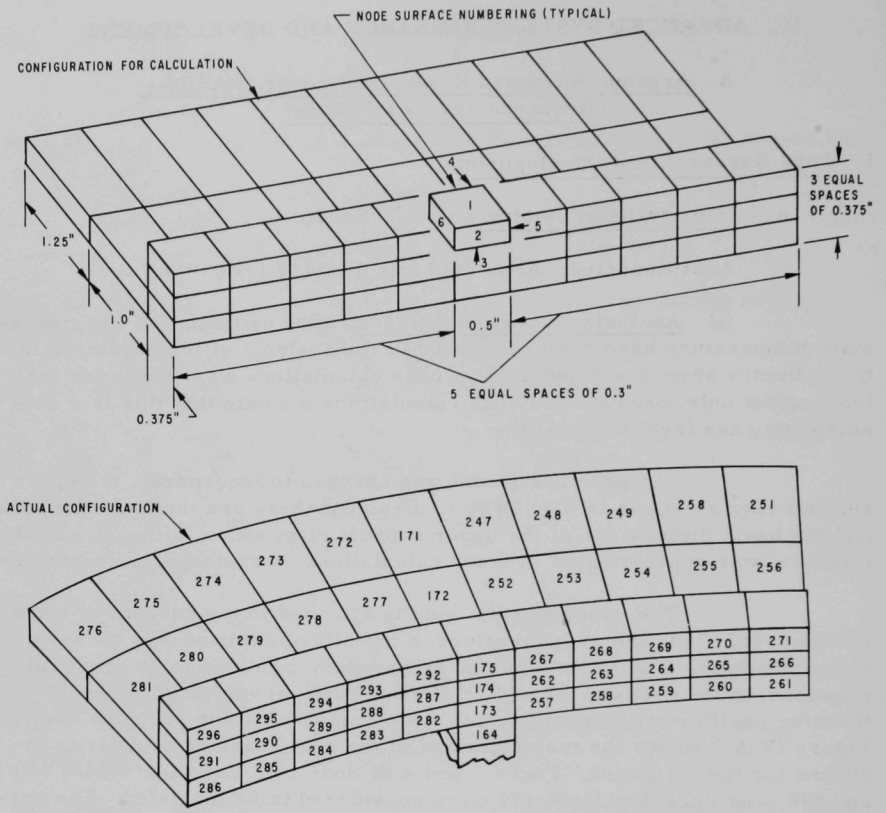

Fig. IV.A.1. Node Numbers and Dimensions for Upper Support Ring-Gusset Attachment

TABLE IV.A.1. Boundary Conditions for Upper Support Ring

Nodes	Film Coefficient[a] (Btu/hr-ft^2-°F)			
	Face 1	Face 2	Face 3	Face 4
171, 247-251, 272-276	250	b	250	250
172, 252-256, 277-281	300	b	300	b
257-261, 282-286	b	300	300	b
262-266, 287-291	b	300	b	b
175, 267-271, 292-296	Insulated	300	b	Insulated

[a]Faces 5 and 6 insulated at extremities, e.g., Face 5 of Node 251, Face 6 of Node 276. Metallurgical bond assumed between extremities.
[b]Metallurgically bonded to adjoining face.

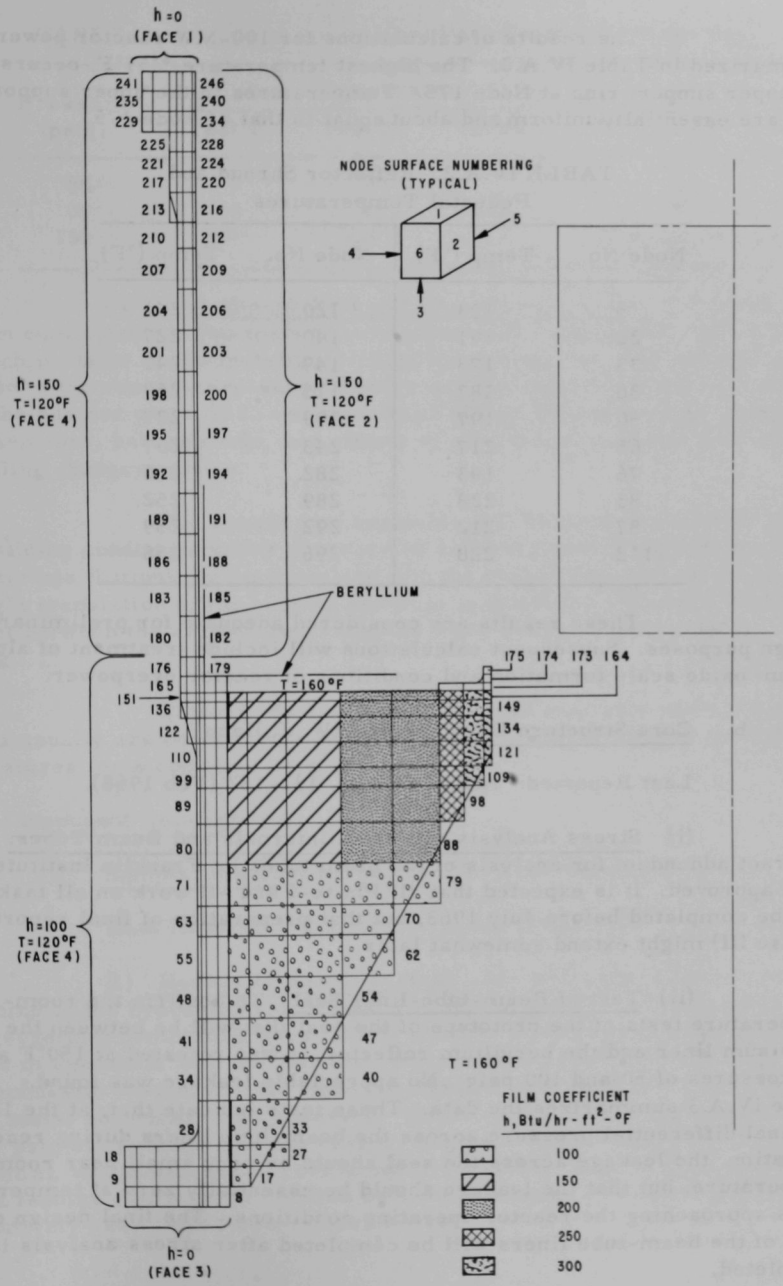

Fig. IV.A.2. Boundary Conditions Used in Calculations of Steady-state Temperature

The results of calculations for 100-MW reactor power are summarized in Table IV.A.2. The highest temperature, 259°F, occurs in the upper support ring at Node 175. Temperatures in the upper support ring are essentially uniform and about equal to that of Node 175.

TABLE IV.A.2. Reflector Shroud and Pedestal Temperatures

Node No.	Temp (°F)	Node No.	Temp (°F)
5	193	120	241
22	191	140	227
33	173	149	240
36	187	175	259
50	197	199	227
65	217	243	207
76	193	282	250
83	228	289	252
87	212	292	259
112	228	296	258

These results are considered adequate for preliminary design purposes. Subsequent calculations will include treatment of aluminum oxide scale formation and conditions of reactor overpower.

b. Core Structure Development (W. J. Kann)

Last Reported: ANL-7427, pp. 131-132 (Feb 1968).

(i) Stress Analysis of Vessel Internals and Beam Tubes. The contract addendum for analysis of the beam tubes by Franklin Institute has been approved. It is expected that all Phase-I and -II work on all tasks will be completed before July 1968, but that preparation of final reports (Phase III) might extend somewhat later.

(ii) Test of Beam-tube-liner Seal. To confirm the room-temperature tests of the prototype of the seal that will be between the aluminum liner and the beryllium reflector, it was retested at 150°F and at pressures of 50 and 100 psig. No appreciable leakage was found. Table IV.A.3 summarizes the data. These tests indicate that, at the 100-psi nominal differential pressure across the beam-tube liners during reactor operation, the leakage across the seal should be very small near room temperature, but that the leakage should be essentially zero at temperatures approaching the reactor operating conditions. The final design details of the beam-tube liners will be completed after stress analysis is completed.

TABLE IV.A.3. Leakage (ml/hr) Past Beam-tube-liner Seal

Pressure (psig)	Room Temperature			150°F
	Test 1	Test 2	Test 3	Test 4
50	0	6		0
100	50	18	175	0
150	575	600		~3 drops in 1 hr

(iii) O-ring-seal Test and Sliding-wear Tests. Drawings have been completed for two tests of core structural components. The first test, which pertains to the metallic O-rings for sealing the core-support adapter plate to the vessel-core-support ledge and the reflector-support pedestal to the adapter plate, is to verify critical design details such as gasket dimensions, bolting loads, and effects of joint translation and rotation on sealing characteristics.

The second test assembly will be used to study the effects of sliding conditions under pressure on several types of hard-surfaced materials that will be incorporated into the vessel internals in areas where slight translation of the bearing surfaces may occur. One such area is the joint between the core-support adapter plate and the vessel-support ledge ring.

These tests are needed because available wear and galling data usually are concerned with either high contact pressures or high temperatures, or a combination of the two.

2. Component Development

a. Sample Irradiation Devices (R. W. Seidensticker)

Last Reported: ANL-7403, p. 135 (Dec 1967).

(i) Hydraulic-rabbit System. The underwater life-cycle testing of the hydraulic-rabbit load station has been terminated after successfully completing about 13,000 cycles, equivalent to an estimated 5 yr of operation with the reactor. Incremental pressure tests were performed with 90-psi air (the expected internal operating pressure) during the tests; no leakage was observed. However, the final hydrostatic test at 250 psig did indicate that the rear O-ring seal had a slight leak (25 psi in 15 min), which was easily corrected by replacing the O-ring. Maintenance of a loading station is simplified by a total-package concept that permits relatively easy replacement under water.

Prototype handling tools for the reflector hydraulic-rabbit facility have been fabricated and are being tested.

(ii) Instrumentation and Control of Prototype Hydraulic Rabbit. Design of the control circuit for the hydraulic-rabbit prototype has been completed. Solid-state logic control elements and the required amplifiers have been ordered; the instrumentation equipment is being procured.

When tests of various sample-detection schemes are completed, final design of this part of the system will be started.

(iii) Rabbit-facility Heat Transfer. The approximate two-dimensional program has been shown to be suitable for studying the effect of facility parameters on steady-state temperature distributions in the internal thermal column (ITC) hydraulic rabbit. Figure IV.A.3 compares various temperature profiles calculated by two codes (both heat-transfer programs consider the sample to be located concentrically within the tube; the effect of sample eccentricity will be studied). The profiles of the coolant and the primary water as calculated by the two codes are almost identical. The only difference between the programs is that the approximate program assumes no axial conduction. The effect of this difference is seen in the tube temperature profile; as expected, the profile calculated by the approximate program is higher. As the conductivity of the tube metal decreases, the difference in temperature profiles decreases. For a range of values of several facility parameters, the only significant difference between temperature profiles calculated by the programs was the difference in tube temperature profiles.

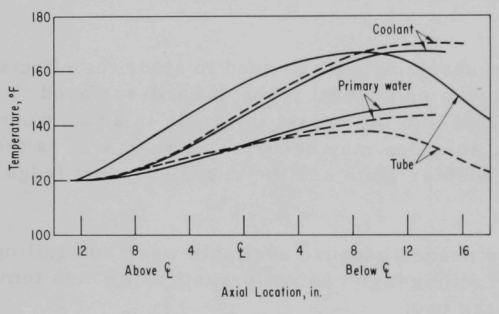

Fig. IV.A.3. Temperature Profiles in Coolant, Primary Water, and Tube of the ITC Hydraulic Rabbit Facility as Calculated by a Two-dimensional Program (dashed lines) and by an Approximate Two-dimensional Program (solid lines)

An approximate two-dimensional program was used to study the parameters of a gas-cooled rabbit facility in the ITC. Facility temperature profiles are shown in Figs. IV.A.4 and IV.A.5 for the parameter values of Table IV.A.4. How parameter variations affect facility temperature profiles is being calculated.

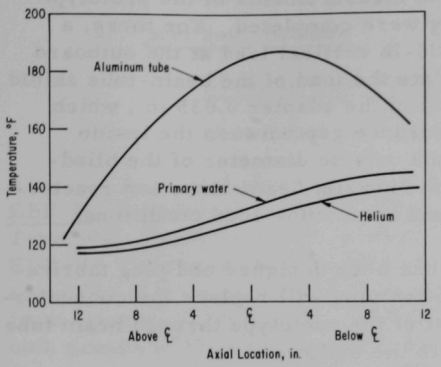

Fig. IV.A.4. Temperature Profiles in Gas-cooled Rabbit Facility in the ITC

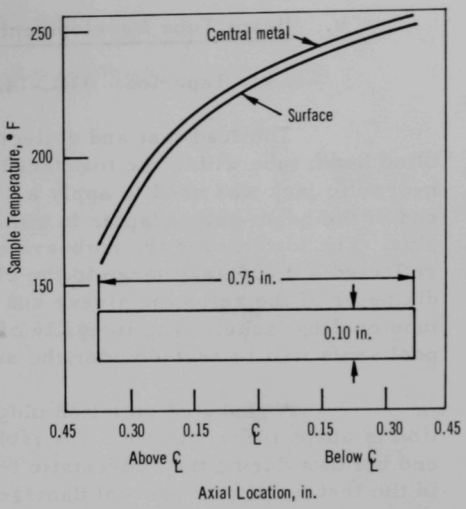

Fig. IV.A.5. Temperature Profiles of Sample in Gas-cooled Rabbit Facility in the ITC

TABLE IV.A.4. Parameters of a Gas-cooled Rabbit Facility

Helium	
Inlet temperature	100°F
Outlet temperature	124°F
Inlet pressure	400 psia
Outlet pressure	380 psia
Flow rate	4 lb_m/min
Primary Water	
Inlet temperature	120°F
Outlet temperature	161°F
Velocity	4 ft/sec
Aluminum Tube	
Outer diameter	0.625 in.
Wall	0.072 in.
Sample	
Material	Cadmium
Diameter	0.10 in.
Length	0.75 in.
Reactor Power	100 MW
Facility heat retained and to be removed by heat exchanger = 2.07 kW	

b. Beam Tube Development (A. R. Jamrog)

Last Reported: ANL-7427, pp. 132-133 (Feb 1968).

The load test and deflection measurements of the prototype blind beam tube within the test facility were completed. For these, a hydraulic jack was used to apply a 2500-lb vertical load at the outboard end of the beam-tube adapter to simulate the load of the beam-tube shield plug. The load moved the outboard end of the adapter 0.035 in., which reflected a 0.005-in. change in the clearance gap between the inside diameter of the reflector sleeve and the outside diameter of the blind-tube cooling jacket. The integrity of the nozzle, beam-tube, and reactor-pool seals will be tested under the same beam-tube-load conditions.

A gasketed isolation plug has been designed and plug fabrication is about 10% complete. The isolation plug will replace the connector-end bellows during the hydrostatic test of the prototype through beam tube in the test facility to prevent damage to the bellows.

c. Internal Thermal Column Development (R. W. Seidensticker)

Last Reported: ANL-7427, p. 133 (Feb 1968).

The ITC test-facility components, which include the breech-lock closure, the simulated ITC tower, and the inner core opening, have been installed in the test chamber of the General-purpose Hydraulic Loop. In preliminary flow tests with these components in the test chamber, severe vibration problems were encountered at flow speeds of only 3 ft/sec in the 5-in.-ID target tower. By trial and error, the problem was isolated to a temporary flat-plate flow orifice that is not a part of the prototype. This orifice had been sized to produce 4-ft/sec fluid speed at 110-psi pressure drop in the ITC. After this temporary orifice plate was removed, flow tests were conducted successfully at speeds up to 17.5 ft/sec (1000 gpm) within the target tower with no indication of any vibration problems.

V. NUCLEAR SAFETY

A. Other Reactor Kinetics--Research and Development

1. Fuel Meltdown Studies with TREAT

a. Meltdown Studies

(i) Ceramic Fuel Studies (C. E. Dickerman)

Last Reported: ANL-7349, p. 124 (June 1967).

(a) Irradiation of Unencapsulated Mixed-oxide Pins in EBR-II. A group of 19 mixed-oxide fuel rods, clad in 0.290-in.-OD Type 304L stainless steel, is awaiting irradiation, unencapsulated, in EBR-II. These pins are intended to be run in the first experimental subassembly of unencapsulated pins, along with 16 similar mixed-oxide pins from General Electric. The preliminary irradiation-data packages for both groups of pins were reviewed as part of the development of criteria for unencapsulated experimental irradiations. As the result of a detailed discussion of experimenters and EBR-II staff, new and expanded data packages have been prepared and sent to the EBR-II Irradiations staff.

(ii) Metallic Fuel Studies (C. E. Dickerman)

Last Reported: ANL-7349, p. 122 (June 1967).

One argon-bonded EBR-II Mark-I pin was melted down in its cladding, without cladding failure, in a TREAT loop experiment designed to assist in analysis of the consequences of a loss-of-bond failure of a single driver pin during EBR-II operation, before the pin had received appreciable burnup. The course of a limited program of follow-up experiments has been under study in joint collaboration with personnel of the EBR-II Operations staff. Before proceeding to investigation of the effects of burnup and of somewhat more realistic simulations, it has been decided to rerun the previous loop experiment for confirmation. Although the encouraging results of that experiment were in agreement with theoretical predictions, there are uncertainties in the effects of such factors as fuel-cladding heat transfer and the severe thermal shock produced in the cladding by fuel slumping when it melts. The Mark-I Integral Loop used for the previous argon-bonded pin experiment is being prepared for the new test.

(iii) Transient Coolant Behavior (C. E. Dickerman)

Last Reported: ANL-7403, p. 140 (Dec 1967).

Preliminary calculations have been performed on TREAT experiments to check the applicability of an existing model of MacFarlane*

*MacFarlane, D., An Analytical Study of the Transient Boiling of Sodium in Reactor Coolant Channels, ANL-7222 (June 1966).

for describing the transient behavior of sodium vaporizing in a fast reactor coolant channel. The sample geometry selected for the loop experiments is that of a single pin, surrounded by a steel flow channel of low heat capacity. Since the major criterion for the pin is that it be a reliable heat source that has a "reasonable" tolerance for overpower without failure, the pin finally chosen on the basis of the calculations is gas-bonded UC, clad by 0.290-in.-OD stainless steel cladding. The calculations indicate that, for a given set of coolant-flow and inlet-temperature conditions, this pin would have a higher cladding heat flux at pin failure than a corresponding gas-bonded oxide. Although EBR-II Mark-I-type pins have been shown to have failure thresholds under transient conditions well in excess of the needs for these experiments, prefailure movements inside the cladding were calculated to occur under conditions that could seriously interfere with analysis of the experiment data.

(iv) Development of Experimental Methods (C. E. Dickerman)

Last Reported: ANL-7419, p. 143 (Jan 1968).

The results of some calculations were reported in ANL-7419 in connection with a study of the physics requirements for hardening the neutron spectrum at the test region in the TREAT reactor for transient experiments on clusters of fast reactor fuel pins. At present this can only be done by filtering low-energy neutrons, a procedure which decreases available sample energy excessively for relatively incomplete filtering. The previously reported converter design yields a hard neutron spectrum similar to that of a fast reactor, with a maximum to minimum power ratio in the 7-pin-cluster test sample smaller than 1.01 (this is the ratio of the power at the "spike" at outer edge of the 6-pin ring to the power at the center of the central pin). It was found that the maximum available energy for melting of the test samples exceeded the energy required to melt completely the $UO_2 + PuO_2$ test sample by 30%. It was also stated in ANL-7419 that the factor could be further increased by allowing some softening of the neutron spectrum in the test section.

In the present extension of this study, the maximum to minimum power ratio in the test sample has been allowed to increase to ~1.07. Also, the maximum allowable temperature in the core has been allowed to increase to 600°C. The maximum allowable converter temperature has remained at 1800°C. These allowances have resulted in increasing the above factor (ratio of energy density available at the test sample to that required for complete adiabatic melting of mixed oxide test sample) from about 1.3 to 2.7, that is, the new "soft spectrum" reference case will produce sample energy input of ~10,000 cal/cc.

The isotopic densities (units of 10^{24} atoms/cc) and characteristics of this converter design are given in Table V.A.1.

TABLE V.A.1. Reference "Softer Spectrum" TREAT Converter

Isotope	Inner Converter (inner ring)	Inner Converter (outer ring)	Outer Converter (inner ring)	Outer Converter (outer ring)	Max to Min Power Ratio in Test Sample	Peak Power in Converter / Center Core Power	Power Ratio Centerline / Core Max	Max Core Temp (°C)	Energy Available at Center of Test Sample / Energy Required for Meltdown of UO_2
	← (x 10^{-24} atoms/cc) →								
^{235}U	0.0020	0.0010	3 x 10^{-4}	1.5 x 10^{-4}	1.075	0.156	40.0	500	2.71
^{238}U	0.0003	0.0001	4.5 x 10^{-5}	2.25 x 10^{-5}					
C			0.0722	0.0722					
Fe			3.34 x 10^{-5}	3.34 x 10^{-5}					

2. Materials Behavior, Equation of State, and Energy Transfer

a. Materials Behavior and Energy Transfer

(i) Studies of High-temperature Properties of Fast Reactor Materials: Heat Capacity of Liquid UO_2 (L. Leibowitz and M. G. Chasanov)

Last Reported: ANL-7403, p. 146 (Dec 1967).

The lack of information about the thermophysical properties of reactor materials at high temperature and pressure has been a major handicap in the calculation of the severity of certain kinds of fast reactor incidents. Experiments are being conducted to measure the heat content of liquid uranium dioxide, which will facilitate estimation of the total energy released and the temperatures attained in the core during destructive nuclear excursions. Drop-calorimetric techniques are being employed, extending to temperatures which have not previously been explored.

In preparation for the work with UO_2, enthalpy measurements were made with tungsten powder. After some initial experimental difficulties, preliminary data were obtained at 2825 and 3125°K. These results are tabulated below, and are compared with the results of Kirillin et al.* and Hein and Flagella.**

Temp (°K)	$H_T - H_{0°K}$ (cal/mole)		
	This Work	Kirillin et al.*	Hein and Flagella**
2825	19,778	19,457	19,384
3125	22,504	22,123	22,305

The agreement with the published values is considered satisfactory.

While the tungsten powder experiments were in progress, prototype capsules containing UO_2 were received. To avoid excessive delays

*Kirillin, V. A., Sheindlin, A. E., Chekhovskoi, V. Ya., and Petrov, V. A., Russ. J. Phys. Chem. 37, 1212 (1963).

**Hein, R. A., and Flagella, P. N., Enthalpy Measurements of UO_2 and Tungsten to 3260°K, GEMP-578 (1968).

in the acquisition of data on the enthalpy of uranium dioxide, exploratory measurements with that material were made before concluding the tungsten work. Preliminary UO_2 results (not reported) show good agreement with the recent work of Hein and Flagella. However, these values are higher than would be expected from extrapolations of earlier measurements by Moore and Kelley* and Conway and Hein.**

At present measurements are continuing simultaneously with UO_2 and tungsten. Attention will be directed initially to a determination of the heat of fusion of UO_2 to help resolve the conflict between the value 18.2 kcal/mole obtained by drop calorimetry by Hein and Flagella† and that of 25.3 kcal/mole obtained by cooling curve techniques.††

3. Coolant Dynamics

a. Critical Flow (H. K. Fauske)

Last Reported: ANL-7427, pp. 141-142 (Feb 1968).

(i) Sodium Tests. Several runs have been made with flashing sodium in the cylindrical-divergent test section. The measured axial temperature and pressure profiles in the flashing region are being analyzed to determine the deviations from the corresponding equilibrium states. Preliminary findings indicate large deviations.

A leak in the test section has caused temporary shutdown of the sodium loop. A new test section is being fabricated.

(ii) Sonic Velocity. The modifications to the experimental facility that will permit tests of steam-water mixtures are almost completed.

b. Coolant Dynamics (R. M. Singer)

Last Reported: ANL-7427, pp. 142-144 (Feb 1968).

(i) Superheat. A second superheat test vessel with a sand-blasted heater surface has been installed and is being tested. The test procedure and pressure-temperature history will be the same as were used in the experiments with the mirror-finished vessel so that the effect of surface characteristics on incipient-boiling superheats can be observed.

---

* Moore, G. E., and Kelley, K. K., J. Amer. Chem. Soc. 69, 2105 (1947).
** Conway, J. B., and Hein, R. A., J. Nucl. Mater. 15, 149 (1965).
† Hein, R. A., and Flagella, P. N., loc. cit.
†† Grossman, L. N., and Kaznoff, A. I., J. Amer. Ceram. Soc. 51, 59 (1968).

(ii) Expulsion. Most of the instrumentation has been installed. The sodium piping and cleanup system are being assembled.

c. Core Component Dynamics (M. W. Wambsganss)

Last Reported: ANL-7419, pp. 154-157 (Jan 1968).

Experimental support of the studies has begun with introductory small-scale explosive tests using powder charges (of less than 1/2 g each) and EBR-II cladding tubes on the "standard" spacing in arrays of 1-19. The introductory tests are establishing the appropriate range of energy releases, materials, and the ignition and packing procedures that will provide consistent results. The aim is to determine such things as the periods and energy-release thresholds for retaining the energy by the bundle packing and the hexagonal can of the subassembly. Then we can study the propagation from subassemblies in the limiting region and beyond. A major goal of the experiments is to explain the partitioning of mechanical energy. For example, the preliminary tests indicate such qualitative features as the partitioning of energy absorbed in gross bending of the tube versus deformation of the cross section, as well as roughly indicating the energy involved in venting a tube in or out of water and the subsequent effect on other tubes in the array.

B. Operations

1. TREAT Operations (J. F. Boland)

Last Reported: ANL-7427, pp. 145-146 (Feb 1968).

a. Reactor Operations. Neutron radiographs were made of unirradiated EBR-II fuel elements to develop techniques for detecting cladding and end-fitting distortion in spent fuel elements. The techniques now appear satisfactory and plans are being formulated for neutron radiographing the lower ends of irradiated EBR-II fuel pins.

Three Zircaloy-clad, UO_2-pellet fuel rods were irradiated in room-temperature water in transparent capsules to obtain data on failure threshold and failure mechanisms. Similar tests are planned for Zircaloy-clad, UO_2-powder fuel rods of similar size, cladding thickness, and fuel enrichment. The data from these experiments will be used to obtain a comparison of failure thresholds and mechanisms for these two types of fuels.

b. Development of Automatic Power-level-control System. Computer simulation of the TREAT reactor with an automatic control system continued. A successful simulation was run of reactor and control-system response to a power demand change of two decades on a 0.1-sec period. The data from this simulation showed that a faster control-rod speed will

be required for terminating the power increase than for any other control function. Additional computer simulations will be required to determine the amount of power overshoot associated with slower power-change rates and slower control-rod speeds. Since the cost of the control system will be strongly dependent on the maximum control-rod speed specified, system response will be evaluated for control-rod speeds that are attainable with several standard-size servo values.

C. Chemical Reaction--Research and Development

1. Chemical and Associated Energy Problems (Thermal)

a. Analysis of Loss-of-coolant Accidents (J. C. Hesson)

Last Reported: ANL-7399, pp. 168-169 (Nov 1967).

Experimental simulations of the environment of Zircaloy-clad, UO_2-core fuel rods following a loss-of-coolant accident in a water-cooled power reactor have continued. In such a situation, the fuel would be subjected to a slowly rising temperature (compared with that of a transient) because of fission product decay heating and the exothermic cladding-steam reaction. In addition, the fuel rods would be subjected to a steam atmosphere and water from an emergency coolant system (unless it fails).

The primary objectives of these out-of-pile simulations are to define, identify, and characterize fuel failure (in terms of change in fuel-rod geometry) so that the behavior of a water-cooled reactor core following a loss-of-coolant accident may be predicted. The program will be useful in providing parameters for fuel failure in loss-of-coolant calculational studies, such as with the CHEMLOC Program.

The results of several scoping experiments using induction heating of single rods and four-rod bundles have been reported previously (see Progress Reports for April 1967, ANL-7329, p. 94, and Nov 1967, ANL-7399, p. 168).

Currently, a series of experiments is being conducted in which single simulated fuel rods are inductively heated in a flowing steam atmosphere to predetermined temperatures and then quenched by cooling water to simulate emergency core cooling. The simulated fuel rods for these tests consist of 1/2-in.-dia UO_2 pellets encased in 12-in.-long sections of Zircaloy tubing (of 0.567-in. OD with a 0.031-in. wall thickness). The rods are evacuated and pressurized to 10 psig with helium. For each test, a rod is placed inside a 0.865-in.-ID quartz tube cell where a central axial section is heated by a 3-in.-long induction coil. A W5-Re/W26-Re thermocouple at the inside surface of the Zircaloy tubing (near the axial center of the induction coil) is used to measure the rod temperature. Steam is

admitted to the bottom of the quartz cell and the cooling water quench is admitted to the cell either by spraying from the top or by flooding from the bottom. The steam flow rate is 2 g/min (0.265 lb/hr), whereas the cooling water flow rate is 190 g/min (25.1 lb/hr).

To heat inductively a single rod to temperatures of the order of 1000 to 2100°C at heating rates of about 5°C/sec and thus simulate loss-of-coolant conditions, heat must be added at a much greater rate than in decay heating of an actual rod. This is necessary because the heat losses from a single rod are much greater than from a rod in a core surrounded by a number of other rods. However, when quenching commences, the heat loss to the cooling water from a single rod becomes more nearly equal to the heat loss of a rod in a core being quenched.

It is extremely difficult to determine at what level the induction heating should be held during the quenching period to simulate the actual conditions experienced by a rod in a reactor core. In these experiments, some tests were conducted with the induction heating power continued during quenching at the level reached at the time quenching was initiated. This results in adding an unknown amount of energy, either more or less energy than needed to simulate the actual case. In other tests, the induction generator was turned off at the time the quenching water flow began.

Preliminary results of the experiments already conducted are shown in Table V.C.1. In considering the results of these tests, it must be borne in mind that the test rods are only 12 in. long with a 3-in.-long heated

TABLE V.C.1. Out-of-pile Loss-of-coolant Experiments Using Inductively Heated Simulated Fuel Rods

Zircaloy-2-clad, UO_2-pellet-core Fuel (See text)
Steam Flow Rate: 2 g/min
Cooling Water Flow Rate: 190 g/min

Run No.	Quench Temp (°C)	Bottom or Top Quench	Heating Rate (°C/sec)	Power On or Off during Quench	Hydrogen Collected (mol)	Remarks
1	2110	Top	6.3	On	<0.1	Rod failed; cladding fragmented.
2	1868	Top	5.2	On	<0.1	Rod failed; cladding fragmented.
3	1646	Bottom	4.7	On	0.093	Rod failed; cladding fragmented.
4	1462	Bottom	4.8	Off	0.025	Rod remained intact.
5	1663	Bottom	5.0	Off	0.062	White band on cladding; rod remained intact.
6	1864	Bottom	5.7	Off	0.081	White band on cladding; rod remained intact on cooling, but failed on handling.
7	1488	Bottom	6.0	On	0.026	Rod remained intact, but some very thin layers of oxide flecked off the cladding.

section, and are not mechanically restrained in the test apparatus. Since the embrittlement and loss of strength of the cladding increase with the degree of cladding oxidation and interaction with the UO_2, unrestrained rods which did not fail in these tests might have failed if subjected to restraints and warpage such as those that could occur in bundles of rods in a reactor core. In addition, the efficiency of cooling bundles of rods may be considerably different than that of cooling single rods. The effects of irradiation and methods of heating (decay versus induction) as well as gas pressure in the rods may also change the results considerably. Nevertheless, these preliminary results indicate that, for the conditions of the tests, the critical quench temperature for unrestrained rod fragmentation would be in the range from 1400 to 1700°C.

Post-test examinations of the cladding and the UO_2 pellets are currently in progress.

b. Pressure Generation due to Particle-coolant Energy Transfer (R. O. Ivins and J. C. Hesson)

Last Reported: ANL-7403, pp. 156-163 (Dec 1967).

In order to analyze adequately the consequences of an accident in a water-cooled thermal reactor in which hot fuel materials are injected and dispersed into the water coolant, knowledge of the manner in which large amounts of energy are transferred from these particles to the coolant is needed. Laboratory-scale experiments are being made, using two different techniques, to obtain heat-transfer and energy-transfer data. The first technique (discussed here) involves determination of boiling heat transfer between a moving sphere and water. The second technique (see ANL-7403, p. 156) employs a pressure transducer to measure the forces generated owing to void formation when hot particles are immersed in a water column.

(i) Transient Heat-transfer Studies in Water. A series of experiments have been performed to study the forced-convection heat transfer from spheres in water. In the experiments, a heated silver metal sphere is propelled through the water by means of a motor-driven swinging arm (see Progress Report for August 1967, ANL-7371, p. 111). The temperature of the sphere is continuously monitored by a thermocouple attached to the sphere through the arm. The rate of heat transfer from the sphere to water is calculated using the time-averaged bulk temperature of the sphere (the arithmetic average temperature before entering and after leaving the water).

Heat-transfer rates from typical recent experiments using a 1/4-in.-dia silver sphere are plotted in Fig. V.C.1 as a function of the average bulk sphere temperature. The heat-transfer rate curves are of the

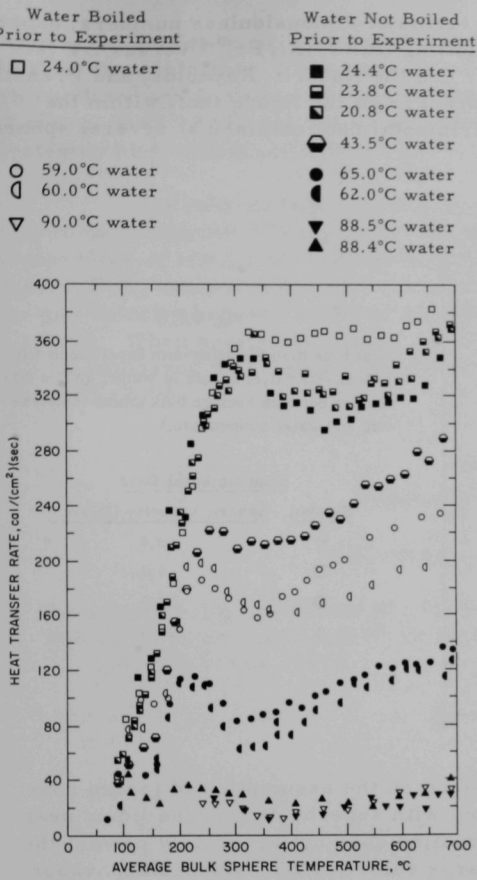

Fig. V.C.1. Heat Flux from Swinging-arm Experiment with 1/4-in.-dia Silver Sphere Moving through Water at 13.9 ft/sec

classic shape for boiling liquids* and show two regimes of boiling: nucleate boiling and film boiling. Nucleate boiling was observed (with water initially at 24°C) at average sphere temperatures from about 100 up to 350°C, with increased rates of heat transfer at the higher temperatures. At average sphere temperatures above 350°C, transition of film boiling occurs, manifested by a decrease in heat transfer rate.

The results shown in Fig. V.C.1 indicate that the effect of heating the water is to lower the temperature at which the transition of film boiling occurs. Dissolved air** in the water also tends to initiate the transition to film boiling at lower temperatures. This effect was less marked at water temperatures of 24 and 90°C than at intermediate temperatures. Heat-transfer rates in the film-boiling region were 75% greater for runs with previously boiled water at 60°C than with water not previously boiled.

The theoretical equation for heat transfer from a sphere (previously given as Eq. (2) in ANL-7371, p. 113) for correlating sodium heat-transfer data has been used to correlate all experimental data obtained with boiled water:

$$q/A = 1.13\left(\frac{U_\infty \rho_\ell C_{p\ell} k_\ell}{D}\right)^{1/2} (T_\ell - T_B). \qquad (1)$$

*Nukiyama, S., "Maximum and Minimum Values of Heat Transmission from Metal to Boiling Water under Atmospheric Pressure," Journal of the Society of Mechanical Engineers (Japan) 36, 367 (1934); Farber, E. A., and Scorah, R. L., "Heat Transfer to Water Boiling under Pressure," Trans. ASME 70, 369 (1948).

**Unboiled water contained oxygen corresponding to amounts present when water is in equilibrium with the atmosphere (about 9 ppm at 20°C), whereas after boiling the oxygen content of the water was only 2 or 3 ppm.

Since Eq. (1) can be expressed in terms of dimensionless numbers, experimental data were correlated by plotting $Nu\Delta T/(Re, Pr)^{0.5}$ versus ΔT (see Fig. V.C.2), where Nu, Re, and Pr are the Nusselt, Reynolds, and Prandtl numbers, respectively. It is apparent from the figure that, within the nucleate-boiling regime, the experimental data obtained at several sphere velocities correlate well.

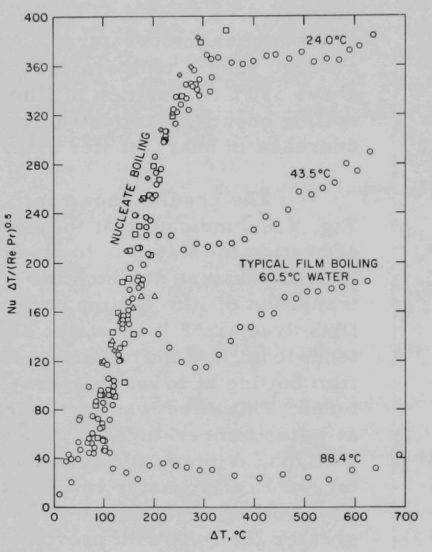

Fig. V.C.2

Heat Flux from Swinging-arm Experiments with 1/4-in.-dia Silver Sphere in Water. (ΔT = difference between average bulk sphere temperature and water temperature.)

Experimental Data

Symbol	Sphere Velocity (ft/sec)
◇	3.4
□	7.2
○	13.9
△	25.5

Since Eq. (1) is based on the assumption of forced convection (negligible vapor formation) with superheating of the liquid near the sphere-liquid interface, the equation does not accurately predict the observed heat-transfer rates at large values of ΔT. Apparently, vapor formation contributes to the higher rates, although superheating of the liquid is nevertheless significant. Future experiments will be directed toward determining the conditions related to water superheating and vapor formation, and toward defining more clearly the contribution of each to heat transfer.

D. Effluent Control Research and Development--Gaseous Effluent Studies

1. Plutonium Volatility Safety

a. Plutonium Hexafluoride Safety (R. W. Kessie)

Last Reported: ANL-7403, pp. 163-164 (Dec 1967).

The volatility of PuF_6, combined with the high toxicity of plutonium, requires that a high degree of cleanup be provided for the off-gas

from an enclosure to provide for the possibility of an accidental release of PuF_6 in the enclosure. Laboratory-scale experiments are underway in which plutonium is removed from the gas stream by the combined process of hydrolysis of PuF_6 and filtration of PuO_2F_2 particles through a series of pretested high-efficiency filters (of 10-cm diameter).

Six runs were performed to determine whether the presence of 1 to 10 m/o fluorine in the gas stream affects plutonium removal. To allow comparison of results with the results of previous runs in which fluorine was absent, PuF_6 concentration was varied between 6×10^{-3} and 26×10^{-3} Torr, the gas velocity between 0.25 and 2.5 cm/sec, and moisture between 0.3 and 5.3 Torr. When analytical results for these experiments are received, they will be compared with results for earlier runs in which fluorine was absent (see ANL-7403).

PUBLICATION

NUCLEAR SAFETY

On the Superheating of Sodium at Low Heat Fluxes
Robert E. Holtz and Ralph M. Singer
ANL-7383 (Nov 1967)

PUBLICATION--GENERAL

Chemical Engineering Division Semiannual Report, January-June 1967
ANL-7375 (Oct 1967)